



Carl-von-Ossietzky Universität Oldenburg

Fakultät II – Informatik, Wirtschafts- und Rechtswissenschaften

Department für Informatik

# Nonlinear Model Predictive Control for Trajectory Tracking and Collision Avoidance of Surface Vessels

Dissertation submitted to obtain the degree of

*Doctor of Engineering (Dr.-Ing.)*

Submitted by

Mohamed Elsayed Hasan Abdelaal, M.Sc.  
born on 01.01.1988 in Cairo

December 2018



Reviewers:

Prof. Dr.-Ing. Axel Hahn

Prof. Dr. Martin Fränzle.

Prof. Dr. Yuanqiao Wen

Date of disputation: 17.12.2018



# Acknowledgements

I would like to express my sincere gratitude to my advisors Prof.Dr.-Ing. Axel Hahn and Prof. Martin Fränzle for the continuous support of my research, their patience, motivation and immense knowledge. Their guidance helped me throughout my research and also during writing this thesis. I could not imagine having a better advisor and mentor for my doctoral study.

Besides my advisors, I would like to thank the rest of my thesis committee: Prof. Dr. Yuanqiao Wen, Prof.Dr.-Ing. Jürgen Sauer and Dr.-Ing. Willem Hagemann, not only for their insightful comments and encouragement, but also for the rich discussion which definitely will help me broaden my research perspective in the future.

My sincere thanks also goes to Aya Mohamed for proofreading this thesis.

I thank my fellow colleagues in the System Analysis and Optimization and Hybrid Systems groups for the stimulating discussions, cooperation, and for all the fun we have had in the last four years.

Finally, I would like to thank my family: my parents and to my brothers for their support throughout writing this thesis and my life abroad in general.



# Abstract

In the past decades, the collision accidents of vessels have drawn much attention due to the bad impact on the maritime environment, and the loss of human lives and money. This leads to developing various collision avoidance systems that act as a decision support system for the crew or as an autonomous system, especially with increasing traffic density and speed as well as growing ship sizes, and the attribution of most of the maritime accidents to humans factors. These systems lack the utilization of the ship maneuverability, represented by the ship dynamics and/or external environmental disturbances. Due to the characteristics of ship motion such as large inertia, time delay and nonlinearities etc., the ship dynamics is a major and important issue for the navigational accuracy and safety of ships, especially in the collision avoidance of ships.

This thesis presents a combined Nonlinear Model Predictive Control (NMPC) for position and velocity tracking of surface vessels, and collision avoidance of static and dynamic objects into a single control scheme. This scheme is suitable for critical maneuvering of autonomous vessels in near-collision situation due to the explicit utilization of the dynamic model and the ship domain in the design. It accounts for sideslip angle and counteracts environmental disturbances. The ship domain of the vessel is assumed to be either circular or elliptical disk. A three-degree-of-freedom (3-DOF) dynamic model is used with only two control variables: namely, surge force and yaw moment. External environmental forces are considered as constant or slowly varying disturbances with respect to the inertial frame, and hence nonlinear with respect to the body frame of the vessel. Nonlinear disturbance observer (NDO) is used to estimate these disturbances in order to be fed into the prediction model and enhance the robustness of the controller. A nonlinear optimization problem is formulated to minimize the deviation of the vessel states from a time varying reference generated over a finite horizon by a virtual vessel. Sideslip angle is considered in the cost function formulation to account for tracking error caused by the transverse external force in the absence of sway control force. Collision avoidance is embedded into the trajectory tracking control problem as a time-varying nonlinear constraint of position states to account for static and

dynamic obstacles. This constraint takes a simple Euclidean distance form for curricular ship domain, and an elliptical disk separation condition for the elliptical case. The effectiveness of the presented approaches are evaluated for three typical collision scenarios; head-on, overtaking and and crossing crossing, using MATLAB and ACADO toolkit for automatic control and dynamic optimization.



# Kurzfassung

Kollisionen von Schiffen erhielten in den letzten Jahren zunehmend Aufmerksamkeit, da sie häufig mit negativen Folgen für die Umwelt, dem Verlust von Menschenleben sowie erheblichen finanziellen Schäden einhergehen. Um solche Unfälle zu verhindern, dienen neue Systeme zur Kollisionsvermeidung der Mannschaft an Bord als Entscheidungshilfe oder arbeiten gar als autonomes System. Dies ist gerade bei der steigenden Verkehrsdichte und Geschwindigkeit auf See notwendig, denn die meisten Unfälle im maritimen Bereich sind auf menschliche Fehler zurückzuführen. Jedoch beziehen diese Systeme die spezifische Manövrierfähigkeit der Schiffe nicht mit ein, die durch die Dynamik der Schiffe und / oder die Umwelteinflüsse repräsentiert werden kann. Aufgrund der Charakteristika von Schiffen, wie etwa eine große Trägheit, zeitliche Verzögerungen und nichtlineares Verhalten, ist die Schiffsdynamik ein wichtiger Bestandteil für die Genauigkeit der Navigation und der Sicherheit der Schiffe, insbesondere bei der Kollisionsvermeidung.

Diese Arbeit zeigt ein kombiniertes Nonlinear Model Predictive Control (NMPC, Nichtlineares Modell für Prädiktive Steuerung). Mit diesem Modell wird die Verfolgung der Position und Geschwindigkeit von Schiffen sowie die Kollisionsvermeidung von statischen und dynamischen Objekten in einem Kontrollschema kombiniert. Dieses Schema ist für kritische Manöver von autonomen Schiffen in Situationen mit beinahe-Kollisionen geeignet, da es in seinem Design explizit das Modell für die Schiffsdynamik sowie die Schiffsdomäne mit einbezieht. Es beachtet den Sideslipwinkel und wirkt Umwelteinflüssen entgegen. Es wird angenommen, dass die Schiffsdomänen entweder rund oder elliptisch ist. Es wird ein Dynamikmodell mit drei Freiheitsgraden (3-DOF, Degrees of Freedom) genutzt, wobei nur zwei Variablen benötigt werden: die Längsachsenkraft und das Gierträgheitsmoment. Externe Umwelteinflüsse werden als konstante oder sich langsam verändernde Störungen einbezogen, wobei das Inertialsystem mit betrachtet wird. Somit wirken diese nicht-linear auf den Rumpf des Schiffes. Ein Nonlinear Disturbance Observer (NDO, Nichtlinearer Störungsbeobachter) wird eingesetzt, um diese Störungen abzuschätzen und an das Vorhersagemodell weiterzugeben, womit die Robustheit des Controllers verbessert werden kann. In der Arbeit wird zudem ein nicht-lineares Optimierungsproblem formuliert, um die Abweichung der Schiffszustände

zu einer zeitvariablen Referenz zu minimieren. Die Referenz wird von einem virtuellen Schiff über einen finiten Zeithorizont berechnet. Der Sideslip-winkel wird in der Kostenfunktion berücksichtigt, um dem Fehler bei der Schiffsverfolgung Rechnung zu tragen, wenn gibt es kein Querkraft. Die Kollisionsvermeidung ist in das Trajektorienverfolgungsproblem als eine zeitvariante, nicht-lineare Bedingung von Positionszuständen integriert, um statische und dynamische Hindernisse zu berücksichtigen. Diese Bedingung nutzt simple Euklidische Distanzen für den Fall, dass eine kreisförmige Schiffsform angenommen wird und eine elliptische Separationsbedingung für den elliptischen Fall. Die Effektivität des Algorithmus' wird für drei typische Kollisionsszenarien evaluiert: frontale Kollision, Überholen und Kreuzung zweier Trajektorien.

# Contents

<b>List of Figures</b>	<b>xv</b>
<b>List of Tables</b>	<b>xvii</b>
<b>List of Abbreviations</b>	<b>xv</b>
<b>1 Introduction</b>	<b>1</b>
1.1 Autonomous Vessels . . . . .	4
1.2 Guidance, Navigation and Control (GNC) . . . . .	7
1.3 Autonomous COLREGs Navigation . . . . .	8
1.4 Main Contributions . . . . .	12
1.5 Thesis Outline . . . . .	14
<b>2 Requirements and Literature Review for Ship Control Systems</b>	<b>17</b>
2.1 Requirements Definition . . . . .	18
2.2 Literature Review . . . . .	20
2.2.1 Vessels Control System . . . . .	20
2.2.2 Model Predictive Control . . . . .	21
2.2.3 Collision Avoidance . . . . .	23
<b>3 Modeling of 3-DOF Marine Vessels Maneuvering Model</b>	<b>25</b>
3.1 Reference Frames . . . . .	26
3.2 Rigid-body Kinematics . . . . .	28
3.3 Rigid-body Kinetics . . . . .	30
3.4 Hydrodynamic Forces and Moments . . . . .	31
3.5 Actuator Forces . . . . .	33
3.6 Environmental Forces . . . . .	35
3.6.1 Wind Forces . . . . .	36
3.6.2 Wave-induced Forces . . . . .	37
3.7 Simplification . . . . .	39

<b>4</b>	<b>Nonlinear Model Predictive Control</b>	<b>41</b>
4.1	Introduction . . . . .	41
4.2	NMPC Formulation . . . . .	43
4.3	NMPC Formulation for Tracking Problems . . . . .	47
4.4	NMPC Formulation for Tracking Problems with Time-varying Constraints . . . . .	49
4.5	Stability . . . . .	50
4.6	Optimal Control Problem Formulation . . . . .	52
4.6.1	Direct Single Shooting . . . . .	54
4.6.2	Direct Collocation . . . . .	54
4.6.3	Direct Multiple Shooting . . . . .	55
4.7	ACADO Toolkit . . . . .	56
<b>5</b>	<b>Disturbance Estimation</b>	<b>59</b>
5.1	Introduction . . . . .	59
5.2	Disturbance Observer Based Control (DOBC) . . . . .	61
5.3	Nonlinear Disturbance Observer . . . . .	63
5.4	Robust Nonlinear Disturbance Observer . . . . .	64
5.5	Case Study: Vessels Disturbance . . . . .	67
5.5.1	Case 1 . . . . .	70
5.5.2	Case 2 . . . . .	72
5.5.3	Case 3: Discretization Effect . . . . .	72
<b>6</b>	<b>NMPC for Trajectory Tracking of Surface Vessels</b>	<b>77</b>
6.1	Introduction . . . . .	77
6.2	Nominal Trajectory Tracking . . . . .	80
6.2.1	Simulation Results . . . . .	81
6.3	Disturbances Counteraction . . . . .	86
6.3.1	Sideslip Angle Compensation . . . . .	88
6.3.2	Simulation Results . . . . .	91
<b>7</b>	<b>Last-line of Defense Collision Avoidance of Surface Vessels</b>	<b>101</b>
7.1	Introduction . . . . .	101
7.1.1	Ship Domain . . . . .	102
7.1.2	Navigation Information System . . . . .	104
7.2	NMPC for Collision Avoidance . . . . .	106
7.2.1	Circular Ship Domain . . . . .	107
7.2.2	Elliptical Ship Domain . . . . .	109

7.2.3	COLREGs Compliance . . . . .	113
7.3	Simulation Results . . . . .	118
7.3.1	Circular Ship Domain . . . . .	118
7.3.2	Elliptical Ship Domain . . . . .	125
7.4	Discussion . . . . .	131
<b>8</b>	<b>Conclusion and Future Work</b>	<b>139</b>
8.1	Conclusion . . . . .	139
8.2	Future Work . . . . .	140
<b>Appendices</b>		
<b>A</b>	<b>Vessels Parameters</b>	<b>145</b>
<b>B</b>	<b>Mathematical Preliminaries</b>	<b>147</b>
B.1	Young’s Inequality . . . . .	147
B.2	Separation Condition between Two Elliptic Disks . . . . .	148
B.3	Cubic Polynomial . . . . .	149
	<b>References</b>	<b>151</b>



# List of Figures

1.3	COLREGS maneuvers for different situations . . . . .	12
3.2	Earth-fixed $(x_n, y_n, z_n)$ and body-fixed $(x_b, y_b, z_b)$ frames. . . . .	28
5.1	Structure of DOBC . . . . .	62
5.2	NDO block digram for the vessel . . . . .	68
5.3	Simulation results of the NDO proposed in Propostion 5.1 . . . . .	71
5.4	Simulation results of the robust NDO proposed in Propostion 5.2 . . . . .	73
5.5	Simulation results of the discrete version of NDO proposed in Propostion 5.2 . . . . .	75
6.1	NMPC simulation results of the states for scenario 1. . . . .	82
6.2	NMPC simulation results of the control input for scenario 1. . . . .	83
6.3	NMPC simulation results of the trajectory for scenario 1. . . . .	84
6.4	NMPC simulation results of the trajectory for scenario 2. . . . .	84
6.5	NMPC simulation results of the states for scenario 2. . . . .	85
6.6	NMPC simulation results of the control input for scenario 2. . . . .	86
6.7	NMPC-NDO scheme . . . . .	88
6.8	The geometrical relationship between course $\chi$ , heading angle $\psi$ and sideslip angle $\beta$ . . . . .	88
6.9	NMPC-NDO simulation results of the states for scenario 1. . . . .	92
6.10	NMPC-NDO simulation results of the trajectory for scenario 1. . . . .	93
6.11	NMPC-NDO simulation results of the Course angle for scenario 1. . . . .	93
6.12	NMPC-NDO simulation results of the control input for scenario 1. . . . .	95
6.13	NMPC-NDO simulation results of the disturbance estimation $\hat{\mathbf{b}}$ for scenario 1. . . . .	96
6.14	NMPC-NDO simulation results of the trajectory for scenario 2. . . . .	97
6.15	NMPC-NDO simulation results of the states for scenario 2. . . . .	98
6.16	NMPC-NDO simulation results of the course angle for scenario 2. . . . .	99
6.17	NMPC-NDO simulation results of the control input for scenario 2. . . . .	99

7.1	Different famous ship domains[123]. . . . .	104
7.2	Collision avoidance for circular ship domains. . . . .	108
7.3	Elliptic Disk. . . . .	109
7.4	Simulation results of the states for the circular scheme head-on scenario.	119
7.5	Trajectory for scenario 2 for the circular scheme head-on scenario.	120
7.6	Distance tracking error for the circular scheme head-on scenario. .	120
7.7	Simulation results of the control input for for the circular scheme head-on scenario. . . . .	121
7.8	Simulation results of the states for the circular scheme overtaking scenario. . . . .	123
7.9	Trajectory for the circular scheme overtaking scenario. . . . .	124
7.10	Distance tracking error for the circular scheme overtaking scenario.	125
7.11	Simulation results of the control input for the circular scheme overtaking scenario. . . . .	126
7.12	Simulation results of the states for the circular scheme crossing scenario.	127
7.13	Trajectory for the circular scheme crossing scenario. . . . .	128
7.14	Simulation results of the control input for the circular scheme crossing scenario. . . . .	129
7.15	Simulation results of the states for the elliptical scheme head-on scenario. . . . .	130
7.16	Trajectory for the elliptical scheme head-on scenario. . . . .	131
7.17	Simulation results of the control input for the elliptical scheme head-on scenario. . . . .	132
7.18	Simulation results of the states for the elliptical scheme overtaking scenario. . . . .	133
7.19	Trajectory for the elliptical scheme overtaking scenario. . . . .	134
7.20	Simulation results of the control input for the elliptical scheme overtaking scenario. . . . .	135
7.21	Simulation results of the states for the elliptical scheme crossing scenario. . . . .	136
7.22	Trajectory for the elliptical scheme crossing scenario. . . . .	137
7.23	Simulation results of the control input for the elliptical scheme crossing scenario. . . . .	138



# List of Tables

3.1	The SNAME notations for marine vessels[57]	27
5.1	Robust NDO performance index	70
5.2	Discrete NDO performance index	74
6.1	NMPC Parameters for Trajectory Tracking	81
6.2	Initial Conditions	83
6.3	NMPC-NDO Parameters for Trajectory Tracking	91
6.4	Initial conditions for NMPC-NDO scenarios	94
7.1	NMPC-NDO Parameters for Circular Ship Domain Collision Avoidance	118
7.2	NMPC-NDO Parameters for Circular Ship Domain Collision Avoidance	126
A.1	Surface Vessel Parameters	146



## List of Abbreviations

<b>AADC</b>	. . . . .	Active Anti-Disturbance Control
<b>AIS</b>	. . . . .	Automatic Identification System
<b>AL</b>	. . . . .	Autonomy Levels
<b>ARPA</b>	. . . . .	Automatic Radar Plotting Aid
<b>ASC</b>	. . . . .	Autonomous Surface Craft (ASC)
<b>ASV</b>	. . . . .	Autonomous Surface Vehicle (ASVs)
<b>CG</b>	. . . . .	Center of Gravity
<b>COLREGs</b>	. .	International Regulations for Preventing Collisions at Sea
<b>CPA</b>	. . . . .	Closest Point of Approach
<b>CV</b>	. . . . .	Constant Velocity
<b>DCPA</b>	. . . . .	Distance at Closest Point of Approach
<b>DMC</b>	. . . . .	Dynamic Matrix Control
<b>DO</b>	. . . . .	Disturbance observer
<b>DOBC</b>	. . . . .	Disturbance Observer Based Control
<b>DOF</b>	. . . . .	degree-of-freedom
<b>DSC</b>	. . . . .	Dynamic Surface Control
<b>ECEF</b>	. . . . .	Earth-centered Earth-fixed
<b>ECI</b>	. . . . .	Earth-centered inertial
<b>FLS</b>	. . . . .	Fuzzy Logic Systems
<b>GNC</b>	. . . . .	Guidance, Navigation, and Control
<b>GNSS</b>	. . . . .	Global Navigation Satellite System
<b>GPC</b>	. . . . .	Generalized Predictive Control
<b>IMC</b>	. . . . .	Internal Model Control

<b>IMO</b>	. . . . .	International Maritime Organization
<b>INS</b>	. . . . .	Inertial Navigation System
<b>LMI</b>	. . . . .	Linear Matrix Inequality
<b>LQR</b>	. . . . .	Linear Quadratic Regulator (LQR)
<b>LS</b>	. . . . .	Least Squares
<b>MPC</b>	. . . . .	Model Predictive Control
<b>NDO</b>	. . . . .	Nonlinear disturbance observer
<b>NED</b>	. . . . .	North-East-Down
<b>NLP</b>	. . . . .	Non-Linear Programming
<b>NMPC</b>	. . . . .	Nonlinear Model Predictive Control
<b>OCP</b>	. . . . .	Optimal Control Problem
<b>PADC</b>	. . . . .	Passive Anti-Disturbance Control
<b>QP</b>	. . . . .	Quadratic Problem
<b>RAO</b>	. . . . .	Response Amplitude Operator
<b>SMC</b>	. . . . .	Sliding Model Control
<b>SNAME</b>	. . . . .	The Society of Naval Architects and Marine Engineers
<b>TCPA</b>	. . . . .	Time to the Closest Point of Approach
<b>USV</b>	. . . . .	Unmanned Surface Vessel
<b>WF</b>	. . . . .	Wave-Frequency (WF)

# 1

## Introduction

In the past decades, the collision accidents in the maritime domain have drawn much attention from the academic community due to the disastrous consequences on human lives and the impact on the society and the marine environment. Over the centuries, ship navigation has traditionally been performed entirely by human endeavour. Today, however, maritime technology comes to the aid of the ship piloting crew in minimizing navigational errors[1]; especially that most of the maritime accidents (about 80%) are attributed to humans factors[2], and the technological advancements in the marine engineering result in the development of heavy and huge ships with great speed, as well as increase of the traffic density. This technology provides many systems ranging from collision alert and decision support systems for the crew over to autonomous collision avoidance systems that take the necessary action automatically. This also raises the prospect of crewless “ghost” ships crisscrossing the ocean, with the potential for cheaper shipping with fewer accidents.

In addition, there is a trend in the maritime domain to use autonomous or semi-autonomous vessels due to the benefits of reduced personnel and the operational precision in spite of the legal and safety issues concerning letting autonomous vessels travel unsupervised in the near future. One of the most challenging requirements

that increase the possibility of accepting running autonomous vessels is to operate safely. Safe operation means that the vessel can track its planned trajectory accurately and avoid collision with obstacles and encountered vessels.

In this context, designing a precise trajectory tracking and collision avoidance systems become necessary not only for autonomous vessels but also for the manned ships to support the crew, decrease their workload and decrease the human mistakes. Trajectory tracking of vessels is a control system component that utilize the ship maneuverability, represented by the ship dynamic model, to track the planned trajectory, while collision avoidance is usually handled as planning problem that lack the utilization of the dynamic model and/or external environmental disturbances in the design. Due to the characteristics of ship motion such as large inertia, time delay and nonlinearities etc., the ship dynamics is a major and important issue for the navigational accuracy and safety of ships, especially in the collision avoidance of ships. The literature lacks considering this issue except for the very recent research [3, 4].

The sinking of **The Royal Mail Ship (RMS) Titanic** can provide some insights on how a better understanding of the ship dynamics can lead to a better collision avoidance systems. The RMS Titanic has sunk on the night of 14th April to the morning of 15th April 1912 in the North Atlantic Ocean during its voyage from Southampton to New York City. It was the largest passenger liner in service at that time with about 2,224 people on board when she struck an iceberg at around 23:40 (ship's time) on Sunday, 14th of April 1912 while she was at a speed of 22 knots (41 km/h; 25 mph), only 2 knots (3.7 km/h; 2.3 mph) less than her maximum speed of 24 knots (44 km/h; 28 mph)[5]. The RMS Titanic was in close encounter head-on situation with an iceberg when the fleet noticed that. One of the fleet rang the lookout-bell three times and telephoned the bridge to inform Sixth Officer James Moody. After thanking Fleet, Moody relayed the message to Murdoch, who ordered Quartermaster Robert Hichens to change the ship's course[6]. The First Officer Murdoch had ordered the helm hard-a-starboard (rudder hard-a-port) which

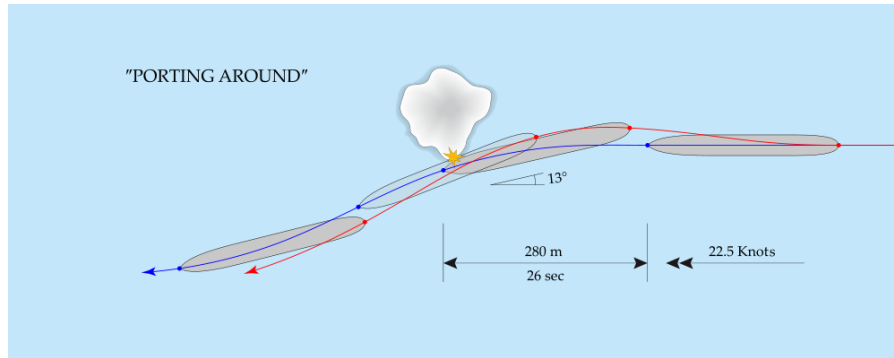


**Figure 1.1:** Diagram of Titanic's course at the time of the collision with the iceberg. (Blue: path of bow. Red: path of stern.)

turns her to port side while ordering the engines full astern. The change of heading was just in time to avoid the head-on collision, but the change in direction caused the ship to strike the iceberg with a glancing blow as shown in Figure 1.1. An underwater spur of ice scraped along the starboard side of the ship for about seven seconds which led to a flood of five compartments.

In [7], Captain Lewis Marmaduke Collins, Atlantic Pilotage Authority, has said that many experts assumed the damage of the aft could have been avoided by Murdoch ordering the helm hard-a-port, which turned her back to starboard, after he had turned to port with a hard-a-starboard helm. This could happen due to the drifting behavior of the ship dynamics during maneuvering as when a ship is trying to turn to the port side, it drifts for sometime in the starboard side. Employing this dynamic behavior, Titanic was able to swing around the iceberg by ordering the helm hard-a-port after the hard-a-starboard helm order.

In this context, this thesis considers the problem of ship motion control, i.e. trajectory tracking or path following, while taking into consideration collision avoidance to act as a last-line of defense scheme. This is achieved by employing the nonlinear dynamics of the ship as well as its geometry, represented by its ship domain, in the collision avoidance design. Such a collision avoidance maneuvering needs to be accurate and hence considering environmental disturbance is necessary. The main motivation driving this work is the development of an integrated motion

control and collision avoidance. This scheme has an increasing attention during the last decade in different domains such as robotics and automotive.

This chapter gives an overview of the autonomous vessels and its benefits followed by the components of the ship control system. After that, a brief overview of the safety rules that is used during collision risk is presented. The main contributions of this research are given at the end of the chapter followed by the thesis structure.

## 1.1 Autonomous Vessels

The trend is clear that higher level of automation is entering, not only the maritime domain, but also all sectors of transportation[8]. Although the international shipping law states that ocean-going vessels must be properly crewed which makes Unmanned Surface Vessels (USVs) not allowed in international waters, a discussion began in 2017 at UN's International Maritime Organization (IMO) that could allow USVs to operate across oceans. The USVs has many benefits such as[9]:

- Reduced personnel cost.
- Less need for personnel in exposed areas and thus improved personnel safety.
- Reduced risk and smaller consequences from operator errors.
- Increased operational precision.
- Wide weather window of operations.
- Flexible vehicles with reduced emissions and thus more eco-friendly operations.
- New vehicle designs and concepts of operation.

The vessel automation can be categorized into different autonomy levels (AL), from simple decision support system to full autonomous vessel, as described in [10]:



- **Decision support:** This corresponds to current advanced ship types with Automatic Radar Plotting Aid (ARPA) system as an anti-collision system, electronic chart systems and common automation systems like autopilot. The crew is still in direct command of ship operations and continuously supervises all operations. This level normally corresponds to "no autonomy".
- **Automatic:** The ship has more advanced automation systems that can complete certain operations without human interaction, e.g. dynamic positioning or automatic berthing. The operation follows a pre-programmed sequence and will request human intervention if any unexpected events occur or when the operation completes. The shore control center (SCC) or the bridge crew is always available to intervene and initiate remote or direct control when needed.
- **Constrained autonomous:** The ship can operate fully automatic in most situations and has a predefined selection of options for solving commonly encountered problems, e.g. collision avoidance. It has defined limits to the options it can use to solve problems, e.g. maximum deviation from planned track or arrival time. It will call on human operators to intervene if the problems cannot be solved within these constraints. The bridge personnel continuously supervises the operations and will take immediate control when requested to by the system. Otherwise, the system will be expected to operate safely by itself.
- **Fully autonomous:** Overall decisions on navigation and operation are calculated by the system. Consequences and risks are calculated. The system acts based on its analysis and calculations of its own capability and the surroundings' reaction. Knowledge about the surroundings and previous and typical events are included at a machine intelligent level.

There are many potential benefits to be gained from autonomous ships. It is assumed that autonomous ships would have fewer accidents because the majority of maritime accidents involve collisions or groundings, caused by humans. In its 2016 annual overview, the European Maritime Safety Agency found that 62% of the 880 accidents occurring globally (2011-2015) were caused by "human erroneous action". Given the role of human error in maritime incidents, it is assumed that autonomous or unmanned vessels could be safer. At the same time, the risks inherent in having a crew, such as injury or loss of life, will be significantly reduced or even eliminated. In this context, The operation of autonomous ships will need to be at least as safe as existing vessels if they are to secure regulatory approval, the support of ship owners, operators, seafarers and wider public acceptance.

The research of autonomous vessels covers a lot of disciplines which includes but not limited to:

- **Improved sensor system:** by developing new efficient algorithms for sensor fusion of inertial, magnetic, range/position, velocity and imaging sensors employing observer theory.
- **Obstacles Detecion:** by using fusion of different equipments such as Radar, camera or AIS data to sense and detect the obstacle or crossing vessel, and categorize them. This includes also intelligent prediction of ships trajectories.
- **Collision avoidance:** by developing collision avoidance algorithms using optimization and heuristic search methods.
- **Track keeping:** by developing robust controller which is able to follow the planned path or track a reference trajectory.

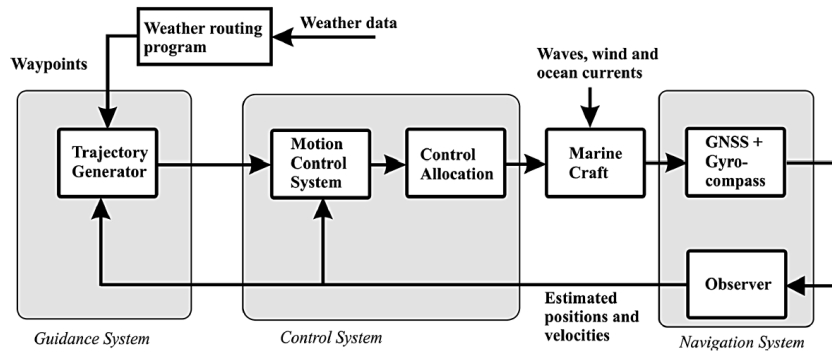


Figure 1.2: GNC block diagram[11].

## 1.2 Guidance, Navigation and Control (GNC)

The ship motion control system can be divided into three components or layers denoted as the guidance, navigation and control. The diagram in Figure 1.2 shows the three components and how they interact with each other. Although the diagram shows these systems interact with each other through signal flow, they could be more tightly coupled and even represented by one system for modern control systems. The tasks of the blocks are classified according to [11]:

**Guidance** is the action or the system that continuously computes the reference (desired) position, velocity and acceleration of a marine craft to be used by the motion control system. The basic components of a guidance system are motion sensors, external data such as weather data (wind speed and direction, wave height and slope, current speed and direction) and a computer. The computer collects and processes the information and then feeds the results to the motion control system. In many cases, advanced optimization techniques are used to compute the optimal trajectory or path for the ship to follow. This might include sophisticated features such as fuel optimization, minimum time navigation, weather routing, collision avoidance, formation control and synchronization.

**Navigation** is the science of directing a craft by determining its position, course and distance traveled. In some cases velocity and acceleration are determined as

well. This is usually done by using a Global Navigation Satellite System (GNSS) combined with Inertial Navigation System (INS) which consists of motion sensors such as accelerometers and gyroscopes. It originally denotes the art of ship driving, including steering and setting the sails.

**Control**, or more specifically motion control, is the action of determining the necessary control forces and moments to be provided by the craft in order to satisfy a certain control objective. The desired control objective is usually seen in conjunction with the guidance system. Examples of control objectives are minimum energy, setpoint regulation, trajectory-tracking, path-following and maneuvering control. Constructing the control algorithm involves the design of feedback and feedforward control laws. The outputs from the navigation system, position, velocity and acceleration are used for feedback control while feedforward control is implemented using signals available in the guidance system and other external sensors.

### 1.3 Autonomous COLREGs Navigation

The International Regulations for Preventing Collisions at Sea (COLREGs) are published by the International Maritime Organization (IMO) and set out, among other things, the navigation rules to be followed by ships and other vessels at sea to prevent collisions between two or more vessels[12]. By 2016, COLREGs were ratified in 156 countries and included in national laws[13]. It is considered as a universal and definitive guide for executing standard avoidance maneuvers.

COLREGs consist of six parts where of which Part B: *Steering and sailing* pertains to navigation practice and conduct of vessel in different visibility conditions. Part A: *General* describes the application and scope, legal responsibility, and general definitions used. Part C and D handle lights and shapes, and Sound and light signals, respectively. Exemption of these rules is described in Part E while Part F deals with the verification of compliance with the provisions of the convention.

Despite its thoroughness, COLREGs was designed with seafaring personal in the loop and relies on the common sense, not only to determine if a situation currently applies, but also to exploit flexibility in the actions prescribed in a rule[14]. Moreover, the COLREGS itself can be disregarded or at least relaxed in critical situation which could be understood from the following rules:

**Rule 2 - Responsibility**

- (a) Nothing in these Rules shall exonerate any vessel, or the owner, master or crew thereof, from the consequences of any neglect to comply with these Rules or of the neglect of any precaution which may be required by the ordinary practice of seamen, or by the special circumstances of the case.
- (b) In construing and complying with these Rules due regard shall be had to all dangers of navigation and collision and to any special circumstances, including the limitations of the vessels involved, which may make a departure from these Rules necessary to avoid immediate danger.

**Rule 16 - Action by give-way vessel**

Every vessel which is directed to keep out of the way of another vessel shall, as far as possible, take early and substantial action to keep well clear.

**Rule 17 - Action by Stand-on Vessel**

- (a) (i) Where one of two vessels is to keep out of the way, the other shall keep her course and speed.
- (ii) The latter vessel may however take action to avoid collision by her manoeuvre alone, as soon as it becomes apparent to her that the vessel required to keep out of the way is not taking appropriate action in compliance with these Rules.
- (b) When, from any cause, the vessel required to keep her course and speed finds herself so close that collision can not be avoided by the action of the give-way vessel alone, she shall take such action as will best aid to avoid collision.

- (c) A power-driven vessel which takes action in a crossing situation in accordance with subparagraph (a)(ii) of this Rule to avoid collision with another power-driven vessel shall, if the circumstances of the case admit, not alter course to port for a vessel on her own port side.
- (d) This Rule does not relieve the give-way vessel of her obligation to keep out of the way

Simply, Rule 17 states that the stand-on vessel must do any necessary maneuvers to avoid collision if it becomes clear that the give-way vessel is not taking appropriate action, or when so close that collision can no longer be avoided by the actions of the give-way vessel alone. Rule 2 identify the responsibility of the vessel not only to follow COLREGs but also to do everything necessary to avoid the risk of collision and the dangers of navigation. This shows the softness or flexibility of the rules.

The three primary rules that must be incorporated in an effective collision avoidance system are as follows: Rule 13: Overtaking, Rule 14: Head-on and Rule 15: Crossing [15], which are depicted in Figure 1.3 and are stated below:

### **Rule 13 - Overtaking Situation**

- (a) Notwithstanding anything contained in the Rules of Part B, Sections I and II, any vessel overtaking any other shall keep out of the way of the vessel being overtaken.
- (b) A vessel shall be deemed to be overtaking when coming up with another vessel from a direction more than  $22.5^\circ$  abaft her beam, that is, in such a position with reference to the vessel she is overtaking, that at night she would be able to see only the sternlight of that vessel but neither of her sidelights.
- (c) When a vessel is in any doubt as to whether she is overtaking another, she shall assume that this is the case and act accordingly.

- (d) Any subsequent alteration of the bearing between the two vessels shall not make the overtaking vessel a crossing vessel within the meaning of these Rules or relieve her of the duty of keeping clear of the overtaken vessel until she is finally past and clear.

#### **Rule 14 - Head-on Situation**

- (a) When two power-driven vessels are meeting on reciprocal or nearly reciprocal courses so as to involve risk of collision each shall alter her course to starboard so that each shall pass on the port side of the other.
- (b) Such a situation shall be deemed to exist when a vessel sees the other ahead or nearly ahead and by night she would see the mast head lights of the other in a line or nearly in a line and or both sidelights and by day she observes the corresponding aspect of the other vessel.
- (c) When a vessel is in any doubt as to whether such a situation exists she shall assume that it does exist and act accordingly.

#### **Rule 15 - Crossing Situation**

When two power-driven vessels are crossing so as to involve risk of collision, the vessel which has the other on her own starboard side shall keep out of the way and shall, if the circumstances of the case admit, avoid crossing ahead of the other vessel

The overtaking rule gives the vessel the choice to pass on either the port (left) or star-board (right) side but must issue the appropriate signal and keep clear from the vessel being overtaken. Rule 14 forces both vessels in head-on situation to alter the course to starboard side immediately and do not wait for the other vessel to act. In crossing situation, the vessel that has the other on her starboard must alter her course to starboard side early so the other vessel knows your intentions. It is recommended in crossing situation to cross astern and avoid crossing ahead if possible.

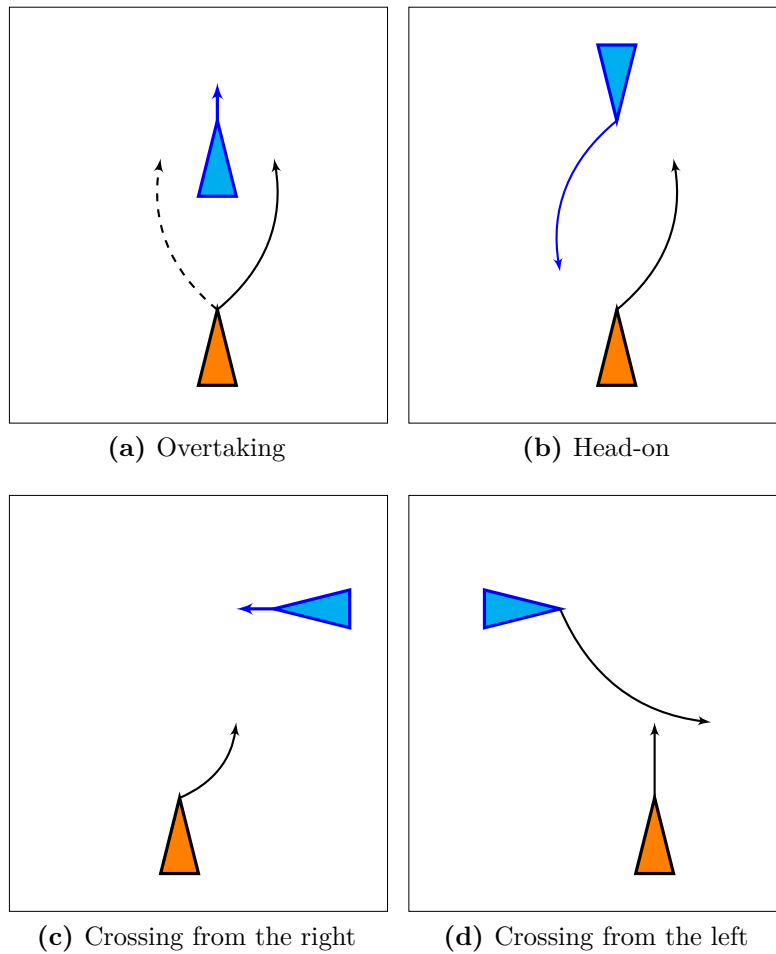


**Figure 1.3:** COLREGS maneuvers for different situations

## 1.4 Main Contributions

This thesis presents an accurate collision avoidance scheme for surface vessels that is handled as an optimization-based control system problem to eliminate the insufficiency of neglecting the ship dynamics in the process of avoiding collision. This scheme is integrated into the trajectory tracking algorithm and is supported by a disturbance counteraction component. This approach is intended to act as a last-line of defense collision avoidance system due to its ability to employ the nonlinear dynamics of the vessel and its efficient computation time.

The main contribution can be summarized as:



- Provide a systematic way to design an optimization-based trajectory tracking nonlinear controller for surface vessel in the framework of Nonlinear Model Predictive Control that respects the control input limits because most of the other techniques lack this. The design is achieved with the aid of the ACADO toolkit for dynamic optimization. The optimization problem is solved over a finite prediction horizon that minimizes the states deviation from the planned reference states with sideslip angle compensation due to the underactuated workspace of the vessel. This technique can be directly applied to a wide range of ship models which therefore can be considered as a universal technique.
- Design of a Nonlinear Disturbance Observer (NDO) to estimate constant or slowly time varying disturbance acting on the vessel due to model uncertainty, wind forces, waves effect and other unmodeled terms. This relaxes the design of nonlinear control design of systems subjected to disturbances to a disturbance-free design problem while considering estimated disturbances as extra states or control inputs. Unlike linear MPC, NMPC does not have an integrator action and therefore the NDO is integrated into it to achieve an offset-free tracking.
- Provide a last-line of defense autonomous collision avoidance system that overcome the lack of utilizing the nonlinear maneuverability of the vessel, i.e dynamic model, into the collision avoidance design. The collision avoidance system is based on NMPC framework and is integrated into the trajectory tracking controller as an operational constraint. This provides a superior accuracy over traditional path planning techniques specially in close-quarters situations[4], which contributes to safer autonomous vessels. The scheme has two variants; one is considering a circular ship domain of the vessel and formulating the collision avoidance as a separation condition among circular disks, and the other that is considering an elliptical ship domain that suits

better the ship geometry. The circular formulation is simple and can be used for open seas, and the elliptical formulation can be used for narrow channels and dense traffic areas.

## 1.5 Thesis Outline

This thesis is organized as follows:

**Chapter 2** provides the requirements from a proper design of a motion control system that has a collision avoidance feature, and the literature review for the trajectory tracking and collision avoidance systems.

**Chapter 3** provides an overview of surface vessels modeling including both kinematics and kinetics in addition to the reference frames of the measurement. It also describes external disturbance modeling and actuator dynamics. Moreover, a simplification of the ship dynamics is presented to be valid for algorithms presented in the following chapters.

**Chapter 4** describes the NMPC formulation for setpoint stabilization, tracking problems, and how time varying constraints are handled. In addition, an overview of the NMPC stability is briefed and the techniques used for discretization and solution of the optimization problem are presented.

**Chapter 5** describes the design of a nonlinear disturbance observer to estimate the disturbance acting on a class of nonlinear systems, and gives a Disturbance Observer Based Control (DOBC) general guidelines that are employed in the following chapters. A case study for the environmental disturbance acting on a surface vessel is provided at the end of the chapter with MATLAB/Simulink simulations.

**Chapter 6** provides the formulation of NMPC for trajectory tracking of surface vessels with disturbance counteraction and sideslip angle compensation. The evaluation of this scheme is done via MATLAB/Simulink simulations.

**Chapter 7** provides the scheme of integrating collision avoidance into the NMPC

tracking problem for circular and elliptical ship domain with COLREGs rules compliance.



# 2

## Requirements and Literature Review for Ship Control Systems

Due to the great interest in autonomous control of surface vessels from both academia and industry and the big concern for the safety of autonomous ships, providing a more accurate collision avoidance system as an integrated component in the control problem become necessary. The necessity of this research comes from the fact that the nonlinear dynamic models, compared to only kinematic, represent the motion of the vessel precisely which opens the door for a unified vessel control system. Moreover, this philosophy adds the flexibility to include the effect of the environmental forces on the dynamic model into the collision avoidance design. External environmental forces, such as those induced by wind and waves, increase the collision risk dramatically specially in dense traffic areas and narrow channels[16].

In this thesis, the motion control problem of surface vessel is extended beyond set-point stabilization to include collision avoidance. This is seen as an essential component for a safe and successful application of USVs in the near future or as a decision support system for the crew. The traditional motion control problem of vessel considers only trajectory tracking or path following while collision avoidance

is handled traditionally as an online path planning problems [13, 17] that lacks the utilization of the ship dynamic model and considers motion models like constant velocity and constant rate of turn. Employing a dynamic model of the vessel will increase the degrees of freedom over motion models by being able to change the speed of the vessel therefore increase its maneuverability. In addition, wind and waves have a great impact on the tracking error of the controller which may degrades the collision avoidance scheme.

In this context, we present in section 2.1 the requirements of the ship control system to achieve trajectory tracking and collision avoidance. These requirements are derived from both the traditional control systems and the collision avoidance requirements. In section 2.2, different approaches that were used for trajectory tracking with a focus on model predictive control and collision avoidance are reviewed.

## 2.1 Requirements Definition

In this section, our point of view of the requirements of a good design of the motion control system for surface vessels are presented.

**R1 Solution Optimality:** The vessel must find the optimal control action, i.e. optimal forces and moments, to achieve minimum deviation from the planned reference trajectory which is parameterized by a sequence of way-points and speed. This optimization problem must respect the dynamic model of the ship and its control inputs limitation, i.e. maximum forces and moments. The acceptable position tracking error, the equivalent of cross track error for trajectory tracking problem, is about 7% of the ship width [18].

**R2 Environmental Disturbance Counteraction:** External disturbance can bring adverse effects on the controller performance in the sense of the tracking error if they are not included in the design of the trajectory tracking problem [19]. The disturbances refer to not only the environmental disturbances

due to waves, but also uncertainties from the dynamic model of the vessel including unmodeled dynamics, parameter perturbations, and simplified nonlinear couplings. Therefore, the controller must be able to reject the disturbances implicitly an integrator action [11] or explicitly via a disturbance observer[19].

**R3 Ship domain:** The ships vary widely in geometry, from few meters length to few hundred meters. Including a proper ship domain is necessary for a successful collision avoidance design.

**R4 Dynamics-based Collision Avoidance:** One of the requirements that we define is to employ the nonlinear dynamic model of the vessel into the collision avoidance design in order to use it as a last line of defense. The idea behind this requirements is to make use of the great research contribution on dynamic modeling of vessels which is surely represents the vessel motion much better than just kinematic and planar motion models such as those used in [13, 17]. The accurate collision avoidance maneuvering is characterized by achieving a minimum distance among the separated ship domains. A great review on modeling of vessel can be found in [11].

**R5 Common Intention Knowledge:** There is a wide research on estimating the intentions of encountered vessels using acoustics [20] or using AIS data [21]. The collision avoidance algorithm must be flexible to take into consideration the prediction of the other ships that could be done via any technique or even via direct ship to ship communication. This leads to the ability of adding any sophisticated prediction technique in the future and helps in the future research of network control systems.

**R6 Action to Avoid Collision:** The collision avoidance maneuver should obey the direction states in rules 13, 14 and 15 of The International Regulations for Preventing Collisions at Sea (COLREGs). The compliance of these rules

should be soft in special circumstances which may make a departure from these rules necessary to avoid immediate danger according to rule 2.

**R7 Computation time:** The computation time of the trajectory tracking and the collision avoidance should be suitable for the sampling interval of the system which is selected based on the dynamics speed of the ship and will be different from one to another. There is no strict rule for the value of the computation time to be neglected, however a computation time of about 7.0% of the sampling interval was considered negligible in [22]. Therefore, we will restrict our acceptable delay to be no more than 5.0%.

## 2.2 Literature Review

This section provides a review of relevant literature on the control system of vessels, receding horizon control and collision avoidance.

### 2.2.1 Vessels Control System

In recent years, trajectory tracking and path following problems have been studied using various control techniques. Dynamic Surface Control (DSC) was one of the popular techniques. In [23], DSC is used for global tracking of underactuated vessel in a modular way that cascaded kinematic and dynamic linearizations can be achieved. The control structure obtained is much simpler than the traditional backstepping-based controllers such that it is beneficial from the practical application point of view. In [24, 25], an adaptive form of DSC is used for formation control of Autonomous Surface Vehicles (ASVs) moving in a leader-follower formation under ocean disturbances. The adaptation is based on Neural Network (NN) due to its ability of learning nonlinear dynamics. The problem of following a straight line path for an underactuated ship is considered in [26]. T-S fuzzy system is used as an approximator of the unknown nonlinearities which is adapted by "minimum-learning-parameters" (MLP) algorithm, then DSC approach is used as a controller.



In [27], Dynamic Positioning (DP) is handled via vectorial backstepping algorithm for ships in the presence of time-varying unknown bounded environmental disturbances. In [28], a backstepping controller is designed, based on global exponential disturbance observer and Lyapunov's direct methods, to solve the path-tracking problem of underactuated ships under tracking error constraints. In [29], an automatic adaptive steering control design for full-actuated vessels is presented. The adaptive law is combined with a control design including a Linear Quadratic Regulator (LQR) and a Riccati based anti-windup compensator. The controller also takes into consideration input constraints, wind and wave effect and parametric uncertainty. In [30], trajectory tracking problem is addressed for 3-DOF underactuated unmanned surface vessel using a state feedback based backstepping control algorithm with relaxed Persistent Exciting (PE) conditions of yaw velocity. In [31], a recursive technique is presented for trajectory tracking of nonholonomic systems by the means of backstepping, and is demonstrated by simulating an articulated vehicle and a knife edge system. In [32], a methodology to design state and output feedback controller was presented by means of Lyapunov's direct method and backstepping after model transformation to Serret-Frenet frame.

Although the aforementioned techniques give good trajectory tracking results, they lack handling neither control inputs nor states constraints, and therefore they can not be used in solving collision avoidance problem.

### 2.2.2 Model Predictive Control

Model Predictive Control (MPC) has got attention for the vessel control problems and for other domains too due to its ability to handle states and controls constraints systematically of the system [33]. In [34], NMPC is used for trajectory tracking of full actuated Autonomous Surface Craft (ASC) in the presence of ocean disturbances which is assumed to be constant with experimental validation that validate the real-time implementation of the algorithm. In [35], a control law based on MPC

and line-of-sight (LOS) guidance law is proposed, where the lookahead distance parameter of the LOS guidance law is chosen to be time-varying and is updated with the MPC algorithm. LOS based MPC is also presented in [36], for the path following of underactuated marine surface vessels employing successive linearization along the LOS model. In [37], model predictive control is applied for tracking problem of underactuated surface vessels, employing the affine property of the system model. The kinematic is simplified by applying frame transformation to the position states independent of the choice of the inertial frame. Nonlinear functions of the System are evaluated using optimal states obtained at the previous instant which leads to significant numerical errors for large horizons[38]. In [39], NMPC is used for trajectory tracking of underactuated vessels employing direct multiple shooting technique that leads to less numerical error.

Online optimization of the MPC dynamic optimization problem is the key to determine whether it can be used for real application or not. Recurrent Neural Networks (RNN) has emerged a promising way for solving linear programming, quadratic programming (QP), general convex programming and pseudoconvex optimization problems. In [40], the Hopfield neural network was used to implement generalized predictive control for systems with constrained inputs and outputs, but the control performance was compromised as a result of suboptimal solutions for optimization problems. In [41], a structured multi-layer neural network implementing the gradient projection algorithm was applied to linear MPC with a proof that the training algorithm converges to the optimal solution. In [42], a dual neural network was applied for the multi-stage optimization problem of Multi-variable generalized predictive control taking into consideration the constraints on the input and output signals of the control system. In [43], two neural networks with simple structures were applied for solving linear programming and QP problems for linear MPC. An interesting approach was presented in [44] where the echo state network was used to model the unknown nonlinear autoregressive exogenous (NARX) systems

and the simplified dual network was applied for solving the reformulated quadratic optimization problems in MPC. In [45], a two-layer recurrent neural network was applied for solving reformulated convex optimization problems for nonlinear affine systems with additive uncertainties.

### 2.2.3 Collision Avoidance

Conventionally, collision avoidance is treated as a controller independent planning problem that might not be achievable by the controller and hence degrade the safety of the vessel[46]. For instance, an evolutionary algorithm is presented in [47] to find a safe and optimal trajectory of surface vessels in a well known environment by using the vessel's kinematic model. A more sophisticated evolutionary approach is presented in [48–50] by adding specialized operators to shape the convergence of the optimization. In [51], a fuzzy logic approach is presented for collision avoidance of large ships by formulating the problem into an optimization problem and solving it using a particle swarm algorithm. Fuzzy-neural inference network is also used in [52] for ship collision avoidance. A graph-theoretic solution on an appropriately-weighted directed graph representation of the navigation area is presented in [53]. The graph is obtained via 8-adjacency integer lattice discretization and utilization of the  $A^*$  algorithm. The aforementioned techniques lack utilizing neither the nonlinear dynamics of the ship nor the effect of the disturbances, and therefore, they are not suitable for close-quarters and can not be used as a last-line of defense collision avoidance system.

Recently, control techniques have been developed to include collision avoidance as an objective while designing the controllers. The work presented in this thesis is inspired by the work presented in [54], where the problem of tracking and formation of multiagent linear systems is solved with collision avoidance as a state constraint for the optimization problem, and extends it to nonlinear systems employing the great development in nonlinear optimization tools. In [55], a centralized MPC

is used for collision avoidance of networked vehicles by successively linearizing the nonlinear prediction model using Taylor series, but neither elliptical safety zones nor disturbance counteraction are handled. Moreover the model used there assumes a constant velocity for the vehicle which might be suitable for big ships, but restrict the maneuverability of small ones. In [46], MPC techniques are applied for the nonlinear model of kinematically redundant space robot to approach an un-cooperative target in complex space environment. For the sake of deriving a linearized version of the space robot, feedback linearization is used and hence collision avoidance can be formulated as a Linear Matrix Inequality (LMI). This method can not be applied to complex safety zones like the elliptic disks.

Handling the ship dynamics into the collision avoidance problem started to get the attention of the researchers after starting this research. In [3], behavioral based offline MPC is used for collision avoidance of ships as an upper layer above the autopilot controller. Using simulated predictions of the trajectories of the obstacles and ship, compliance with the Convention on COLREGs and collision hazards associated with each of the alternative control behaviors are evaluated on a finite prediction horizon, and the optimal control behavior is selected. In [4], the neglect of the ship maneuverability in the process of avoiding collision is overcome by employing the dynamic calculation model of collision avoidance parameter to calculate the dynamic Distance at Closest Point of Approach (DCPA) and Time to the Closest Point of Approach (TCPA) in real-time when ship is maneuvering. For the aforementioned research, they are using simulation to account for the dynamics and not utilizing the great development in the dynamic optimization domain, and they do not account for neither external disturbances nor elliptical ship domains.

# 3

## Modeling of 3-DOF Marine Vessels Maneuvering Model

The key for a successful vessel motion control system is using a proper mathematical dynamic model for the ship under control which is accurate enough to obtain good results. This includes good understanding of the motion physics to build a model, in addition to find a suitable technique to estimate its parameters. Highly accurate model might be so complex for the control theory or the optimization techniques, while the simplification of the model makes the problem feasible and gives acceptable results[56].

In this chapter, some preliminaries regarding reference frames and motion variables are reviewed followed by the mathematical modeling of the 3-DOF maneuvering model and different forces that act on the vessel. At the end, the simplified model, used in the rest of the thesis, is presented.

The marine surface vessel has six degrees of freedom (DOF), six independent parameters that define its configuration, i.e. its position and orientation.

**Definition 3.1** (Degree-of-Freedom (DOF)). [11] *For a vessel, DOF is the set of independent displacements and rotations that completely specify the displaced*

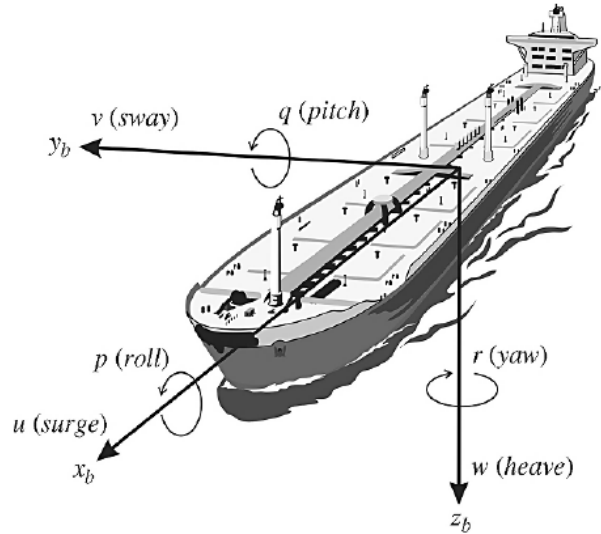


**Figure 3.1:** The 6-DOF velocities  $u$ ,  $v$ ,  $w$ ,  $p$ ,  $q$  and  $r$  in the body-fixed reference frame  $b = (x_b, y_b, z_b)$ [11].

*position and orientation of the vessel. A vessel that can move freely in the 3-D space has a maximum of 6 DOFs, three translational and three rotational components*

The first three coordinates, and their time derivatives, correspond to the position and translational velocity along the  $x$ ,  $y$  and  $z$  axes, while the other three coordinates and their time derivatives are used to describe orientation and angular velocity. The Society of Naval Architects and Marine Engineers (SNAME) has standardized the names and symbols of these motion components as surge, sway, heave, roll, pitch and yaw (see Figure 3.1 and Table 3.1).

### 3.1 Reference Frames

The motion variable of the vessels are usually expressed globally into two earth-centered reference frames and locally into two geographical reference frames.

#### Earth-Centered Reference Frames

**ECI:** The Earth-Centered Inertial (ECI) frame  $i = (x_i, y_i, z_i)$  is an inertial frame in which bodies, whose net force acting upon them is zero, are not accelerated and

Newton's laws of motion can be applied. The origin of  $\{i\}$  is located at the center  $o_i$  of the Earth.

**ECCF:** The Earth-centered Earth-fixed (ECEF) reference frame  $\{e\} = (x_e, y_e, z_e)$  has its origin  $o_e$  fixed to the center of the earth but the axes rotate relative to the inertial frame ECI, which is fixed in space, at the angular rate of rotation of the earth. For vessels moving at relatively low speed, the Earth rotation can be neglected and hence  $\{e\}$  can be considered to be inertial.

### Geographic Reference Frames

**NED:** The North-East-Down (NED) coordinate system  $\{n\} = (x_n, y_n, z_n)$  with origin  $o_n$  is defined as the tangent plane on the surface of the earth moving with the vessel, but with axes pointing in different directions than the body-fixed axes of the vessel. For this system the  $x$ -axis points towards true north, the  $y$ -axis points towards east while the  $z$ -axis points downwards normal to the earth's surface. This frame is fixed to earth and the location of  $\{n\}$  relative to  $\{e\}$  is determined by using two angles  $l$  and  $\mu$  denoting the longitude and latitude, respectively.

This reference is valid for vessels operating in a local area where the longitude and latitude are approximately constant. The navigation space is assumed to be an earth fixed tangent plane on the surface of the earth. This is called flat earth navigation and is assumed to be inertial where Newton's laws still apply. The

**Table 3.1:** The SNAME notations for marine vessels[57]

DOF	Forces and moments	Linear and angular velocities	Positions and Euler angles
motions in the $x$ direction (surge)	$X$	$u$	$x$
motions in the $y$ direction (sway)	$Y$	$v$	$y$
motions in the $z$ direction (heave)	$Z$	$w$	$z$
rotation about the $x$ axis (roll, heel)	$K$	$p$	$\phi$
rotation about the $y$ axis (pitch, trim)	$M$	$q$	$\theta$
rotation about the $z$ axis (yaw)	$N$	$r$	$\psi$

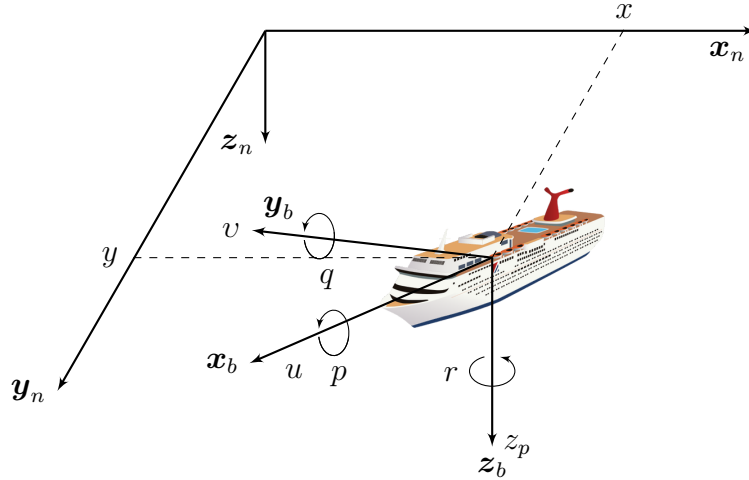


**Figure 3.2:** Earth-fixed  $(x_n, y_n, z_n)$  and body-fixed  $(x_b, y_b, z_b)$  frames.

position and orientation of the vessel are expressed relative to it.

**Body-fixed Reference Frame:** The body-fixed reference frame  $\{b\} = (x_b, y_b, z_b)$  with origin  $o_b$  is fixed on the vessel and is moving with it. It is used to express the linear and angular velocities of the vessel. The origin  $o_b$  is usually chosen to coincide with a point midships in the water line named  $CO$  or geometric center point. The body axes  $x_b$ ,  $y_b$  and  $z_b$  are chosen to coincide with the principal axes of inertia, and they are usually defined as (see Figure 3.2):

- $x_b$  - longitudinal axis (directed from aft to fore).
- $y_b$  - transversal axis (directed to starboard).
- $z_b$  - normal axis (directed from top to bottom).

## 3.2 Rigid-body Kinematics

The rigid-body dynamics can be divided into two parts: the kinematics which treats only geometrical aspects of the motion and the kinetics which is the analysis of the forces causing the motion. Although the motion of the vessels are expressed in 6-DOF, the motion variables can be simplified in just 3-DOF under the following assumptions[58]:



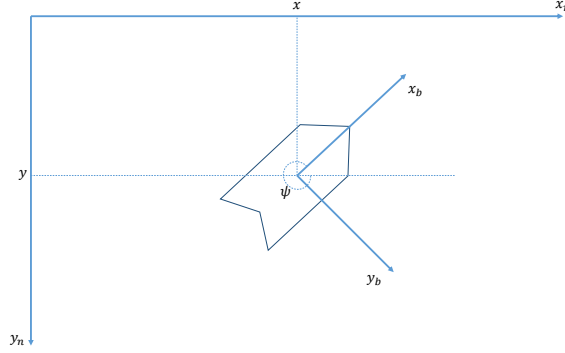


**Figure 3.3:** Horizontal Plane Coordinates

**Assumption 3.1.** *The ship is longitudinally and laterally metacentrically stable with small amplitudes  $\phi = \theta = \dot{\phi} = \dot{\theta} \approx 0$*

**Assumption 3.2.** *The ship is floating with  $z \approx 0$ .*

These assumptions are valid and lead to acceptable results when the focus is on the horizontal motion of the ship [11]. Based on the aforementioned assumptions, the dynamics of the roll, pitch and heave can be ignored and the resulting model can be used for the purpose of the maneuvering in the horizontal plane as shown in Figure 3.3. This model is called the 3-DOF maneuvering model and will be used in this thesis. The states of the model can be chosen to be  $\boldsymbol{\eta} = [x, y, \psi]^T$  expressed in the NED frame and  $\boldsymbol{v} = [u, v, r]^T$ . The 3-DOF kinematics relates the earth-fixed velocity vector (measured w.r.t NED frame) to the body-fixed velocity vector (measured w.r.t body-fixed frame) as follows:

$$\dot{\boldsymbol{\eta}} = R(\psi)\boldsymbol{v} \quad (3.1)$$

where

$$R(\psi) = \begin{bmatrix} \cos(\psi) & -\sin(\psi) & 0 \\ \sin(\psi) & \cos(\psi) & 0 \\ 0 & 0 & 1 \end{bmatrix}$$

is the 3-DOF horizontal rotation matrix[11]. It has the properties that  $R(\psi)^T R(\psi) = I$  for all  $\psi$ .

### 3.3 Rigid-body Kinetics

The kinetics of the rigid body are equations that describe the effect of the forces causing the motion which acts on the vessel Center of Gravity (CG). The CG point will be located at a distance  $x_g$  along the  $x_b$ -axis of the body reference frame  $\{b\}$  under the following assumption:

**Assumption 3.3.** *The ship is port-starboard symmetric.*

By Newton's second law, it can easily shown that the horizontal motion of a rigid body takes the form[59]:

$$M_{RB}\dot{\mathbf{v}} + C_{RB}(\mathbf{v})\mathbf{v} = \boldsymbol{\tau}_{RB} \quad (3.2)$$

where

$$M_{RB} = \begin{bmatrix} m & 0 & 0 \\ 0 & m & mx_g \\ 0 & mx_g & I_z \end{bmatrix}$$

is the rigid-body inertial matrix,  $m$  is the mass of the ship,  $I_z$  is the moment of inertia about the  $z_b$ -axis, the Coriolis matrix is represented as[60]:

$$C_{RB}(\mathbf{v}) = \begin{bmatrix} 0 & 0 & -m(x_g r + v) \\ 0 & 0 & mu \\ m(x_g r + v) & -mu & 0 \end{bmatrix},$$

and  $\boldsymbol{\tau}_{RB}$  is the forces and moment vector, and is defined by:

$$\boldsymbol{\tau}_{RB} = \boldsymbol{\tau} + \boldsymbol{\tau}_H + \mathbf{w}(t) \quad (3.3)$$

where  $\boldsymbol{\tau} = [\tau_u \ \tau_v \ \tau_r]^T$  is the actuator forces and moment in the surge, sway and yaw,  $\boldsymbol{\tau}_H$  accounts for the hydrodynamic effect, and  $\mathbf{w}(t)$  is the exogenous disturbances due to, for instance, waves and wind forces[61].

### 3.4 Hydrodynamic Forces and Moments

The Hydrodynamic forces and moment, represented by  $\boldsymbol{\tau}_H$ , are due to added mass, radiation-induced potential damping and some other hydrodynamic phenomena that are not yet fully understood[58]. They depend on the relative velocity between the ship hull and the fluid which is defined in [58], under the assumption of nonrotational fluid, as:

$$\boldsymbol{v}_r := \boldsymbol{v} - \boldsymbol{v}_c = [u_r, v_r, r]^T \quad (3.4)$$

where  $\boldsymbol{v}_c := R(\psi)^T \boldsymbol{v}_c$  is the current velocity w.r.t. the body reference frame,

$$\boldsymbol{v}_c := \begin{bmatrix} V_c \cos(\beta_c) \\ V_c \sin(\beta_c) \\ 0 \end{bmatrix} \quad (3.5)$$

is the current velocity w.r.t. the earth fixed frame, and  $V_c$  and  $\beta_c$  are the current speed and angle. According to that, the hydrodynamic effect is modeled as[62]:

$$\boldsymbol{\tau}_H = -M_A \dot{\boldsymbol{v}}_r - C_A(\boldsymbol{v}_r) \boldsymbol{v}_r - d(\boldsymbol{v}_r) \quad (3.6)$$

where  $M_A$  is the added mass matrix,  $C_A(\boldsymbol{v}_r)$  accounts for added Coriolis and centripetal terms, and  $d(\boldsymbol{v}_r)$  sums up the damping effect. Following the notation of SNAME (1950)[57],  $M_A$  can be represented as:

$$M_A = \begin{bmatrix} X_{\dot{u}} & 0 & 0 \\ 0 & -Y_{\dot{v}} & -Y_{\dot{r}} \\ 0 & -N_{\dot{v}} & -N_{\dot{r}} \end{bmatrix} \quad (3.7)$$

where assumption 3.3 is still applied and its elements are called hydrodynamic derivatives; for instance the hydrodynamic added mass moment  $N$  around the  $z$ -axis due to an acceleration  $\dot{v}$  in the  $y$  direction is written as:

$$N = -N_{\dot{v}} \dot{v}, \quad N_{\dot{v}} := \frac{\partial N}{\partial \dot{v}}. \quad (3.8)$$

$C_A(\mathbf{v}_r)$  can be computed using Theorem 3.2 in [60] if the  $M_A$  is symmetric which is not the case. Therefore, the added mass kinetic energy is modified as:

$$T_A = \frac{1}{2} \mathbf{v}_r^T M_A \mathbf{v}_r = \frac{1}{4} \mathbf{v}_r^T (M_A + M_A^T) \mathbf{v}_r = \frac{1}{2} \mathbf{v}_r^T \bar{M}_A \mathbf{v}_r$$

where  $\bar{M}_A = \frac{1}{2}(M_A + M_A^T) = \bar{M}_A^T$  is the symmetric equivalent of  $M_A$  which can be used to derive  $C_A(\mathbf{v}_r)$  from Theorem 3.2 in [60] which gives[58]:

$$C_A(\mathbf{v}_r) = \begin{bmatrix} 0 & 0 & Y_{\dot{v}} \mathbf{v}_r + \frac{1}{2}(N_{\dot{v}} + Y_{\dot{r}})r \\ 0 & 0 & -X_{\dot{u}} u_r \\ -Y_{\dot{v}} \mathbf{v}_r - \frac{1}{2}(N_{\dot{v}} + Y_{\dot{r}})r & X_{\dot{u}} u_r & 0 \end{bmatrix}. \quad (3.9)$$

The damping vector  $d(\mathbf{v}_r)$  is the most uncertain component of the hydrodynamic forces and moment and has many representations in the literature.

**Odd Functions:** Abkowitz proposed a truncated Taylor series for  $d(\mathbf{v}_r)$  [63]. Since, in general,  $d(\mathbf{v}_r)$  is dissipative for both positive and negative relative velocities, it must be an odd function and hence, only odd terms in the Taylor expansion are required. Using first and third order terms only:

$$\begin{aligned} d(\mathbf{v}_r) &= \begin{bmatrix} X_D(\mathbf{v}_r) \\ Y_D(\mathbf{v}_r) \\ N_D(\mathbf{v}_r) \end{bmatrix} \\ &= \begin{bmatrix} -X_u u_r - X_{uuu} u_r^3 \\ -Y_v v_r - Y_r r - Y_{vvv} v_r^3 - Y_{vvr} v_r^2 r - Y_{vrr} v_r r^2 - Y_{rrr} r^3 \\ -N_v v_r - N_r r - N_{vvv} v_r^3 - N_{vvr} v_r^2 r - N_{vrr} v_r r^2 - N_{rrr} r^3 \end{bmatrix} \end{aligned} \quad (3.10)$$

**Modulus Functions:** In [64] and [65] gave another representation using a second order modulus function as follows:

$$\begin{aligned} d(\mathbf{v}_r) &= \begin{bmatrix} X_D(\mathbf{v}_r) \\ Y_D(\mathbf{v}_r) \\ N_D(\mathbf{v}_r) \end{bmatrix} \\ &= \begin{bmatrix} -X_u u_r - X_{|u|} |u_r| u_r \\ -Y_v v_r - Y_r r - Y_{|v|v} |v_r| v_r - Y_{|v|r} |v_r| r - Y_{|r|v} |r| v_r - Y_{|r|r} |r| r \\ -N_v v_r - N_r r - Y_{|v|v} |v_r| v_r - N_{|v|r} |v_r| r - N_{|r|v} |r| v_r - N_{|r|r} |r| r \end{bmatrix} \end{aligned} \quad (3.11)$$

The parameters of (3.10) and 3.11 are usually identified experimentally via system identification techniques . During the identification experiment, the hydrodynamic model can be changed for another one that best fit the experimental data. It is common to separate the linear and nonlinear terms of  $d(\mathbf{v}_r)$  as:

$$d(\mathbf{v}_r) = D_L \mathbf{v}_r + D_{NL}(\mathbf{v}_r) \mathbf{v}_r \quad (3.12)$$

where the linear term is defined by

$$D_L = \begin{bmatrix} -X_u & 0 & 0 \\ 0 & -X_v & -Y_r \\ 0r & -N_v & -N_r \end{bmatrix}, \quad (3.13)$$

the nonlinear term for the truncated Taylor series is defined by

$$D_{NL}(\mathbf{v}_r) = \begin{bmatrix} -X_{uuu}u_r^2 & 0 & 0 \\ 0 & -Y_{vvv}v_r^2 - Y_{vrr}r^2 & -Y_{vvr}v_r^2 - Y_{rrr}r^2 \\ 0 & -N_{vvv}v_r^2 - N_{vrr}r^2 & -N_{vvr}v_r^2 - N_{rrr}r^2 \end{bmatrix}, \quad (3.14)$$

and the nonlinear term for second order modulus function is defined by

$$D_{NL}(\mathbf{v}_r) = \begin{bmatrix} -X_{|u|} |u_r| & 0 & 0 \\ 0 & -Y_{|v|} |v_r| - Y_{|r|} |r| & -Y_{|v|r} |v_r| - Y_{|r|r} |r| \\ 0 & -N_{|r|} |r| - Y_{|v|} |v_r| & -N_{|v|r} |v_r| - N_{|r|r} |r| \end{bmatrix} \quad (3.15)$$

According to the aforementioned description the model of the surface vessel 3.2 becomes:

$$M_{RB} \dot{\mathbf{v}} + M_A \dot{\mathbf{v}}_r + C_{RB}(\mathbf{v}) \mathbf{v} + C_A(\mathbf{v}_r) \mathbf{v}_r + D_L \mathbf{v}_r + D_{NL}(\mathbf{v}_r) \mathbf{v}_r = \boldsymbol{\tau} + \mathbf{w}(t) \quad (3.16)$$

### 3.5 Actuator Forces

The forces and moment vector  $\boldsymbol{\tau} \in R^3$  are generated by a set of actuators. In the 3-DOF, each  $i^{th}$  actuator generates forces  $\mathbf{F}_i = [F_{x,i} F_{y,i}]^T \in R^2$  and the position of the actuator w.r.t the body frame denotes by  $(l_{x,i}, l_{y,i})$ , determines the corresponding moment. The most common actuators for surface vessels are:

- **Main propellers:** The main propellers of the craft are mounted aft of the hull. It produces a thrust force in the surge direction defined by[58]:

$$\mathbf{F}_i = \begin{bmatrix} T_{|n_i|n_i}|n_i|n_i - T_{|n_i|u}|n_i|u_r \\ 0 \end{bmatrix} \quad (3.17)$$

where  $n_i$  is the revolutions per second of the propeller, and  $T_{|n_i|n_i}$  and  $T_{|n_i|u}$  can be assumed to be constant parameters function of the blades diameter  $d_i$ .

- **Aft Rudders:** Rudders are the primary steering device for conventional vessels. They are usually located aft of the vessel, usually in conjunction with the main propeller and usually take the same index. They produce mainly a lift force  $F_{y,i}$  in the sway direction and a small drag force  $F_{x,i}$  in the surge direction, which is negligible for control system analysis. The generated forces are:

$$\mathbf{F}_i = \begin{bmatrix} -D_{|\delta_i|}|\delta_i||u_{rud,i}|u_{rud,i} \\ L_{\delta_i}\delta_i - L_{|\delta_i|\delta_i}|\delta_i||u_{rud,i}|u_{rud,i} \end{bmatrix} \approx \begin{bmatrix} 0 \\ L_{\delta_i}\delta_i - L_{|\delta_i|\delta_i}|\delta_i||u_{rud,i}|u_{rud,i} \end{bmatrix} \quad (3.18)$$

where  $L_{\delta_i}$ ,  $L_{|\delta_i|\delta_i}$  and  $D_{|\delta_i|}$  are constant parameters, and  $u_{rud,i}$  is the relative velocity of the fluid at the rudder surface which is different than  $u_r$  if the rudder is installed in front of the propeller and is modeled as a function by:

$$u_{rud,i} = u_r + k_u \left( \sqrt{\max\{0, \frac{8}{\pi\rho d_i^2}F_{x,i} + u_r^2\}} - u_r \right)$$

where  $k_u \approx 0.5$  when the rudder is close to the propeller.

- **Control surfaces:** Control surfaces are similar to the rudder but usually placed at different locations to produce lift and drag forces. For 3-DOF models, they are modeled similar to the rudders by (3.18) with  $u_{rud,i} = u_r$ .
- **Azimuth thrusters:** Azimuth thrusters are rotatable thrusters that can produce two force components as a function of the thruster revolution per

second  $n_i$  and rotation angle  $\alpha_i$ :

$$\mathbf{F}_i = \begin{bmatrix} [T_{|n_i|n_i}|n_i|n_i - T_{|n_i|u}|n_i|u_r] \cos(\alpha_i) \\ [T_{|n_i|n_i}|n_i|n_i - T_{|n_i|u}|n_i|u_r] \sin(\alpha_i) \end{bmatrix} \quad (3.19)$$

Suppose a virtual generic vessel that has two thrusters in conjunction with two rudders (indexed together by 1,2) and two azimuth thruster(indexed by 3,4). The actuator forces are related to control forces and moment  $\boldsymbol{\tau}$  by

$$\boldsymbol{\tau} = B f_a(u_r, n, \delta, \alpha) \quad (3.20)$$

where  $n = [n_1, n_2, n_3, n_4]^T, \delta = [\delta_1, \delta_2]^T, \alpha = [\alpha_3, \alpha_4]^T$ ,  $f_a(u_r, n, \delta, \alpha) = [F_{x,1}, F_{x,2}, F_{x,3}, F_{x,4}, F_{y,1}, F_{y,2}, F_{y,3}, F_{y,4}]^T \in R^8$ , and

$$B = \begin{bmatrix} 1 & 1 & 1 & 1 & 0 & 0 & 0 & 0 \\ 0 & 0 & 0 & 0 & 1 & 1 & 1 & 1 \\ l_{y,1} & l_{y,2} & -l_{y,3} & l_{y,4} & l_{x,1} & l_{x,2} & l_{x,3} & l_{x,4} \end{bmatrix} \in R^{3 \times 8} \quad (3.21)$$

is the actuator configuration matrix.

### 3.6 Environmental Forces

The vessel is affected by environmental disturbances represented by the vector  $\mathbf{w}(t)$ . These external environmental forces is mainly due to the wind and waves. The currents can be considered as an external disturbance if the relative velocity between the hull and the fluid  $\mathbf{v}_r$  is omitted for simplification and  $\mathbf{v}$  is used instead. It is common to assume the principle of superposition when considering wind and wave disturbances and therefore:

$$\mathbf{w}(t) := \boldsymbol{\tau}_{wind} + \boldsymbol{\tau}_{wave}. \quad (3.22)$$

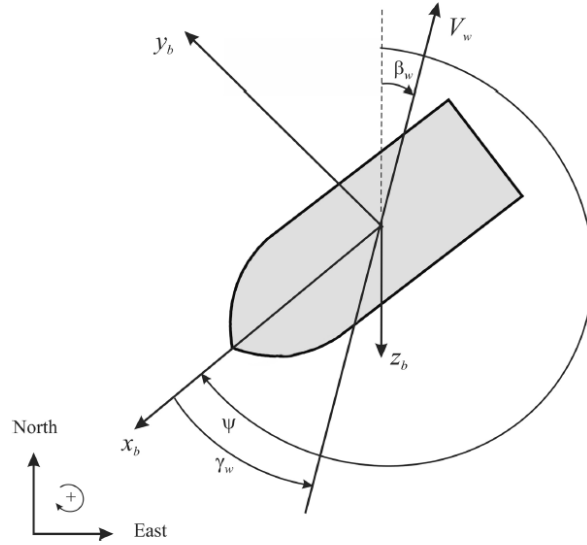


**Figure 3.4:** Wind speed  $V_w$ , wind direction  $\beta_w$  and wind angle of attack  $\gamma_w$  relative to the bow[11].

### 3.6.1 Wind Forces

Let  $V_w$ ,  $\beta_w$  and  $\gamma_w$  denote the wind speed, wind direction and angle of attack, respectively (see Figure 3.4). The 3-DOF wind forces and moment acting on a marine craft are computed as[11]:

$$\boldsymbol{\tau}_{wind} = \frac{1}{2} \rho_a V_{rw}^2 \begin{bmatrix} C_X(\gamma_{rw}) A_{Fw} \\ C_Y(\gamma_{rw}) A_{Lw} \\ C_N(\gamma_{rw}) A_{Lw} L_{oa} \end{bmatrix} \quad (3.23)$$

where  $\rho_a$  is the air density,  $L_{oa}$  is the over all length of the ship,  $A_{Fw}$  and  $A_{Lw}$  are the frontal and lateral projected areas above the water line, respectively,  $C_X(\gamma_w)$ ,  $C_Y(\gamma_w)$ , and  $C_N(\gamma_w)$  are the wind coefficients which can be obtained experimentally,

$$V_{rw} = \sqrt{u_{rw}^2 + v_{rw}^2} \quad (3.24)$$

is the relative wind speed,

$$\gamma_{rw} = -atan2(v_{rw}, u_{rw}) \quad (3.25)$$



is the relative angle of attack. The relative velocity components are:

$$u_{rw} = u - u_w \quad (3.26)$$

$$v_{rw} = v - v_w \quad (3.27)$$

while the components of  $V_w$  in the earth fixed frame are:

$$u_w = V_w \cos(\beta_w - \psi) \quad (3.28)$$

$$v_w = V_w \sin(\beta_w - \psi) \quad (3.29)$$

Since only the mean wind forces and moments can be compensated by the vessel actuators, the wind speed measurement should be filtered via a low-pass filter before using it as a feed forward signal for the controller.

### 3.6.2 Wave-induced Forces

The wave-induced forces can be modeled as two components:

**First-order wave-induced forces:** Wave-Frequency (WF) motion observed as zero-mean oscillatory motions.

**Second-order wave-induced forces:** Wave drift forces observed as nonzero slowly varying components.

The waves forces and moments will be the sum of both as follows:

$$\boldsymbol{\tau}_{wave} = \boldsymbol{\tau}_{wave1} + \boldsymbol{\tau}_{wave2} \quad (3.30)$$

It is common to design a cascaded notch and low-pass filter to remove the oscillatory effect of First-order wave-induced forces, and employ an integral action to counteract the Second-order wave-induced forces. There are three main approaches for modeling the wave forces:

- Force Response Amplitude Operators (RAOs).
- Motion RAOs

- Linear state-space models (WF models)

Response amplitude operators methods require that the RAO tables are computed using a hydrodynamic program since the wave forces depend on the geometry of the craft. These two methods will be skipped in this thesis and more details can be found in [11]. The following lines describe the linear state-space models which are of a great interest due to its simplicity.

It is preferred for control application to approximate the wave response model with linear models. The wave model is chosen, for each degree of freedom, to be a second order transfer function with an oscillating frequency  $\omega_{0i}$ , damping factor  $\lambda_i$  and a constant gain  $k_{wi}$  as:

$$h(s) = \frac{k_{wi}s}{s^2 + 2\lambda_i\omega_{0i}s + \omega_{0i}^2} \quad (3.31)$$

where  $i = \{1, 2, 3\}$ . It is convenient to define the gain according to:

$$k_{wi} = 2\lambda_i\omega_{0i}\sigma_i \quad (3.32)$$

where  $\sigma_i$  is a constant describing the wave intensity. A linear state-space model can be obtained by defining  $\dot{x}_{w1} = x_{w2} \in R^3$  and  $x_{w2} = y_w \in R^3$  as state variables. This implies that the state-space model, for the 3-DOF, can be written as:

$$\dot{\mathbf{x}}_w = A_w \mathbf{x}_w + E_w \mathbf{w}_w \quad (3.33)$$

$$y_w = C_w^T \mathbf{x}_w \quad (3.34)$$

where  $\mathbf{w}_w \in R^3$  is a vector of zero-mean white noise. Expanding this equation yields:

$$\begin{bmatrix} \dot{\mathbf{x}}_{w1} \\ \dot{\mathbf{x}}_{w2} \end{bmatrix} = \begin{bmatrix} 0 & I \\ A_{w21} & A_{w22} \end{bmatrix} \begin{bmatrix} \mathbf{x}_{w1} \\ \mathbf{x}_{w2} \end{bmatrix} + \begin{bmatrix} 0 \\ E_{w2} \end{bmatrix} \mathbf{w}_w \quad (3.35)$$

$$y_w = \begin{bmatrix} 0 & I \end{bmatrix} \begin{bmatrix} \mathbf{x}_{w1} \\ \mathbf{x}_{w2} \end{bmatrix} \quad (3.36)$$

where  $A_{w21} = -diag\{\omega_{01}^2, \omega_{02}^2, \omega_{03}^2\}$ ,  $A_{w22} = -diag\{2\lambda_1\omega_{01}\sigma_1, 2\lambda_2\omega_{02}\sigma_2, 2\lambda_3\omega_{03}\sigma_3\}$ , and  $E_{w2} = diag\{k_{w1}, k_{w2}, k_{w3}\}$ . Based on that, the wave forces and moments can be expressed as[59]:

$$\boldsymbol{\tau}_{wave} = \boldsymbol{y}_w + \boldsymbol{d} \quad (3.37)$$

where  $\boldsymbol{d} \in R^3$  is the wave drift forces which are usually modeled as slowly-time varying bias terms (Wiener processes).

### 3.7 Simplification

The nonlinear model 3.16 is complex for the control objective due to the dependency on  $\boldsymbol{v}_c$  which must be measured or estimated. In [66],  $\boldsymbol{v}$  is only used as a velocity state and the effect of ocean current dynamics, in addition to other slowly varying disturbances and nonlinear hydrodynamics[56], are captured by a slowly time varying bias  $\boldsymbol{b}$  in the earth frame. This gives the following simplified model:

$$M\dot{\boldsymbol{v}} + C(\boldsymbol{v})\boldsymbol{v} + D\boldsymbol{v} = \boldsymbol{\tau} + R(\psi)^T\boldsymbol{b} + \boldsymbol{w}(t) \quad (3.38)$$

where  $M := M_{RB} + M_A$ ,  $C(\boldsymbol{v}) := C_{RB}(\boldsymbol{v}) + C_A(\boldsymbol{v})$ , and  $D(\boldsymbol{v}) := D_L + D_{NL}(\boldsymbol{v})$ . Most ships have port/starboard symmetry but fore/aft nonsymmetry. This nonsymmetry leads to the nonzero off-diagonal terms in the inertia and damping matrices. However, these terms are small compared to the main diagonal terms [56]. Therefore, the diagonally simplified matrices will be:

$$\begin{aligned} M &= \begin{bmatrix} m_{11} & 0 & 0 \\ 0 & m_{22} & 0 \\ 0 & 0 & m_{33} \end{bmatrix}, D = \begin{bmatrix} d_{11} & 0 & 0 \\ 0 & d_{22} & 0 \\ 0 & 0 & d_{33} \end{bmatrix} \\ C(\boldsymbol{v}) &= \begin{bmatrix} 0 & 0 & -m_{22}v \\ 0 & 0 & m_{11}u \\ m_{22}v & -m_{11}u & 0 \end{bmatrix} \end{aligned} \quad (3.39)$$

with

$$\begin{aligned} m_{11} &= m - X_{\dot{u}}, m_{22} = m - Y_{\dot{v}}, m_{33} = I_z - N_{\dot{r}} \\ d_{11} &= -X_u, d_{22} = -Y_v, d_{33} = -N_r \end{aligned}$$

The system 3.38 with the kinematic 3.1 can be represented in the state space model, the desirable representation for control systems, as follows:

$$\dot{\mathbf{x}} = \mathcal{F}(\mathbf{x}) + g\mathbf{u} + g_b(\mathbf{x})\mathbf{b} + \boldsymbol{\omega} \quad (3.40)$$

Here,  $\mathbf{x} = [\boldsymbol{\eta} \ \mathbf{v}]^T$ ,  $\mathbf{u} = \boldsymbol{\tau}$ ,  $\mathcal{F}(\mathbf{x}) = \begin{bmatrix} R(\psi)\mathbf{v} \\ -M^{-1}\{C(\mathbf{v})\mathbf{v} + D\mathbf{v}\} \end{bmatrix}$ ,  $g = \begin{bmatrix} \mathbf{0} \\ M^{-1} \end{bmatrix}$ , and  $g_b(\mathbf{x}) = \begin{bmatrix} \mathbf{0} \\ M^{-1}R(\psi)^T \end{bmatrix}^T$ .

If the ship is equipped only with two aft thruster, the sway force will be zero and the dynamics (3.40) can be rewritten as:

$$\dot{\mathbf{x}} = \mathcal{F}(\mathbf{x}) + g\mathbf{u} + g_b(\mathbf{x})\mathbf{b} + \boldsymbol{\omega} \quad (3.41)$$

Here,  $\mathbf{x} = [\boldsymbol{\eta} \ \mathbf{v}]^T \in \mathbb{R}^6$ ,  $\mathbf{u} = \Gamma_{23}\boldsymbol{\tau} = [\tau_u \ \tau_r]^T \in \mathbb{R}^2$ ,  $\mathcal{F}(\mathbf{x}) = \begin{bmatrix} R(\psi)\mathbf{v} \\ -M^{-1}\{C(\mathbf{v})\mathbf{v} + D\mathbf{v}\} \end{bmatrix} \in \mathbb{R}^6$ ,  $g = \begin{bmatrix} \mathbf{0} \\ M^{-1}\Gamma_{23}^T \end{bmatrix} \in \mathbb{R}^6 \times \mathbb{R}^2$ ,  $g_b(\mathbf{x}) = \begin{bmatrix} \mathbf{0} \\ M^{-1}R(\psi)^T \end{bmatrix}^T \in \mathbb{R}^6 \times \mathbb{R}^3$ , and  $\Gamma_{23} = \begin{bmatrix} 1 & 0 & 0 \\ 0 & 0 & 1 \end{bmatrix}$

This simplification can not be used except if the the controller or the collision avoidance system has a disturbance estimation component to estimate the unmeasured value of  $\mathbf{b}$  in (3.40) or (3.41). Otherwise, the prediction model will lead to large tracking offset as shown in Chapter 6.

# 4

## Nonlinear Model Predictive Control

### 4.1 Introduction

Model Predictive Control (MPC), also known as Receding Horizon Control and Moving Horizon Optimal Control, has roots in optimal control. It has been widely adopted in industry as an effective mean to deal with multivariable constrained control problems. It was first presented in [67] but, due to lack of sufficiently fast computers, was first developed in the late 1970s at the Shell Oil Company for chemical processes[68]. At this time MPC has been used for linear system, with quadratic cost and linear constraints, as the algorithms were fast enough for the slow dynamics of the chemical systems[69]. It started to gain a huge scientific interest in the 1980s after the papers on Dynamic Matrix Control (DMC)[70, 71], and the first comprehensive exposition of Generalized Predictive Control (GPC) [72, 73].

The basic concept of MPC is to use a dynamic model of the system to forecast its behavior, and optimize the forecast to produce the best decision — the control move at the current time (see Figure 4.1). The term Model Predictive Control (MPC) describes a class of computer control algorithms that control the future predicted output of a system through the use of an explicit system model. This is

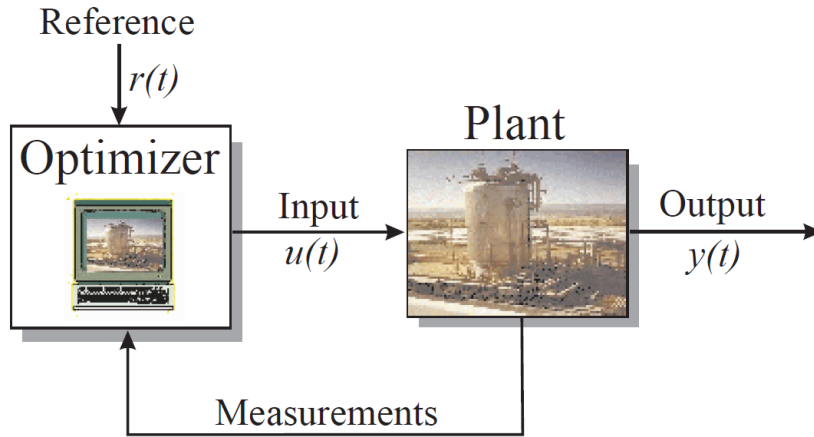


**Figure 4.1:** Basic structure of Model Predictive Control.

achieved by employing the prediction to formulate and solve a dynamic optimization problem online where tracking error, namely the difference between the predicted output and the desired reference, is minimized over a future horizon, possibly subject to constraints on the control inputs (manipulated variable) and the outputs. This optimization problem is solved in discrete control interval suitable for the system dynamics. At each control interval the MPC algorithm computes an open-loop sequence of control inputs adjustments. The first input in the optimal sequence is injected into the system, and the entire optimization is repeated at subsequent control intervals.

The basic concept of MPC is to use a dynamic model of the system to forecast its behavior, and optimize the forecast to produce the best decision — the control move at the current time (see Figure 4.1). The term Model Predictive Control (MPC) describes a class of computer control algorithms that control the future predicted output of a system through the use of an explicit system model.

## 4.2 NMPC Formulation

Consider a general continuous time-invariant nonlinear state space model of the system under control in the form of:

$$\dot{\mathbf{x}}(t) = f(\mathbf{x}, \mathbf{u}) \quad (4.1)$$

subject to the constraints:

$$\begin{aligned} \mathbf{x}(t) &\in \mathbb{X} \subseteq \mathbb{R}^n, \\ \mathbf{u}(t) &\in \mathbb{U} \subseteq \mathbb{R}^m, \end{aligned} \quad (4.2)$$

where  $\mathbf{x} \in \mathbb{R}^n$  is the state vector;  $\mathbf{u} \in \mathbb{R}^m$  is the control vector;  $f(\cdot, \cdot)$  is continuous,  $\mathbb{X} \subseteq \mathbb{R}^n$  and  $\mathbb{U} \subseteq \mathbb{R}^m$  define the allowable state and control set respectively. The best closed loop performance is obtained from the solution of the following infinite horizon Optimal Control Problem (OCP)[74]:

$$\begin{aligned} \text{OCP}_\infty : \min_{\mathbf{u}(\cdot)} V_\infty(\mathbf{x}, \mathbf{u}(\cdot)) &= \int_{\tau=0}^{\infty} \ell(\mathbf{x}(\tau), \mathbf{u}(\tau)) d\tau \\ \text{subject to :} & \\ \dot{\mathbf{x}}(t) &= f(\mathbf{x}, \mathbf{u}) \text{ with } \mathbf{x}(0) = \mathbf{x}_0 \\ \mathbf{x}(t) &\in \mathbb{X}, \\ \mathbf{u}(t) &\in \mathbb{U}, \forall t \in [0, \infty) \end{aligned}$$

The goal of the controller is to steer the states of the system to a constant reference  $\mathbf{x}^{ref} \equiv \mathbf{x}_* \in \mathbb{X}$ . A necessary condition to find a feedback law that stabilizes the system at  $\mathbf{x}_*$  is that there exists a control value  $\mathbf{u}_* \in \mathbb{U}$  such that:

$$\mathbf{x}_* = f(\mathbf{x}_*, \mathbf{u}_*) \quad (4.3)$$

We can assume that  $\mathbf{x}_* = 0$  and  $\mathbf{u}_* = 0$  without loss of generality: if it is not the case we can replace  $f(\mathbf{x}, \mathbf{u})$  by  $f(\mathbf{x} + \mathbf{x}_*, \mathbf{u} + \mathbf{u}_*) - \mathbf{x}_*$ . We denote the solution of the problem  $\text{OCP}_\infty$  and the optimal value function by  $V_\infty^*(\mathbf{x})$  and  $\mathbf{u}_\infty^*(\cdot, \mathbf{x})$ , respectively. The evolution of the closed loop system is given by:

$$\dot{\mathbf{x}}(t) = f(\mathbf{x}, \mathbf{u}_\infty^*(t, \mathbf{x})) \quad (4.4)$$

Although the control law  $\mathbf{u}_\infty^*(t, \mathbf{x})$  provides excellent closed-loop properties, it is impractical to be used due to the following reasons[75]:

- A feedback control, rather than an open-loop, is usually necessary because of uncertainty.
- Solution of the optimal control problem  $\text{OCP}_\infty$  yields the optimal control  $\mathbf{u}_\infty^*(0, \mathbf{x})$  for the state  $\mathbf{x}$  but does not provide a control law.
- Difficulty to use dynamic programming for relatively large state dimension or long horizons.

Even if we accept optimizing only for the currently measured value of  $\mathbf{x}$ , the problem remains formidable because of intractable optimization over a semi-infinite interval  $[0, \infty)$  and in infinite dimensional optimization over a time function  $\mathbf{u}(\cdot)$  which stays difficult for the finite-horizon case. The above formulation could be characterized using *indirect methods* like calculus of variations, Pontryagin's maximum principle [76] and dynamic programming [77]. This characterizations could only be used to analytic exact representation of the solution for very limited special cases[75].

In order to avoid the aforementioned issues which hinder utilizing model predictive control, finite horizon optimal control formulation is presented instead with the aid of the so-called *direct methods* for problem characterizations. They are characterized by discretization and finite parameterization being introduced in the optimal control problem formulation which is then directly solved with numerical methods. In order to reformulate the problem into a finite-dimensional and practical setting, we will make the following assumptions that will allow the integral and differentiation operators to be approximated by numerical integration methods.

- The optimization problem will be solved only for the currently measured or estimated value of the states  $\mathbf{x}_{t_k}$ .
- The prediction horizon is finite of a given value  $T_p$ .



- The input signal  $\mathbf{u}(\cdot)$  is assumed to be piecewise constant over the horizon  $T_p$  with a regular sampling interval  $T_s$  such that  $T_p$  is an integer multiple of  $T_s$  (i.e.  $T_p = NT_s$ ), and is characterized by a sequence  $\mathbf{U}_N = \text{col}(U_0, \dots, U_{N-1}) \in \mathbb{R}^{mN}$  such that  $\mathbf{u}(t) = \mu(t, \mathbf{U}_N) = U_k$  for  $t_k \leq t < t_{k+1}$ .
- An approximate solution to the ordinary differential equation(4.1) is assumed to be available for the current initial condition in the form of  $\mathbf{x}(t) = \phi(t, \mathbf{U}_N, \mathbf{x}(t_k))$  at the discrete time instants  $T_d = \{t_{k+1}, t_{k+2}, \dots, t_{k+N} = T_p\}$ .
- The infinite number of control and state constraints are converted to a finite number and evaluated only at the discrete time instants  $T_d$ .

**Remark:** In general, it is not necessary for the time instants  $T_d$  to coincide with sampling instants used for the characterization and parametrization of the control input, but in this thesis it is assumed so.

**Remark:** A simulation of the ODEs embedded in the function  $\phi(\cdot)$  may incorporate additional intermediate time-steps not included in  $T_d$ .

Details about practical reformulation and discretization of the problem will be described in section 4.6 while the problem will be kept in its continuous form. Based on that, the NMPC regulation problem (or setpoint stabilization) can be achieved by repeatedly solving the following OCP[74]:

$$\begin{aligned} \text{OCP}_{T_p} : \min_{\mathbf{u}(\cdot)} V_{T_p}(\mathbf{x}_{t_k}, \mathbf{u}(\cdot)) &= \int_{\tau=t_k}^{t_k+T_p} \ell(\mathbf{x}(\tau), \mathbf{u}(\tau)) d\tau + V_f(\mathbf{x}(t_k + T_p)) \\ \text{subject to :} & \\ \dot{\mathbf{x}}(t) &= f(\mathbf{x}, \mathbf{u}) \text{ with } \mathbf{x}(t_k) = \mathbf{x}_{t_k} \\ \mathbf{x}(t) &\in \mathbb{X}, \forall t \in [t_k, t_k + T_p) \\ \mathbf{u}(t) &\in \mathbb{U}, \forall t \in [t_k, t_k + T_p) \\ \mathbf{x}(t_k + T_p) &\in \mathbb{X}_f \end{aligned}$$

where  $l(\cdot, \cdot) : \mathbb{X} \times \mathbb{U} \rightarrow \mathbb{R}_0^+$  is the stage cost function,  $V_f(\cdot)$  and  $\mathbb{X}_f$  are the terminal cost and terminal set, respectively which are used for guaranteeing stability,  $T_p$

is the prediction horizon period. The stage cost function should be selected such that if we are in the equilibrium  $\mathbf{x}_*$  and the control value  $\mathbf{u}_*$  is used, the cost is zero, and outside the equilibrium the cost is positive, i.e.,

$$\ell(\mathbf{x}_*, \mathbf{u}_*) = 0 \quad \text{and} \quad \ell(\mathbf{x}, \mathbf{u}) > 0 \quad \forall \mathbf{x} \in \mathbb{X}, \mathbf{u} \in \mathbb{U} \text{ with } \mathbf{x} \neq \mathbf{x}_* \quad (4.5)$$

As discussed in [78], the stage cost function is usually defined as the weighted norm of the states and control inputs:

$$\ell(\mathbf{x}(t), \mathbf{u}(t)) = \|\mathbf{x}(t)\|_Q + \|\mathbf{u}(t)\|_R \quad (4.6)$$

Here  $Q$  and  $R$  are positive semidefinite weighing matrices. Control action is penalized because that makes the optimization problem easier and avoids control values of high energy[79]. The basic algorithm for regulation or set-point stabilization is [80]:

---

**Algorithm 4.1** Basic NMPC Algorithm

---

- 1: Set the time index  $k = 0$ , the sampling interval  $T_s$ , and the prediction horizon  $T_p = NT_s$ .
  - 2: Measure the value of the states  $\mathbf{x}(t_k)$  or estimate them.
  - 3: Solve the discretized form of the optimization problem  $\text{OCP}_{T_p}$  over the discrete time instants  $T_d$  and get the optimal control sequence  $[\mathbf{u}(t_k) \cdots \mathbf{u}(t_{k+N-1})]$  and the corresponding predicted states  $[\mathbf{x}(t_k) \cdots \mathbf{x}(t_{k+N})]$ .
  - 4: Apply only the first control element  $\mathbf{u}(t_k)$ .
  - 4: wait for the next sample and set the time index  $k = k + 1$ , then go to step 2.
- 

Therefore, NMPC is considered as a nonlinear state feedback  $\mathbf{u}(t_k) = \mathcal{K}(\mathbf{x}(t_k))$  obtained online from an optimal control problem, that minimizes a Least Squares (LS) objective function penalizing the deviation of the system states and inputs from the reference states, using a nominal model and the last available measurement or an accurate estimation of the states.

### 4.3 NMPC Formulation for Tracking Problems

The tracking problem considers following a time-varying reference  $\mathbf{x}^{ref}(t)$  which should be considered in the NMPC formulation. This requires not only the stage cost function to be time varying, but also the terminal cost, constraints and possibly state and control constraints. Similar to the regulation case, we assume that the reference  $\mathbf{x}^{ref}(t)$  is a trajectory of the system 4.1, i.e.

$$\dot{\mathbf{x}}^{ref}(t) = f(\mathbf{x}^{ref}, \mathbf{u}^{ref})$$

for an admissible reference control input  $\mathbf{u}^{ref}(t) \in \mathbb{U}$ , i.e.  $\mathbf{x}^{ref} \in \mathbb{X}$ . This leads to an explicit time dependence in the formulation of the optimal control problem as assuming that these references are constantly equal to 0 would lead to time varying coordinate transformations in  $\mathbb{X}$  and  $\mathbb{U}$ . Therefore,  $\mathbf{x}^{ref}$  and  $\mathbf{u}^{ref}$  must be considered in the stage cost function  $\ell$  to keep track of the current time in the optimal control problem. As a result,  $\ell : t \times \mathbb{X} \times \mathbb{U} \rightarrow \mathbb{R}_0^+$  becomes a time varying function that vanishes if and only if we are exactly on the reference. In the tracking problem, equation (4.5) becomes:

$$\ell(t, \mathbf{x}^{ref}, \mathbf{u}^{ref}) = 0 \quad \text{and} \quad \ell(t, \mathbf{x}, \mathbf{u}) > 0 \quad \forall \mathbf{x} \in \mathbb{X}, \mathbf{u} \in \mathbb{U} \text{ with } \mathbf{x} \neq \mathbf{x}^{ref}. \quad (4.7)$$

One possible choice for the stage cost function is the norm of the deviation of the states and control inputs from the references (instead of the 0), i.e. the regulation case (4.6) becomes:

$$\ell(t, \mathbf{x}(t), \mathbf{u}(t)) = \|\mathbf{x}(t) - \mathbf{x}^{ref}\|_Q + \|\mathbf{u}(t) - \mathbf{u}^{ref}\|_R. \quad (4.8)$$

Here  $Q$  and  $R$  are still positive semidefinite weighing matrices.

Based on that, the NMPC tracking problem can be achieved by repeatedly solving the following optimal control problem[80]:

$$\begin{aligned}
\text{OCP}_{T_p}^t : \min_{\mathbf{u}(\cdot)} V_{T_p}(t, \mathbf{x}_{t_k}, \mathbf{u}(\cdot)) &= \int_{\tau=t_k}^{t_k+T_p} \ell(\tau, \mathbf{x}(\tau), \mathbf{u}(\tau)) d\tau + V_f(t, \mathbf{x}(t_k + T_p)) \\
\text{subject to :} & \\
\dot{\mathbf{x}}(t) &= f(\mathbf{x}, \mathbf{u}) \text{ with } \mathbf{x}(t_k) = \mathbf{x}_{t_k} \\
\mathbf{x}(t) &\in \mathbb{X}, \forall t \in [t_k, t_k + T_p) \\
\mathbf{u}(t) &\in \mathbb{U}, \forall t \in [t_k, t_k + T_p) \\
\mathbf{x}(t_k + T_p) &\in \mathbb{X}_f(t)
\end{aligned}$$

where  $\ell(\cdot, \cdot, \cdot)$  is the stage cost function,  $V_f(\cdot, \cdot)$  and  $\mathbb{X}_f(\cdot)$  are the terminal cost and terminal set, respectively which are used for guaranteeing stability,  $T_p$  is the prediction horizon period. In general, the terminal region  $\mathbb{X}_f(\cdot)$  is time varying, unlike the regulation case, to bound the states evolution to be closer to the reference trajectory beyond the prediction horizon. The algorithm for the trajectory tracking problem is:

---

**Algorithm 4.2** Tracking NMPC Algorithm

---

- 1: Set the time index  $k = 0$ , the sampling interval  $T_s$ , and the prediction horizon  $T_p = NT_s$ .
  - 2: Measure the value of the states  $\mathbf{x}(t_k)$  or estimate them, and get the reference trajectory  $\mathbf{x}^{ref}$  and controls  $\mathbf{u}^{ref}$  over the horizon .
  - 3: Solve the discretized form of the optimization problem  $\text{OCP}_{T_p}$  over the discrete time instants  $T_d$  and get the optimal control sequence  $\mathbf{U}_N^* = [\mathbf{u}^*(t_k) \cdots \mathbf{u}^*(t_{k+N-1})]$  and the corresponding predicted states  $\mathbf{X}_N^* = [\mathbf{x}^*(t_k) \cdots \mathbf{x}^*(t_{k+N})]$ .
  - 4: Apply only the first control element  $\mathbf{u}^*(t_k)$ .
  - 4: wait for the next sample and set the time index  $k = k + 1$ , then go to step 2.
-

## 4.4 NMPC Formulation for Tracking Problems with Time-varying Constraints

Although the state and control constraints usually represent physical constraints and therefore are represented by time invariant sets, for some other applications, like the one presented in this thesis, the constraints may result from operational constraints and therefore it may be needed to formulate them as time-varying over the horizon. Even if the physical model is time invariant similar to (4.1), there is a need to represent it as a time varying system which allows for known disturbances and exogenous input signals to be accounted for in the optimal control problem formulation.

Consider a time varying nonlinear system described by the state space model:

$$\dot{\mathbf{x}}(t) = f(t, \mathbf{x}, \mathbf{u}) \quad (4.9)$$

subject to the time varying constraints:

$$\begin{aligned} \mathbf{x}(t) \in \mathbb{X}(t) &\subseteq \mathbb{R}^n, \\ \mathbf{u}(t) \in \mathbb{U} &\subseteq \mathbb{R}^m, \end{aligned} \quad (4.10)$$

where  $\mathbf{x} \in \mathbb{R}^n$  is the state vector;  $\mathbf{u} \in \mathbb{R}^m$  is the control vector;  $f(\cdot, \cdot, \cdot)$  is continuous,  $\mathbb{X}(\cdot) \subseteq \mathbb{R}^n$  and  $\mathbb{U} \subseteq \mathbb{R}^m$  define the allowable time-varying state and control set, respectively. The operational constraints are usually defined for the states only over a finite future horizon, so the control constraints will be kept time invariant.

The NMPC tracking problem with time varying state constraints is achieved by repeatedly solving the following optimal control problem[80]:

$$\begin{aligned} \text{OCP}_{T_p, t}^t : \min_{\mathbf{u}(\cdot)} V_{T_p}(t, \mathbf{x}_{t_k}, \mathbf{u}(\cdot)) &= \int_{\tau=t_k}^{t_k+T_p} \ell(\tau, \mathbf{x}(\tau), \mathbf{u}(\tau)) d\tau + V_f(t, \mathbf{x}(t_k + T_p)) \\ \text{subject to :} & \\ \dot{\mathbf{x}}(t) &= f(t, \mathbf{x}, \mathbf{u}) \text{ with } \mathbf{x}(t_k) = \mathbf{x}_{t_k} \\ \mathbf{x}(t) &\in \mathbb{X}(t), \forall t \in [t_k, t_k + T_p) \\ \mathbf{u}(t) &\in \mathbb{U}, \forall t \in [t_k, t_k + T_p) \\ \mathbf{x}(t_k + T_p) &\in \mathbb{X}_f(t) \end{aligned}$$

**Remark:** It is also possible to include states and control mixed constraints in the form of  $\mathbf{h}(\mathbf{x}, \mathbf{u}) \leq 0$ , but it is omitted here because it is not used in our application.

## 4.5 Stability

To guarantee asymptotic stability by using the control law  $\mathbf{u}(t_k) = \mathcal{K}(\mathbf{x}(t_k))$ , it is desirable to use infinite prediction and control horizons, i.e., set  $T_p = \infty$  in the aforementioned OCPs, but it is not feasible to get the solution of the infinite horizon nonlinear optimization problem[81]. On the other hand, stability can be guaranteed for finite horizon problems by suitably choosing a terminal cost  $V_f(\mathbf{x}(\cdot))$  and a terminal attractive region  $\mathbb{X}_f$ . This result has been studied in [81–84]. The following assumption is a necessary condition which is required to guarantee the stability[85]:

**Assumption 4.1.** *There exist an auxiliary control law  $\mathcal{K}_f(\mathbf{x})$ , a terminal set  $\mathbb{X}_f$  and a terminal penalty  $V_f$  such that, letting  $\phi_f(t, \mathbf{x}(t_k))$  the solution of the closed-loop system:*

$$\dot{\mathbf{x}}(t) = f(\mathbf{x}, \mathcal{K}_f(\mathbf{x}(t))) \quad (4.11)$$

with the initial state  $\mathbf{x}(t_k)$ , the following conditions hold:

- $\mathbb{X}_f \subset \mathbb{X}$ ,  $\mathbb{X}_f$  is closed, and  $0 \in \mathbb{X}_f$
- $\mathcal{K}(\mathbf{x}) \in \mathbb{U}, \forall \mathbf{x} \in \mathbb{X}_f$
- $\mathbb{X}_f$  is positively invariant for (4.11)
- $V_f(\cdot) : \mathbb{R}^n \rightarrow \mathbb{R}$  is such that  $\forall \mathbf{x}(t_k) \in \mathbb{X}_f$

$$\begin{aligned} & V_f(\phi_f(t_{k+1}, \mathbf{x}(t_k))) - V_f(\mathbf{x}(t_k)) \\ & \leq - \int_{\tau=t_k}^{t_{k+1}} \left\{ \left\| \phi_f(\tau, \mathbf{x}(t_k)) \right\|_Q^2 + \left\| \mathcal{K}_f(\phi_f(\tau, \mathbf{x}(t_k))) \right\|_R^2 \right\} d\tau \quad (4.12) \end{aligned}$$

**Note:** The control law  $\mathcal{K}_f(\cdot)$  is never applied to the system but it is only used in simulation in order to obtain the terminal set and the terminal penalty.

Based on Assumption 4.1, many techniques were introduced in the literature to guarantee the stability of the MPC algorithm:

**Terminal Equality Constraint:** The first technique found in the literature is to use a terminal equality constraint  $\mathbb{X}_f = 0$  [86, 87]. The terminal control law and the terminal penalty are defined only in the origin such that the following trivial functions can be chosen:  $V_f(\mathbf{x}) \equiv 0$  and  $\mathcal{K}_f(\mathbf{x}) \equiv 0$ . The disadvantage of using this method is the excessive control action required to steer the states to the origin, specially for short prediction horizon.

**Quadratic Terminal Penalty:** The second well known method is to use a quadratic terminal penalty and a linear auxiliary control law [84]. This can be achieved by linearizing the system (4.9):

$$A = \left. \frac{\partial f}{\partial \mathbf{x}} \right|_{\mathbf{x}=0, \mathbf{u}=0}, B = \left. \frac{\partial f}{\partial \mathbf{u}} \right|_{\mathbf{x}=0, \mathbf{u}=0}$$

The auxiliary (terminal) control law is designed to be  $\mathcal{K}_f(\mathbf{x}) = K\mathbf{x}$  where  $K$  is designed with linear control theory such that  $A_{cl} = A + BK$  is Hurwitz. The terminal penalty is selected to be a quadratic function  $V_f(\mathbf{x}) = \mathbf{x}^T P \mathbf{x}$  where  $P$  is the solution of the following Lyapunov function:

$$(A_{cl} + k_\epsilon I)^T P + P (A_{cl} + k_\epsilon I) = \bar{Q} \quad (4.13)$$

where  $\bar{Q} = Q + K^T R K$  and  $k_\epsilon$  is a positive scalar which satisfies  $k_\epsilon < -\lambda_{max}(A_{cl})$ .

The terminal region is defined as a level set of the terminal penalty:

$$\mathbb{X}_f := \left\{ \mathbf{x} \in \mathbb{R}^n \mid \mathbf{x}^T P \mathbf{x} \leq \alpha \right\} \subset \mathbb{X} \quad (4.14)$$

such that

1.  $K\mathbf{x} \in \mathbb{U} \quad \forall \mathbf{x} \in \mathbb{X}_f$ ;

2.  $\mathbb{X}_f$  is positively invariant for the closed loop system driven by the control law  $\mathbf{u} = K\mathbf{x}$ ;
3.  $\forall \mathbf{x} \in \mathbb{X}_f$ ,  $\frac{d}{dt}\mathbf{x}^T P \mathbf{x} \leq -\mathbf{x}^T \bar{Q} \mathbf{x}$  is satisfied for the closed loop system driven by the control law  $\mathbf{u} = K\mathbf{x}$ .

**Infinite-Horizon Closed-loop Costing:** The third method, presented in [88], relies on being able to design a general stabilizing nonlinear control law and use it as the terminal penalty. Based on that, an infinite horizon cost can be used, and the terminal penalty will be:

$$V_f(\mathbf{x}(t_k)) = \int_{\tau=t_k}^{\infty} \left\{ \|\phi_f(\tau, \mathbf{x}(t_k))\|_Q^2 + \|\mathcal{K}_f(\phi_f(\tau, \mathbf{x}(t_k)))\|_R^2 \right\} d\tau$$

The terminal region is defined as:

$$\begin{aligned} \mathbb{X}_f := \{ \bar{\mathbf{x}} \in \mathbb{R}^n \mid \phi_f(\tau, \mathbf{x}(t_k)) \subset \mathbb{X}, \\ \mathcal{K}_f(\phi_f(\tau, \mathbf{x}(t_k))) \in \mathcal{U}, t > \bar{t}, \\ V_f(\mathbf{x}(\bar{\mathbf{x}})) \text{ is bounded} \} \subset \mathcal{X} \quad (4.15) \end{aligned}$$

**Long Horizon:** One of the interesting techniques is to rely only on selecting a relatively long horizon. In [89], it is shown that there is always a finite horizon for which the NMPC scheme is stabilizing without the use of a terminal cost or terminal constraints.

## 4.6 Optimal Control Problem Formulation

Having a successful usage of the aforementioned NMPC problems requires a proper formulation of an optimization problem. There are two possible categories when it comes to dynamic optimization problems; indirect and direct methods. Indirect methods, such as calculus of variations and dynamic programming, consider the continuous NMPC as it is and does not require discretization of the problem. They provide exact analytic solution of the optimal control problem [74]. They



are not common to be used for the nonlinear optimal control problems due to their inability to handle a wide class of systems because they require a guess of the optimal control structure[74]. Direct methods are more desirable for solving NMPC optimization problem.

The main idea behind the direct methods are introducing the discretization and finite parameterization into the optimal control problem formulation which is then directly solved with numerical methods. The choice of the numerical optimization formulation strategy will have significant impact on both the need for computational resources and the quality of the solution in NMPC. Given that, direct numerical optimal control techniques are reviewed in this section which are classified into two approaches [90]:

- **The sequential approach:** The ODE (4.1) is solved via numeric simulation when evaluating the cost and constraint functions which make the sampled intermediate states  $\mathbf{x}(t_k) \cdots \mathbf{x}(t_{k+N})$  disappear from the problem formulation by substitution into the cost and constraint functions, while the control trajectory parameters  $\mathbf{U}_N$  are treated as unknowns. This leads to a sequence of simulate-optimize iterations, often known as Direct Single Shooting, [91–93].
- **The simultaneous approach:** The ODE (4.1) is discretized based on a suitable sampling interval and the resulting finite set of nonlinear algebraic equations are treated as nonlinear equality constraints. In this case, both the control sequence  $\mathbf{U}_N^* = [\mathbf{u}^*(t_k) \cdots \mathbf{u}^*(t_{k+N-1})]$  and the corresponding predicted states  $\mathbf{X}_N = [\mathbf{x}(t_k) \cdots \mathbf{x}(t_{k+N})]$  are handled as unknowns. There are two main methods which use this approach; direct multiple shooting [94–97], and collocation methods [98–100].

In the following, the three most common formulation techniques that are used in numerical optimal control; single shooting, direct collocation and multiple shooting,

are reviewed followed by the reasons to choose one of them to be used considering our research application.

### 4.6.1 Direct Single Shooting

In this method, numerical solution of the nonlinear differential equation  $\mathbf{x}(t_k) = \phi(t_k, \mathbf{U}_N, \mathbf{x}(0))$  is substituted into the the cost and constraints, and therefore, the ODE 4.9 is eliminated from the problem. The optimization problem become as follows:

$$\begin{aligned} \min_{\mathbf{U}_N} V_{T_p}(\mathbf{x}_0, \mathbf{U}_N) &\triangleq \sum_{k=1}^N \ell(t_k, \phi(t_k, \mathbf{U}_N, \mathbf{x}(0)), \mu(t_k, \mathbf{U}_N)T_s + V_f(T_p, \phi(T_p, \mathbf{U}_N, \mathbf{x}(0)))) \\ \text{subject to :} & \\ \mathbf{x}(t_k) &\in \mathbb{X}(t_k), \forall t_k \in T_d \\ \mathbf{u}(t_k) &\in \mathbb{U}, \forall t_k \in T_d \\ \mathbf{x}(t_{k+N}) &\in \mathbb{X}_f(t_{k+N}) \end{aligned}$$

where  $\phi(\cdot)$  results from either explicit or implicit integration schemes. For example, explicit integration scheme gives the following difference equation:

$$\mathbf{x}_{k+1} = F(t_k, \mathbf{x}(t_k), \mu(t_k, \mathbf{U}_N)), \mathbf{x}(t_0) = \mathbf{x}(0) \quad (4.16)$$

that leads to the following prediction:

$$\phi(t_k, \mathbf{U}_N, \mathbf{x}(0)) = F(t_{k-1}, \dots F(t_1, F(t_0, \mathbf{x}(0), \mu(t_0, \mathbf{U}_N)), \mu(t_1, \mathbf{U}_N)), \dots \mu(t_{k-1}, \mathbf{U}_N)) \quad (4.17)$$

### 4.6.2 Direct Collocation

In direct collocation, the nonlinear algebraic equations resulting from discretization of the continuous ones are kept into the optimization problem instead of substituting the numerical solution of  $\mathbf{x}_{t_k}$ . Hence, the predicted states  $[\mathbf{x}(t_1) \dots \mathbf{x}(t_N)]$  are treated as unknown decision variables:

$$\begin{aligned}
& \min_{\mathbf{U}_N, \mathbf{x}(t_1) \cdots \mathbf{x}(t_N)} V_{T_p}(\mathbf{x}(t_1) \cdots \mathbf{x}(t_N), \mathbf{U}_N, \mathbf{x}_0) \triangleq \\
& \quad \sum_{k=1}^N \ell(t_k, \mathbf{x}_{t_k}, \mu(t_k, \mathbf{U}_N)) T_s + V_f(T_p, \mathbf{x}(T_p)) \\
& \quad \text{subject to :} \\
& \quad \quad \mathbf{x}(t_k) \in \mathbb{X}(t_k), \forall t_k \in T_d \\
& \quad \quad \mathbf{u}(t_k) \in \mathbb{U}, \forall t_k \in T_d \\
& \quad \quad \mathbf{x}(t_{k+N}) \in \mathbb{X}_f(t_{k+N}) \\
& \quad F(t_k, \mathbf{x}_{k+1}, \mathbf{x}(t_k), \mu(t_k, \mathbf{U}_N)) = 0, \quad \mathbf{x}(t_0) = \mathbf{x}(0)
\end{aligned}$$

where  $F(\cdot)$  is a function defined according to the discretization scheme. This allows for both explicit and implicit integration to be used. The algebraic equations result from the implicit discretization are solved simultaneously with the optimization problem.

### 4.6.3 Direct Multiple Shooting

Direct multiple shooting combines elements of both direct single shooting and direct collocation. The nonlinear continuous ODE is discretized to a set of algebraic equations which included and solved simultaneously in the optimization problem as equality constraints (as in collocation), and the ODE solver is used to simulate the ODE in each time interval  $t_k \leq t \leq t_{k+1}$  as follows:

$$\begin{aligned}
& \min_{\mathbf{U}_N, \mathbf{x}(t_1) \cdots \mathbf{x}(t_N)} V_{T_p}(\mathbf{x}(t_1) \cdots \mathbf{x}(t_N), \mathbf{U}_N, \mathbf{x}_0) \triangleq \\
& \quad \sum_{k=1}^N \ell(t_k, \mathbf{x}_{t_k}, \mu(t_k, \mathbf{U}_N)) T_s + V_f(T_p, \mathbf{x}(T_p)) \\
& \quad \text{subject to :} \\
& \quad \quad \mathbf{x}(t_k) \in \mathbb{X}(t_k), \forall t_k \in T_d \\
& \quad \quad \mathbf{u}(t_k) \in \mathbb{U}, \forall t_k \in T_d \\
& \quad \quad \mathbf{x}(t_{k+N}) \in \mathbb{X}_f(t_{k+N}) \\
& \quad \quad \mathbf{x}(t_{k+1}) = \phi(t_k, \mu(t_k, \mathbf{U}_N), \mathbf{x}(t_k)), \quad \mathbf{x}(t_0) = \mathbf{x}(0)
\end{aligned}$$

where  $\phi(\cdot)$  is defined by the simulation of the ODE. The main advantage of multiple shooting is the usage of an arbitrary ODE solver between the time instants of  $T_d$  such that adaptive discretization schemes might be used due to stiff dynamics.

In this thesis, Direct Multiple Shooting is used due to the following reasons [74]:

- Although the simultaneous approach involves a larger number of constraints and therefore leads to bigger problems, the cost and constraint function evaluation is much simpler.
- The sequential approach may use a separate ODE and optimization solvers which may, in some cases, be simple and convenient specially for industrial applications.
- The simultaneous approach not only requires an initial control trajectory guess, but also one for the state trajectory. The availability of a good initial guess for the state trajectory is an advantage that can be exploited by the simultaneous approach.
- Direct multiple shooting technique provides additional flexibility to both direct single shooting and direct collocation as it decouples the discretization grids of the constraints and the discretization grid of the ODE integration.

## 4.7 ACADO Toolkit

The open-source ACADO Code Generation toolkit [101] is used in the implementation of the NMPC algorithms presented in this thesis. Based on a symbolic representation of optimal control problems, ACADO generates an optimized and self-contained C code with static memory for a good real-time performance. The C code can be integrated into MATLAB as MATLAB executable (mex) files. The main steps of the implementation are briefly described as follows:

- The continuous state space model is symbolically defined using C-code or the MATLAB interface, then it is simplified employing automatic differentiation tools and using zero entries in the Jacobian matrix. The result is an efficient real time C-code for the integration of the continuous nonlinear system which will be used for the prediction.
- The optimization problem cost function and constraints are symbolically defined, parametrized by the aforementioned direct multiple shooting technique, and the resulting, large but sparse, Quadratic Problem (QP) is condensed.
- The discretized QP is then solved with the aid of Gauss-Newton iterative algorithm and a real time iteration (RTI) scheme.



# 5

## Disturbance Estimation

### 5.1 Introduction

A lot of nonlinear systems are subjected to disturbances which affect the controller performance adversely. Therefore, disturbance counteraction is one of the useful techniques of improving the controller design while maintaining the level of complexity. In general, disturbances refer not only to unknown inputs from the external environment of a control system but also to uncertainties of the system model under control including unmodeled dynamics, parameter uncertainty and nonlinear couplings terms, which are difficult to handle[19].

In the field of ship motion control, the hydrodynamic effect is very difficult to model and usually is done experimentally based on some approximations which bring unmodeled dynamics to the control problem[11]. Moreover, the ship will be influenced in open water to severe wind and current forces which degrades the performance of the motion controllers[102].

Motivated by the benefits of disturbance counteraction to improve the control precision and of course the production efficiency of practical engineering systems, many advanced control techniques have been proposed to handle the undesirable

effects caused by unknown disturbances and uncertainties since 1950s. They can be categorized into two categories: Passive Anti-Disturbance Control (PADC) and Active Anti-Disturbance Control (AADC)[19].

The major PADC techniques are:

- *Adaptive Control*: Adaptive control handles the structured parameter perturbation by estimating the parameters of the model online and tune the controller parameters to obtain a fine performance. Adaptive control is very useful when the model is well known but with time varying parameters, and there is a parameter estimation technique to estimate their parameters.
- *Robust Control* : Robust control is an important branch of modern control theory that guarantee an upper bound of the performance given that there exist a known bound for the unknown disturbances or uncertainties. The control design of it is quite conservative as it considers the worst case of the uncertainties or disturbances. The robustness of this controller is generally obtained at the price of sacrificing the transient performance of other featured points[19].
- *Sliding Model Control (SMC)* : SMC is a robust discontinuous controller which can handle plant structured and unstructured uncertainties and disturbances. The main drawback of SMC is the chattering which is undesirable since it involves high control activity and may excite high frequency dynamics neglected in the course of modeling. In the recent years, some techniques have been emerged to solve chattering and to achieve convergence to the sliding surface, most of them are based on Fuzzy Logic Systems (FLS) which can reduce the chattering as in [103].
- *Internal Model Control (IMC)* : IMC is a simple and intuitive way to attenuate the effects of external disturbances in control systems. It is only available for linear systems and is very sophisticated for high-dimensional systems due



to the requirement of calculating the inverse of a high dimensional transfer function matrix.

The aforementioned techniques use a feedback regulation to compensate the unknown disturbances, rather than feedforward compensation, based on the tracking error between the reference input and the measured outputs. The main drawbacks for these schemes is the relative slow reaction to the disturbances specially in the presence of strong disturbances [19]. One disadvantage of PADC techniques is that a new technique must be developed for each new nonlinear controller scheme.

Active Anti-Disturbance Control (AADC) methods have been proposed to overcome the limitations of PADC methods. The main idea behind them is to directly counteract disturbances by feed-forward compensation control design based on disturbance measurements or estimations. Traditional feed-forward control is considered as the earliest AADC methods where a sensor is firstly employed to measure the disturbances; secondly, the model of disturbance channel is built; finally, a feedforward controller, which employs the disturbance measurement and both models of the process and disturbance channels, is designed to counteract the disturbances. In most of the practical systems the disturbance is not measured and therefore estimation of the disturbance become beneficial. Disturbance observer (DO) is one of the most effective and popular disturbance estimation techniques.

## **5.2 Disturbance Observer Based Control (DOBC)**

Disturbance Observer Based Control (DOBC) is framework used to handle control problems subject to disturbances. Within this framework, instead of considering the control problem for a nonlinear system under disturbances as a single one, it is divided into two subproblems, each with its own design objectives. The first subproblem is the same as the control problem for a nonlinear system without disturbances and its objective is to stabilize the nonlinear plant and achieve the performance specifications such as tracking or regulation. The second subproblem

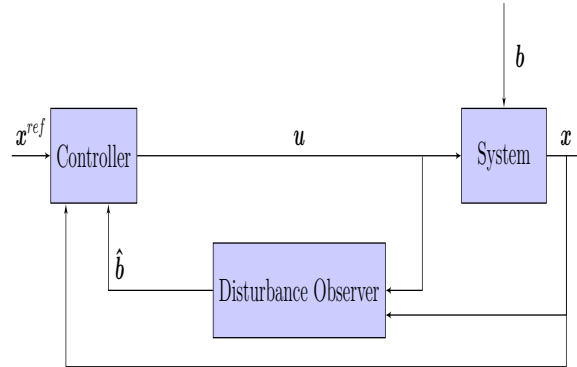


**Figure 5.1:** Structure of DOBC

is to attenuate disturbances. A nonlinear disturbance observer is designed to deduce external disturbances and then to compensate for their influence using proper feedback[104].

A general design procedures for the DOBC scheme are:

1. Design a nonlinear controller for system to achieve stability and other performance specifications under the assumption that the disturbance is measurable.
2. Design a disturbance observer to estimate the disturbance.
3. Integrate the disturbance observer with the controller by replacing the disturbance in the control law with its estimation yielded by the disturbance observer.

A block digram showing the structure of BODC is shown in Figure5.1. As seen from this figure, the composite controller consists of two components: a controller designed based on the nominal model, (i.e. ignoring the disturbance or assuming that it is measurable) and a disturbance observer, which are integrated together to achieve disturbance counteraction. The advantage of this scheme is the deign flexibility as the controller design is separated from the disturbance observer and generally speaking can be used for linear and nonlinear systems subject to simple additive disturbance or a more complex ones.

### 5.3 Nonlinear Disturbance Observer

In this section, a Nonlinear Disturbance Observer (NDO) is presented for a class of nonlinear system, affine system, subjected to a constant nonlinear disturbance. Consider the following affine nonlinear system represented in state space:

$$\dot{\mathbf{x}} = \mathcal{F}(\mathbf{x}) + g(\mathbf{x})\mathbf{u} + g_b(\mathbf{x})\mathbf{b} \quad (5.1)$$

where  $\mathbf{x} \in \mathbb{R}^n$  is the state vector,  $\mathbf{u} \in \mathbb{R}^m$  is the control vector,  $\mathbf{b} \in \mathbb{R}^l$  is the constant but unknown disturbance vector, and  $\mathcal{F}(\cdot)$ ,  $g(\cdot)$  and  $g_b(\cdot)$  are continuous function of appropriate dimensions.

A nonlinear disturbance observer is proposed to estimate the disturbance  $\mathbf{b}$  as follows:

$$\dot{\hat{\mathbf{b}}} = l(\mathbf{x})[\dot{\mathbf{x}} - \mathcal{F}(\mathbf{x}) - g(\mathbf{x})\mathbf{u} - g_b(\mathbf{x})\hat{\mathbf{b}}] \quad (5.2)$$

where  $\hat{\mathbf{b}}$  is the disturbance estimation vector, and  $l(\mathbf{x})$  is the nonlinear gain function of the observer. The estimation error is defined by:

$$\tilde{\mathbf{b}} := \hat{\mathbf{b}} - \mathbf{b}. \quad (5.3)$$

The disturbance error dynamics can be obtained by substituting (5.1) and (5.2) into the time derivative of (5.3):

$$\begin{aligned} \dot{\tilde{\mathbf{b}}} &= \dot{\hat{\mathbf{b}}} - \dot{\mathbf{b}}. \\ &= -l(\mathbf{x})[\dot{\mathbf{x}} - \mathcal{F}(\mathbf{x}) - g(\mathbf{x})\mathbf{u} - g_b(\mathbf{x})\hat{\mathbf{b}}], \\ &= -l(\mathbf{x})g_b(\mathbf{x})\tilde{\mathbf{b}} \end{aligned} \quad (5.4)$$

where the nonlinear gain  $l(\mathbf{x})$  is chosen such that the error dynamics (5.4) is asymptotically stable.

**Remark:** This observer is difficult to use for wide range of applications as it requires the measurement of the states derivative.

**Remark:** For the application of vehicle motion control, accelerometers might be

installed on-board and the derivative of the velocity states can be measured and therefore the the observer (5.2) can be used.

An enhanced observer is proposed to overcome the need to measure the states time derivative [19, 104]:

$$\dot{\mathbf{z}} = -l(\mathbf{x}) [g_b(\mathbf{x})z + g_b(\mathbf{x})p(\mathbf{x}) + \mathcal{F}(\mathbf{x}) + g(\mathbf{x})\mathbf{u}] \quad (5.5a)$$

$$\hat{\mathbf{b}} = \mathbf{z} + p(\mathbf{x}) \quad (5.5b)$$

where  $\mathbf{z} \in \mathbb{R}^l$  is the internal state of the nonlinear observer, and  $p(\mathbf{x}) \in \mathbb{R}^l$  is the nonlinear function to be designed. The nonlinear disturbance observer gain  $l(\mathbf{x}) \in \mathbb{R}^n \times \mathbb{R}^l$  is determined by:

$$l(\mathbf{x}) = \frac{\partial p(\mathbf{x})}{\partial \mathbf{x}}. \quad (5.6)$$

The estimation error is governed according to [19]:

$$\begin{aligned} \dot{\tilde{\mathbf{b}}} &= \dot{\hat{\mathbf{b}}} - \dot{\mathbf{b}} \\ &= -l(\mathbf{x})g_2(\mathbf{x})\tilde{\mathbf{b}} \end{aligned} \quad (5.7)$$

Hence, the NDO design can estimate unknown constant disturbances if the observer gain  $l(\mathbf{x})$  is chosen such that system (5.7) is asymptotically stable.

## 5.4 Robust Nonlinear Disturbance Observer

In this section, we relax the assumption of constant disturbance by letting the disturbance vector  $\mathbf{b}$  to be unknown time varying but bounded. This observer is adapted from the one presented in [105] where the disturbance was additive to the system, not nonlinear.

**Assumption 5.1.** *The disturbance  $\mathbf{b}$  is unknown time-varying but bounded and there exists an unknown positive constant  $\rho$  such that*

$$\|\dot{\rho}(t)\| \leq \rho \quad (5.8)$$

The proposed observer is:

$$\dot{\mathbf{z}} = -l(\mathbf{x}) [g_b(\mathbf{x})z + g_b(\mathbf{x})p(\mathbf{x}) + \mathcal{F}(\mathbf{x}) + g(\mathbf{x})\mathbf{u}] \quad (5.9a)$$

$$\hat{\mathbf{b}} = \mathbf{z} + p(\mathbf{x}) \quad (5.9b)$$

where  $\mathbf{z} \in \mathbb{R}^l$  is the internal state of the nonlinear observer, and  $p(\mathbf{x}) \in \mathbb{R}^l$  and  $l(\mathbf{x}) \in \mathbb{R}^n \times \mathbb{R}^l$  are nonlinear functions to be designed. Define the disturbance estimation error  $\tilde{\mathbf{b}} \in \mathbb{R}^l$ :

$$\tilde{\mathbf{b}} := \hat{\mathbf{b}} - \mathbf{b}. \quad (5.10)$$

From (5.9) and (5.1), we have

$$\begin{aligned} \dot{\hat{\mathbf{b}}} &= -l(\mathbf{x}) [g_b(\mathbf{x})z + g_b(\mathbf{x})p(\mathbf{x}) + \mathcal{F}(\mathbf{x}) + g(\mathbf{x})\mathbf{u}] + \dot{p}(\mathbf{x}) \\ &= -l(\mathbf{x}) [g_b(\mathbf{x})z + g_b(\mathbf{x})p(\mathbf{x}) + \mathcal{F}(\mathbf{x}) + g(\mathbf{x})\mathbf{u}] + \frac{\partial p}{\partial \mathbf{x}} \dot{\mathbf{x}} \\ &= -l(\mathbf{x})g_b(\mathbf{x})\hat{\mathbf{b}} + \frac{\partial p}{\partial \mathbf{x}}g_b(\mathbf{x})\mathbf{b} + \left( \frac{\partial p}{\partial \mathbf{x}} - l(\mathbf{x}) \right) g(\mathbf{x})\mathbf{u} + \left( \frac{\partial p}{\partial \mathbf{x}} - l(\mathbf{x}) \right) \mathcal{F}(\mathbf{x}) \end{aligned} \quad (5.11)$$

if we select  $l(\mathbf{x})$  to be:

$$l(\mathbf{x}) := \frac{\partial p}{\partial \mathbf{x}} \quad (5.12)$$

the estimation disturbance dynamics will be:

$$\dot{\tilde{\mathbf{b}}} = -l(\mathbf{x})g_b(\mathbf{x})\tilde{\mathbf{b}} \quad (5.13)$$

From (5.13) and (5.10) the error dynamics becomes:

$$\dot{\tilde{\mathbf{b}}} = -l(\mathbf{x})g_b(\mathbf{x})\tilde{\mathbf{b}} - \dot{\mathbf{b}} \quad (5.14)$$

Select the candidate Lyapunov function as:

$$V_{do} = \frac{1}{2} \tilde{\mathbf{b}}^T \tilde{\mathbf{b}} \quad (5.15)$$

Using (5.14), (5.8) and Young's inequality (See Appendix B), the time derivative of (5.15) is:

$$\begin{aligned}
\dot{V}_{do} &= \tilde{\mathbf{b}}^T \dot{\tilde{\mathbf{b}}} \\
&= -\tilde{\mathbf{b}}^T l(\mathbf{x}) g_b(\mathbf{x}) \tilde{\mathbf{b}} - \tilde{\mathbf{b}}^T \dot{\mathbf{b}} \\
&\leq -\tilde{\mathbf{b}}^T l(\mathbf{x}) g_b(\mathbf{x}) \tilde{\mathbf{b}} + \|\tilde{\mathbf{b}}\| \|\dot{\mathbf{b}}\| \\
&\leq -\tilde{\mathbf{b}}^T l(\mathbf{x}) g_b(\mathbf{x}) \tilde{\mathbf{b}} + \frac{1}{2} \tilde{\mathbf{b}}^T \tilde{\mathbf{b}} + \frac{1}{2} \|\dot{\mathbf{b}}\|^2 \\
&\leq -\tilde{\mathbf{b}}^T \left( l(\mathbf{x}) g_b(\mathbf{x}) - \frac{1}{2} I \right) \tilde{\mathbf{b}} + \frac{1}{2} \rho^2
\end{aligned} \tag{5.16}$$

**Assumption 5.2.** *The design matrix function  $l(\mathbf{x})$  can be chosen such that the matrix  $\Lambda(\mathbf{x}) := l(\mathbf{x}) g_b(\mathbf{x})$  is positive definite for all  $\mathbf{x}$ , with*

$$\lambda_{\min}(\Lambda) > \frac{1}{2} \tag{5.17}$$

where  $\lambda_{\min}(\cdot)$  denotes the minimum eigenvalue of a matrix.

Following Assumption 5.2, equation (5.15) becomes:

$$\begin{aligned}
\dot{V}_{do} &\leq -\left[ \lambda_{\min}(\Lambda) + \frac{1}{2} \right] \tilde{\mathbf{b}}^T \tilde{\mathbf{b}} + \frac{1}{2} \rho^2 \\
&= -2\alpha V_{do} + C_d
\end{aligned} \tag{5.18}$$

where  $\alpha = \lambda_{\min}(\Lambda) - \frac{1}{2}$  and  $C_d = \frac{1}{2} \rho^2$ . Therefore, we have the following theorem.

**Theorem 5.1.** *Under Assumptions 5.1 and 5.2, the disturbance estimation error vector  $\tilde{\mathbf{b}}$  of the observer constructed by (5.9) settles within the compact set  $\Omega_{\tilde{\mathbf{b}}} = \{\tilde{\mathbf{b}} \in \mathbb{R}^l \mid \|\tilde{\mathbf{b}}\| \leq \xi_{\tilde{\mathbf{b}}}, \xi_{\tilde{\mathbf{b}}} > \sqrt{\frac{C_d}{\alpha}}\}$  which can be made arbitrarily small. The practical stability of the disturbance observer is ensured.*

*Proof.* From the analytic solution of the first order differential equation (5.18), we have

$$0 \leq V_{do}(t) \leq \frac{C_d}{2\alpha} + \left[ V_{do}(0) - \frac{C_d}{2\alpha} \right] e^{-2\alpha t} \tag{5.19}$$

Therefore,  $V_{do}(t)$  is globally uniformly ultimately bounded. From (5.15) and (5.19), we have

$$\|\tilde{\mathbf{b}}\| \leq \sqrt{\frac{C_d}{\alpha} + \left[ V_{do}(0) - \frac{C_d}{2\alpha} \right] e^{-2\alpha t}}, \tag{5.20}$$

which makes  $\tilde{\mathbf{b}}$  uniformly ultimately bounded. For any positive constant  $\xi_{\tilde{\mathbf{b}}} > \sqrt{\frac{C_d}{\alpha}}$  there exists a time constant  $T_{\tilde{\mathbf{b}}} > 0$  such that  $\|\tilde{\mathbf{b}}\| \leq \xi_{\tilde{\mathbf{b}}}$  for all  $t > T_{\tilde{\mathbf{b}}}$ . Thus,  $\tilde{\mathbf{b}}$  converges to  $\Omega_{\tilde{\mathbf{b}}} = \{\tilde{\mathbf{b}} \in \mathbb{R}^l \mid \|\tilde{\mathbf{b}}\| \leq \xi_{\tilde{\mathbf{b}}}\}$ . Selecting the design matrix will influence the convergence rate of the observer. Theorem 5.1 is thus proved.  $\square$

**Remark:** The two observers (5.5) and (5.9) are identical and the robustness again unknown, but bounded, disturbance time derivative can be achieved by the design matrix  $l(\mathbf{x})$ .

## 5.5 Case Study: Vessels Disturbance

In this section, the nonlinear disturbance observer will be used to estimate the disturbance acting on the underactuated vessel modeled by (3.40) with the parameters given in Appendix A. External environmental forces might lead to a big tracking error if they are not considered, implicitly or explicitly, in the controller design; hence, a measurement or estimation of these disturbances is required. The environmental forces are modeled as a slowly time varying bias  $\mathbf{b}$  with respect to the inertial fixed frame acting on the vessel and a vector of white noise  $\boldsymbol{\omega}$  (See section 3.7). The states measurement will be filtered for the high frequency compartments to facilitate the estimation of the low frequency disturbance.

In [102], a nonlinear disturbance observer is designed for vessels under the approximation that  $g_b(\mathbf{x}) = g_b(\boldsymbol{\psi}) \approx g_b(\boldsymbol{\psi} + \boldsymbol{\psi}_w)$ , where  $\boldsymbol{\psi}_w$  is the wave induced yaw disturbance, which is suitable for the dynamic positioning application presented in that paper. The sway force is estimated in [106] while the surge and yaw disturbances are compensated using the integral term of the PID. In this subsection, a nonlinear observer is designed to estimate the three components of the disturbances without approximation of the matrix  $g_b(\mathbf{x})$  based on (5.9). A block diagram of the observer and the disturbance acting nonlinearly on the vessel is shown in Figure 5.2.

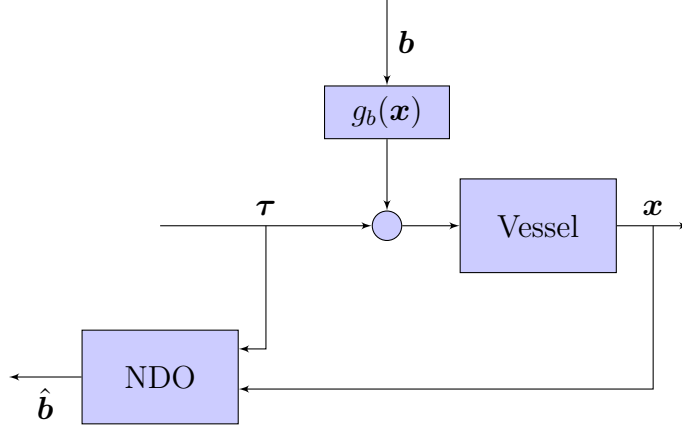


**Figure 5.2:** NDO block diagram for the vessel

For the vessel model (3.40),  $\mathbf{x} \in \mathbb{R}^6$ ,  $\mathbf{u} \in \mathbb{R}^2$ , and  $\mathbf{b} \in \mathbb{R}^3$ , and  $\mathcal{F}(\mathbf{x})$ ,  $g(\mathbf{x})$  and  $g_b(\mathbf{x})$  are smooth in terms of  $\mathbf{x}$ . One possible choice for  $l(\mathbf{x})$  is:

$$l(\mathbf{x}) = K_w g_b(\mathbf{x})^{-1} = K_w \begin{bmatrix} 0 & 0 & 0 \\ 0 & 0 & 0 \\ -m_1 u \sin(\psi) & m_1 u \cos(\psi) & 0 \\ -m_2 v \cos(\psi) & -m_2 v \sin(\psi) & 0 \\ m_1 \cos(\psi) & m_1 \sin(\psi) & 0 \\ -m_2 \sin(\psi) & -m_2 \cos(\psi) & 0 \\ 0 & 0 & m_3 \end{bmatrix}^T \quad (5.21)$$

$K_w \in \mathbb{R}^3 \times \mathbb{R}^3$  is a positive definite matrix that determines the convergence rate of the observer and  $g_b(\mathbf{x})^{-1} \in \mathbb{R}^3 \times \mathbb{R}^6$  is the pseudo inverse of  $g_b(\mathbf{x})$ . By integrating (5.21) with respect to  $\mathbf{x}$ ,  $p(\mathbf{x})$  will be:

$$p(\mathbf{x}) = MR(\psi)^T \mathbf{v} = \begin{bmatrix} m_{11} u \cos(\psi) - m_{22} v \sin(\psi) \\ m_{11} u \sin(\psi) + m_{22} v \cos(\psi) \\ m_{33} r \end{bmatrix}. \quad (5.22)$$

This choice makes the deterministic observer estimation error(5.4) linear with eigenvalues equal to the scalar  $K_w$ :

$$\dot{\tilde{\mathbf{b}}} = -K_w \tilde{\mathbf{b}}. \quad (5.23)$$



**Proposition 5.1.** *Consider the ship dynamics given by (3.40) with a constant unknown disturbance  $\mathbf{b}$  and full states measurement  $\mathbf{x}$  which is filtered to reject the effect of  $\boldsymbol{\omega}$ . A disturbance observer based on (5.9), with  $l(\mathbf{x})$  given by (5.21) and  $p(\mathbf{x})$  by (5.22) makes the error  $\tilde{\mathbf{b}}$  converge asymptotically to the origin.*

*Proof.* If we filtered for the white noise  $\boldsymbol{\omega}$ , the vessel dynamics will be similar to (5.1). Select the candidate Lyapunov function as (5.15). The time derivative of it will be:

$$\dot{V}_{do} = -\tilde{\mathbf{b}}^T K_w \tilde{\mathbf{b}} \quad (5.24)$$

If  $K_w$  is selected to be positive definite then the system (5.7) is globally asymptotically stable with a time constant  $\frac{1}{\lambda_{\min}(K_w)}$ .  $\square$

The next proposition applies Theorem 5.1 to the vessel (3.40).

**Proposition 5.2.** *Consider the ship dynamics given by (3.40) with a time varying unknown disturbance  $\mathbf{b}$  as in Assumption 5.1 and full states measurement  $\mathbf{x}$  which is filtered to reject the effect of  $\boldsymbol{\omega}$ . A disturbance observer based on (5.9), with  $l(\mathbf{x})$  given by (5.21) and  $p(\mathbf{x})$  by (5.22), settles within the compact set  $\Omega_{\tilde{\mathbf{b}}} = \{\tilde{\mathbf{b}} \in \mathbb{R}^3 \mid \|\tilde{\mathbf{b}}\| \leq \xi_{\tilde{\mathbf{b}}}, \xi_{\tilde{\mathbf{b}}} > \sqrt{\frac{C_d}{\alpha}}\}$  which can be made arbitrarily small by appropriately selecting the design matrix  $K_w$ . The practical stability of the disturbance observer is ensured.*

*Proof.* If we filtered for the white noise  $\boldsymbol{\omega}$ , the vessel dynamics will be similar to (5.1). Select the candidate Lyapunov function as (5.15). From (5.21) and Theorem 5.1,  $\alpha = \lambda_{\min}(K_w) - \frac{1}{2}$  and  $C_d = \frac{1}{2}\rho^2$ . If  $K_w$  is selected to be positive definite with  $\lambda_{\min}(K_w) > \frac{1}{2}$  then  $\tilde{\mathbf{b}}$  converges to  $\Omega_{\tilde{\mathbf{b}}} = \{\tilde{\mathbf{b}} \in \mathbb{R}^3 \mid \|\tilde{\mathbf{b}}\| \leq \xi_{\tilde{\mathbf{b}}}\}$ , i.e.  $\tilde{\mathbf{b}}$  is globally uniformly ultimately bounded.  $\square$

### 5.5.1 Case 1

We evaluate the observer proposed in Proposition 5.1 to estimate a piecewise periodic disturbance of a period 300 *sec*. A single period version of it is:

$$\mathbf{b}(t) = \begin{cases} [1800N \ 800N \ 700N \cdot m]^T & 0 \leq t < 150 \\ [600N \ -800N \ -700N \cdot m]^T & 150 \leq t < 300 \end{cases}, \quad (5.25)$$

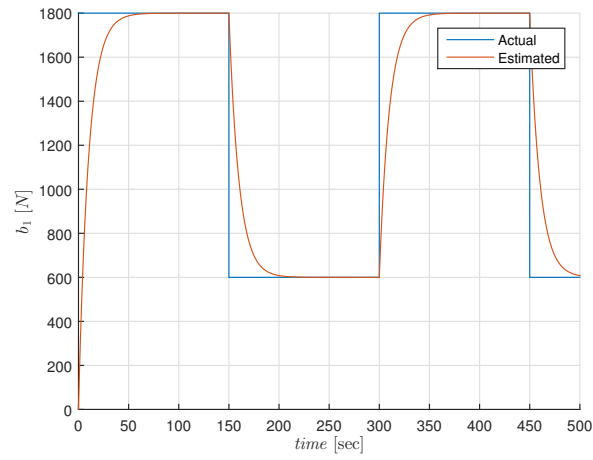
The ship is driven by a piecewise periodic control input that has a period of 200*sec* with a single period given by:

$$\boldsymbol{\tau}(t) = \begin{cases} \begin{bmatrix} 120kN \\ 70kN \cdot m \end{bmatrix} & 0 \leq t < 200 \\ \begin{bmatrix} 60kN \\ -70kN \cdot m \end{bmatrix} & 200 \leq t < 400 \end{cases}. \quad (5.26)$$

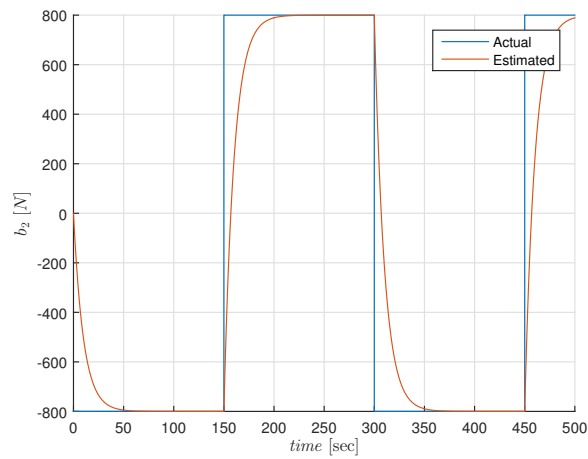
The design matrix  $K_w$  is selected to be  $K_w = \text{diag}(0.1, 0.1, 0.1)$ . Figure 5.3 shows the actual and the estimated disturbances in the surge, sway and yaw velocities. It is clear that the proposed observer tracks the unknown constant disturbance with a settling time of 40 *sec*.

**Table 5.1:** Robust NDO performance index

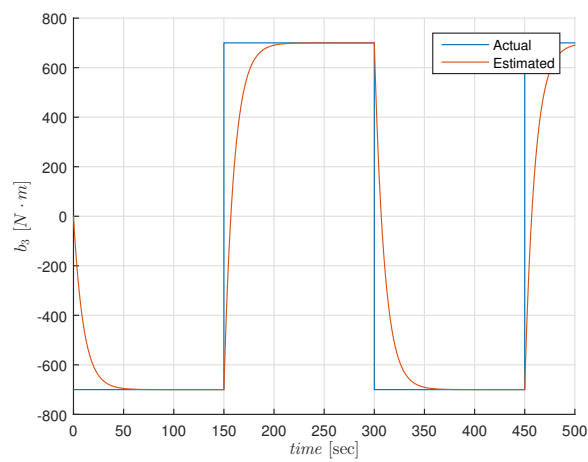
	$\int_0^{500}  b_1(t)  dt$	$\int_0^{500}  b_2(t)  dt$	$\int_0^{500}  b_3(t)  dt$
$K_w = \begin{bmatrix} 0.5 & 0 & 0 \\ 0 & 0.5 & 0 \\ 0 & 0 & 0.5 \end{bmatrix}$	6069.97	4856.40	3642.94
$K_w = \begin{bmatrix} 5.0 & 0 & 0 \\ 0 & 5.0 & 0 \\ 0 & 0 & 5.0 \end{bmatrix}$	608.10	486.52	364.96
$K_w = \begin{bmatrix} 20.0 & 0 & 0 \\ 0 & 20.0 & 0 \\ 0 & 0 & 20.0 \end{bmatrix}$	152.04	121.64	91.25



(a) Surge Disturbance



(b) Sway Disturbance



(c) Yaw Disturbance

**Figure 5.3:** Simulation results of the NDO proposed in Proposition 5.1

### 5.5.2 Case 2

The robust disturbance observer proposed in Proposition 5.2 is evaluated in this subsection. The actual disturbance is assumed to be sinusoidal with a frequency of  $0.01\text{rad}/\text{sec}$  as follows:

$$\mathbf{b}(t) = \begin{bmatrix} 1000 \sin(0.01t) \\ 800 \sin(0.01t + 0.001) \\ 600 \sin(0.01t + 0.003) \end{bmatrix} \quad (5.27)$$

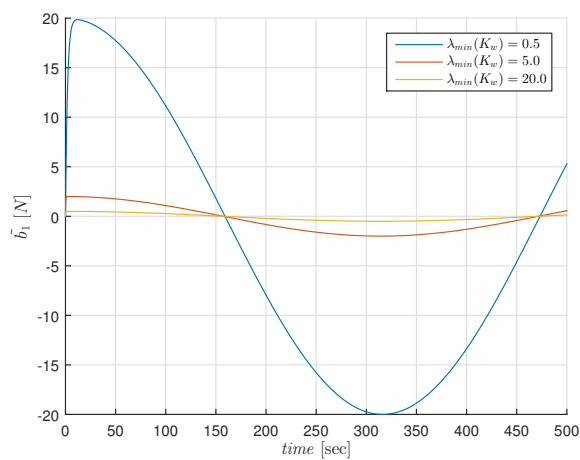
The ship is driven with the same input as in Case 1. The response curves of the three disturbance estimation errors under different observer parameters are shown in Figure 5.2. The design matrix  $K_w$  is selected to be  $K_w = \text{diag}(0.5, 0.5, 0.5)$ ,  $K_w = \text{diag}(5, 5, 5)$ , and  $K_w = \text{diag}(20, 20, 20)$  which, according to (5.17), imply that the eigenvalues of observer error dynamics are 0.0, 4.5 and 19.5. Furthermore, in order to quantitatively evaluate the effect of the design matrix  $K_w$  on the estimated error, the integral of the absolute estimation error is given in Table 5.1.

It can be observed from Figure 5.2 that a smaller bounds of the estimation error is obtained if the eigenvalues  $K_w$  of observer error dynamics are placed farer away from the imaginary axis which leads also to small absolute integral error as seen in Table 5.1.

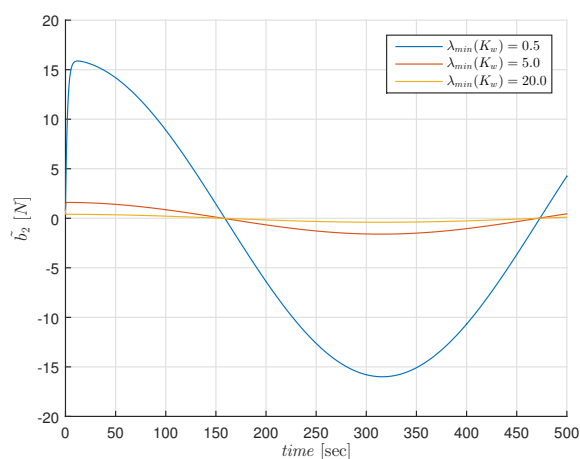
### 5.5.3 Case 3: Discretization Effect

In this subsection we evaluate the performance of the discretized version the NDO. The NDO (5.9) is discretized using a fixed step 4th order implicit Runge–Kutta method. Implicit methods are usually desirable for stiff equations because their region of absolute stability is bigger than the explicit methods.

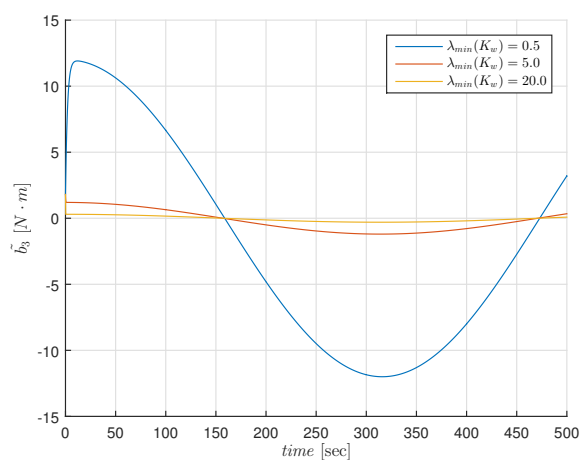
We select the disturbance to be piecewise periodic signal of a period of 300 sec as in (5.25) and the ship is driven by a piecewise periodic input of a period 200sec as in (5.26). The sampling interval is selected to be  $T_s = 1\text{sec}$  and four different



(a) Surge disturbance error



(b) Sway disturbance error



(c) Yaw disturbance error

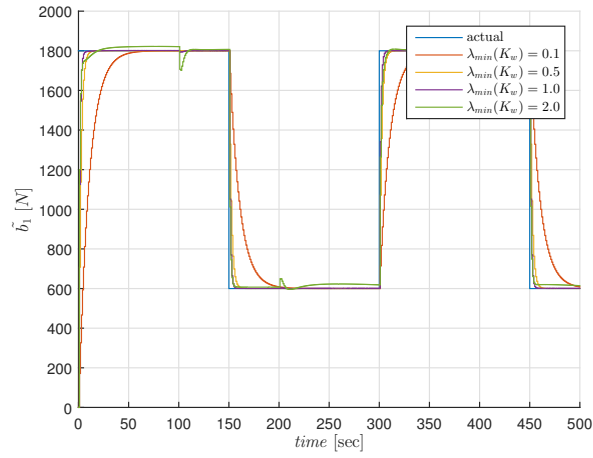
**Figure 5.4:** Simulation results of the robust NDO proposed in Propostion 5.2

**Table 5.2:** Discrete NDO performance index

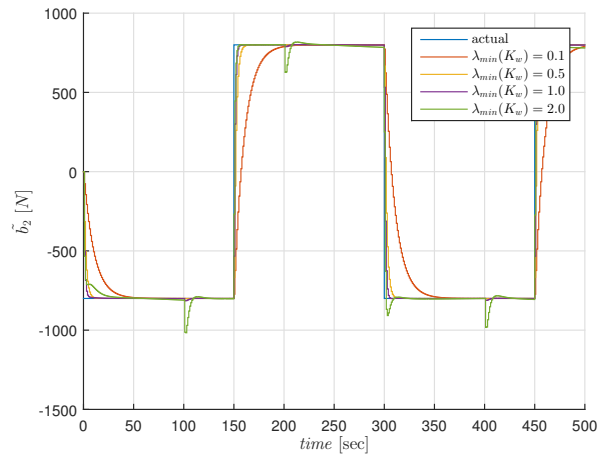
	$\sum_{n=0}^{500}  b_1(nT_s)  dt$	$\sum_{n=0}^{500}  b_2(nT_s)  dt$	$\sum_{n=0}^{500}  b_3(nT_s)  dt$
$K_w = \begin{bmatrix} 0.1 & 0 & 0 \\ 0 & 0.1 & 0 \\ 0 & 0 & 0.1 \end{bmatrix}$	56660.034	57895.267	50657.790
$K_w = \begin{bmatrix} 0.5 & 0 & 0 \\ 0 & 0.5 & 0 \\ 0 & 0 & 0.5 \end{bmatrix}$	13781.75	13258.802	11570.860
$K_w = \begin{bmatrix} 1.0 & 0 & 0 \\ 0 & 1.0 & 0 \\ 0 & 0 & 1.0 \end{bmatrix}$	9141.557	8022.609	6720.0
$K_w = \begin{bmatrix} 2.0 & 0 & 0 \\ 0 & 2.0 & 0 \\ 0 & 0 & 2.0 \end{bmatrix}$	1.5577.836	11857.983	5250.0

values of  $K_w$  are evaluated as depicted in Figure 5.5. The sum of the absolute error over the simulation period is shown in Table 5.2.

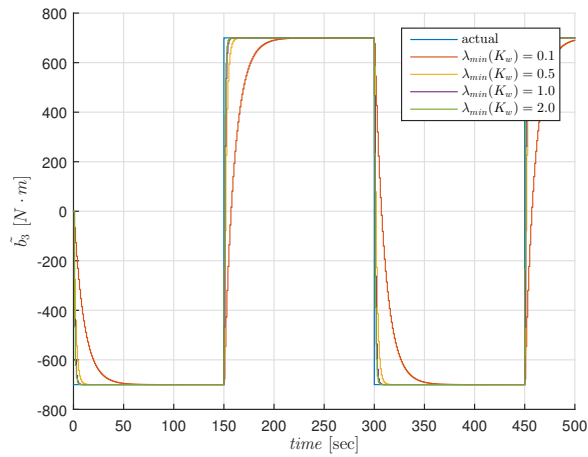
It is clear from Table 5.2 that increasing the gain  $K_w$  leads to a better performance, in terms of lower integral error, until  $K_w = \text{diag}(2, 2, 2)$  when oscillations start to occur. Increasing the gain more than  $K_w = \text{diag}(2, 2, 2)$ , the observer dynamics become unstable.



(a) Surge disturbance



(b) Sway disturbance



(c) Yaw disturbance

**Figure 5.5:** Simulation results of the discrete version of NDO proposed in Proposition 5.2





# 6

## NMPC for Trajectory Tracking of Surface Vessels

### 6.1 Introduction

In order to design a ship motion controller, the control objective must be well defined according to the required motion specification. In this context, there are three important control objectives which are studied in the literature [11]:

- **Setpoint Regulation:** It is a special control objective where the setpoint is constant. Its application in the maritime domain could be dynamic positioning (DP) where the objective is to steer the vessel slowly to the desired position and heading and then maintain them by counteracting environmental forces.
- **Path-Following Control:** The objective of this controller is to steer the vessel to follow a reference path independent of time, i.e. no temporal constraint. Moreover, no restrictions are placed on the temporal propagation along the path. This is typical for ships in transit between continents. The mathematical problem formulation is to design a feedback controller that bounds the position/orientation  $\boldsymbol{\eta}(t)$  of the vessel to remain close to a reference

position  $\boldsymbol{\eta}_r(\alpha)$  which is parametrized by  $\alpha \in R$ , i.e.  $\|\boldsymbol{\eta}(t) - \boldsymbol{\eta}_r(\alpha(t))\|$  converges to a neighborhood of the origin that can be made arbitrarily small. It is required that  $\boldsymbol{\eta}_r$  is sufficiently smooth with respect to  $\alpha$  and its derivatives (with respect to  $\alpha$ ) is bounded[107].

- **Trajectory-Tracking Control:** Here, the control objective is to steer the ship position and velocity to track a time varying reference that is usually generated by a reference model, a vessel dynamic model, or an optimization technique. In this case, the time propagation is taking into consideration which is necessary in near collision situations. The mathematical problem formulation is to design a feedback controller that bounds the states of the vessel or a function of them  $h(\boldsymbol{x}(t))$  to remain close to a reference  $h(\boldsymbol{x}_r(t))$ , i.e.  $\|h(\boldsymbol{x}(t)) - h(\boldsymbol{x}_r(t))\|$  converges to a neighborhood of the origin that can be made arbitrarily small.

From the controllability point of view, the vessels can be classified into two types which are necessary to distinguish before designing a controller. To specify them, the configuration space need to be specified:

**Definition 6.1** (Configuration Space). *The  $n$ -dimensional configuration space is the space of possible positions and orientations that a vessel may attain.*

It is usually described by an  $n$ -dimensional vector of generalized coordinates, that is the least number of coordinates needed to uniquely specify the state of the system. For ships, the configuration space is represented by the generalized positions and velocities,  $\boldsymbol{\eta} \in \mathbb{R}^6$  and  $\boldsymbol{v} \in \mathbb{R}^6$ , and has a dimension  $dim(\boldsymbol{\eta}) = 6$ .

Underactuation and full actuation can be defined with respect to the configuration space in the sense of having number of independent actuators less than and equal to the configuration space, respectively. This can lead to a misconception when it comes to control systems. Suppose that the control objective is to control the horizontal motion of the ship in the 3-DOF (surge, sway and yaw), if the ship

has 3 independent actuators in these 3 direction, the ship will be classified as an underactuated ship as it has a configuration space dimension of  $\dim(\boldsymbol{\eta}) = 6$ , although the desired control objective can be achieved with these three forces and moments. This suggest to classify underactuated and full actuated ship with respect to the workspace of the craft and not the configuration space while designing a motion control system.

**Definition 6.2** (Workspace). *The workspace is a reduced space of dimension  $m < n$  in which the control objective is defined.*

According to that, full actuated and underactuated controlled ship will be defined as:

**Definition 6.3** (Fully actuated vessel). *Fully actuated vessel is a vessel that is equipped with number of independent actuators equal to the dimension of the workspace, i.e. it could produce independent forces and moments in all the directions of the degrees of freedom under control.*

**Definition 6.4** (Underactuated vessel). *Underactuated vessel is a vessel that is equipped with a number of independent actuators less than the dimension of the workspace, i.e. it could not produce independent forces and moments in all the directions of the degrees of freedom under control.*

Based on these definitions, a vessel with a horizontal motion objective is full actuated when it has actuators that produce independent forces in the surge, sway and yaw directions, and is underactuated when it does not have. Most of the ships are equipped with two independent aft thrusters or with one main aft thruster and a rudder and therefore underactuated. In the first case, the sway force is zero while the sway force and the yaw moment are dependent in the second case. It is easier to control a fully actuated vessel while Underactuation adds control restrictions and decreases the controllability of the ship. Unfortunately, most ships are underactuated since they can not produce control forces and moments in all DOFs under control.

In the following sections, we utilize different NMPC formulations to solve the trajectory tracking problem of the simplified underactuated ship model provided in (3.41) and with the parameters given in Appendix A.

## 6.2 Nominal Trajectory Tracking

In this section, NMPC is used to solve the trajectory tracking problem for the nominal underactuated vessel (3.40), i.e. assuming no disturbance:

$$\dot{\mathbf{x}} = \mathcal{F}(\mathbf{x}) + g\mathbf{u} \quad (6.1)$$

A time-varying reference trajectory is generated by a virtual ship with the same dynamics as (3.41):

$$\dot{\mathbf{x}}^{ref} = \mathcal{F}(\mathbf{x}^{ref}) + g\mathbf{u}^{ref} \quad (6.2)$$

where  $\mathbf{x}^{ref} = [\boldsymbol{\eta}^{ref} \ \mathbf{v}^{ref}]^T$  is the reference states vector, and  $\mathbf{u}^{ref}$  is the reference control input vector. The same assumptions, as in [37], are adopted throughout this chapter:

**Assumption 6.1.** *All ship state variables (position, orientation and velocities) are measurable or can be accurately estimated.*

**Assumption 6.2.** *The reference velocities and positions are smooth over time.*

Hence, the NMPC control objective is to steer the vessel states  $\mathbf{x}$  to follow the reference states  $\mathbf{x}^{ref}$  while satisfying the following actuator constraints:

$$\begin{aligned} \tau_{u\min} &\leq \tau_u \leq \tau_{u\max}, \\ \tau_{r\min} &\leq \tau_r \leq \tau_{r\max}. \end{aligned} \quad (6.3)$$

where  $\tau_{u\min}$  and  $\tau_{r\min}$  are the minimum surge force and yaw moment, respectively, and  $\tau_{u\max}$  and  $\tau_{r\max}$  are the maximum surge force and yaw moment, respectively. The optimal control problem formulation for trajectory tracking will be similar to  $\text{OCPT}_{T_p}^t$ :

$$\begin{aligned}
\min_{\mathbf{u}(\cdot)} V_{T_p}(t, \mathbf{x}_{t_k}, \mathbf{u}(\cdot)) &= \int_{\tau=t_k}^{t_k+T_p} \ell(\tau, \mathbf{x}(\tau), \mathbf{u}(\tau)) d\tau \\
\text{subject to :} & \\
\dot{\mathbf{x}}(t) &= f(\mathbf{x}, \mathbf{u}) = \mathcal{F}(\mathbf{x}) + g\mathbf{u} \text{ with } \mathbf{x}(t_k) = \mathbf{x}_{t_k} \\
\mathbf{u}(t) &\in \mathbb{U}, \forall t \in [t_k, t_k + T_p)
\end{aligned}$$

where the stage cost function is selected to be:

$$\ell(t, \mathbf{x}(t), \mathbf{u}(t)) = \|\mathbf{x}(t) - \mathbf{x}(t)^{ref}\|_Q + \|\mathbf{u}(t) - \mathbf{u}(t)^{ref}\|_R, \quad (6.4)$$

the feasible control set  $\mathbb{U}$  is defined by

$$\mathbb{U} = \{\mathbf{u} \mid \mathbf{u}_{min} \leq \mathbf{u} \leq \mathbf{u}_{max}, \mathbf{u} \in \mathbb{R}^2, \mathbf{u}_{min} = \begin{bmatrix} \tau_{u_{min}} \\ \tau_{r_{min}} \end{bmatrix}, \mathbf{u}_{max} = \begin{bmatrix} \tau_{u_{max}} \\ \tau_{r_{max}} \end{bmatrix}\}. \quad (6.5)$$

### 6.2.1 Simulation Results

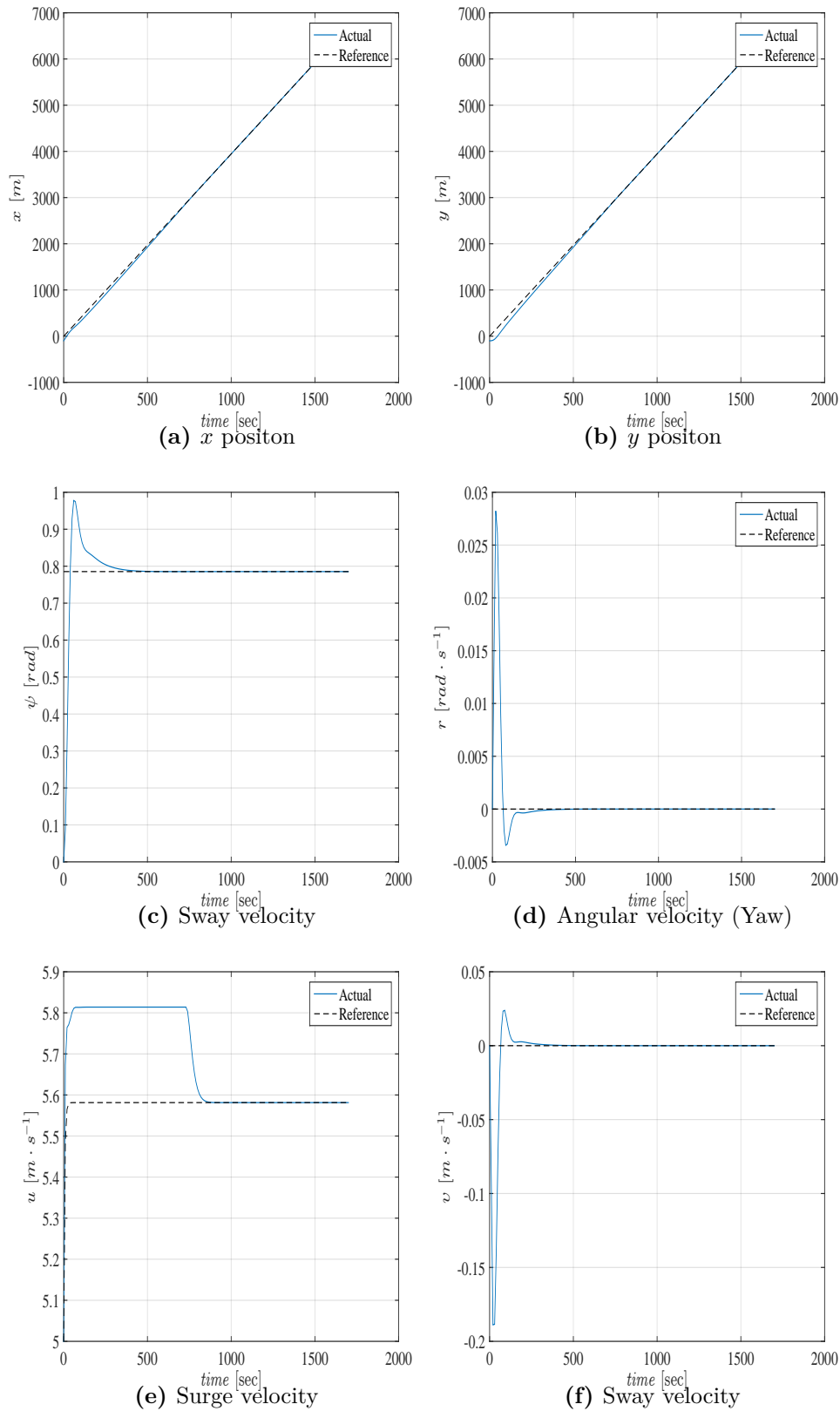
To assess the performance of this algorithm, two simulation scenarios are presented using MATLAB with the aid of ACADO toolkit and qpOASES solver. These results have been obtained on 3.3 GHz core i5 CPU with 8 GB RAM. The NMPC parameters are given in Table 6.1.

**Table 6.1:** NMPC Parameters for Trajectory Tracking

Parameter	Value
$T_p$	150.0 sec
$T_s$	5.0 sec
$N$	30
$Q$	$diag(5, 5, 5, 0.2, 0.2, 0.2)$
$R$	$diag(0.001, 0.001)$

#### Scenario 1

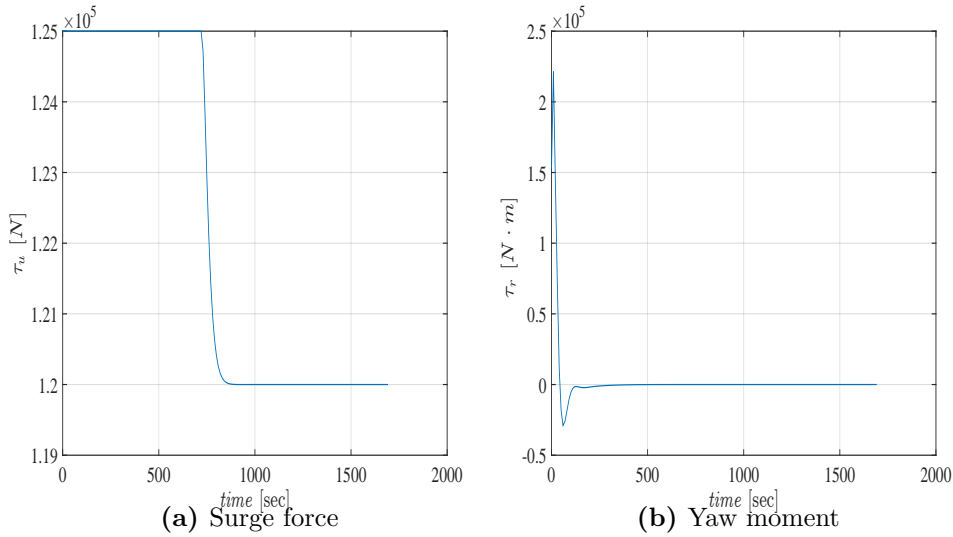
A straight line reference is generated by applying  $\tau_u^{ref}(t) = 120.0$  kN and  $\tau_r^{ref}(t) = 0.0$  N.m without excitation for the yaw velocity as  $r^{ref}(t) = 0$ , and the reference initial conditions and the actual ship initial condition are given in Table 6.2:



**Figure 6.1:** NMPC simulation results of the states for scenario 1.

**Table 6.2:** Initial Conditions

Reference Initial Condition	Value	Actual Initial Condition	Value
$x^{ref}$	0.0 m	$x$	-100.0 m
$y^{ref}$	0.0 m	$y$	-100.0 m
$\psi^{ref}$	$\frac{\pi}{4}$ rad	$\psi$	0.0 rad
$u^{ref}$	5.0 m/sec	$u$	5.0 m/sec
$v^{ref}$	0.0 m/sec	$v$	0.0 m/sec
$r^{ref}$	0.0 rad/sec	$r$	0.0 rad/sec

**Figure 6.2:** NMPC simulation results of the control input for scenario 1.

The surge, sway, and yaw velocities are depicted in Figures 6.1e, 6.1f and 6.1d, respectively, while the positions and heading are depicted in Figures 6.1a, 6.1b and 6.1c. The tracked trajectory of the vessel is presented in Figure 6.3, and the surge force and yaw moments are demonstrated in Figure 6.2a and 6.2b. It is shown that the vessel can follow the straight line reference trajectory without the need to sway velocity ( $v$ ) excitation, which can not be achieved in many backstepping techniques such as [108], while satisfying the control law bounds constraint as shown in Figure 6.2.

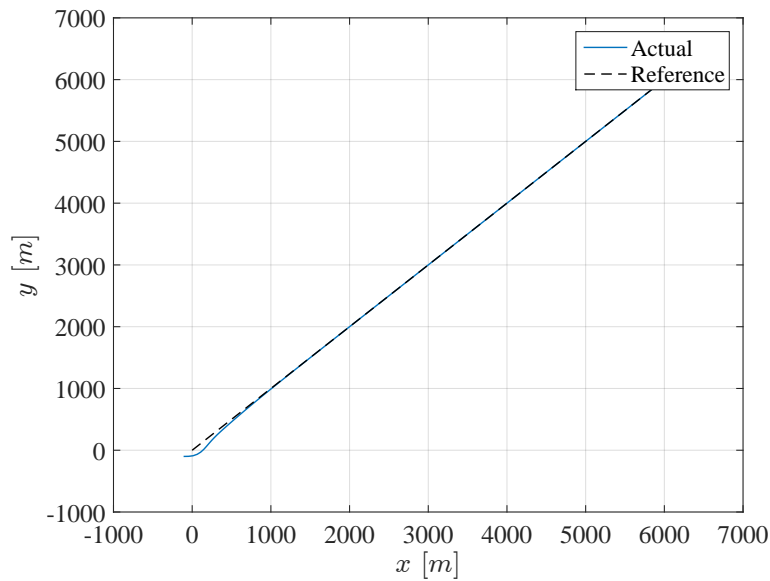


**Figure 6.3:** NMPC simulation results of the trajectory for scenario 1.

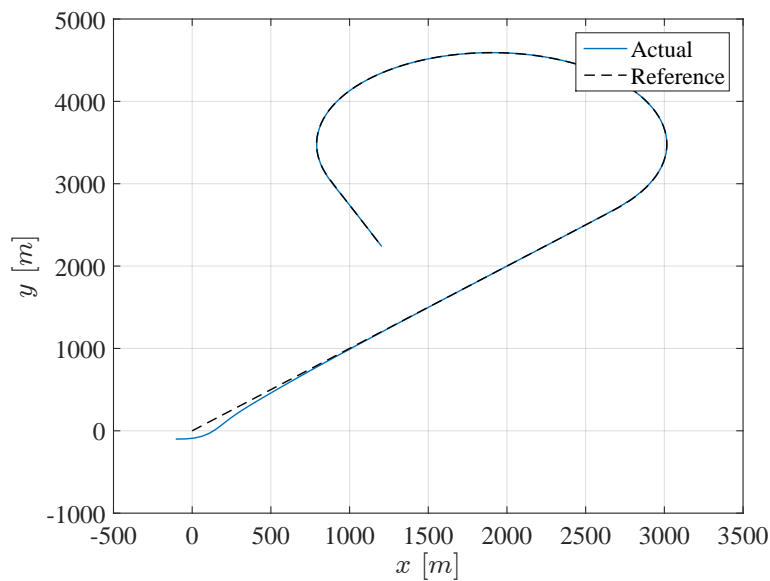


**Figure 6.4:** NMPC simulation results of the trajectory for scenario 2.

## Scenario 2

To assess the performance of the proposed technique, a curved reference path is fed to the algorithm with reference initial condition and vessel initial condition as in Scenario 1 and with the same NMPC parameters.

The tracking trajectory of the vessel is presented in Figure 6.4, and the surge,



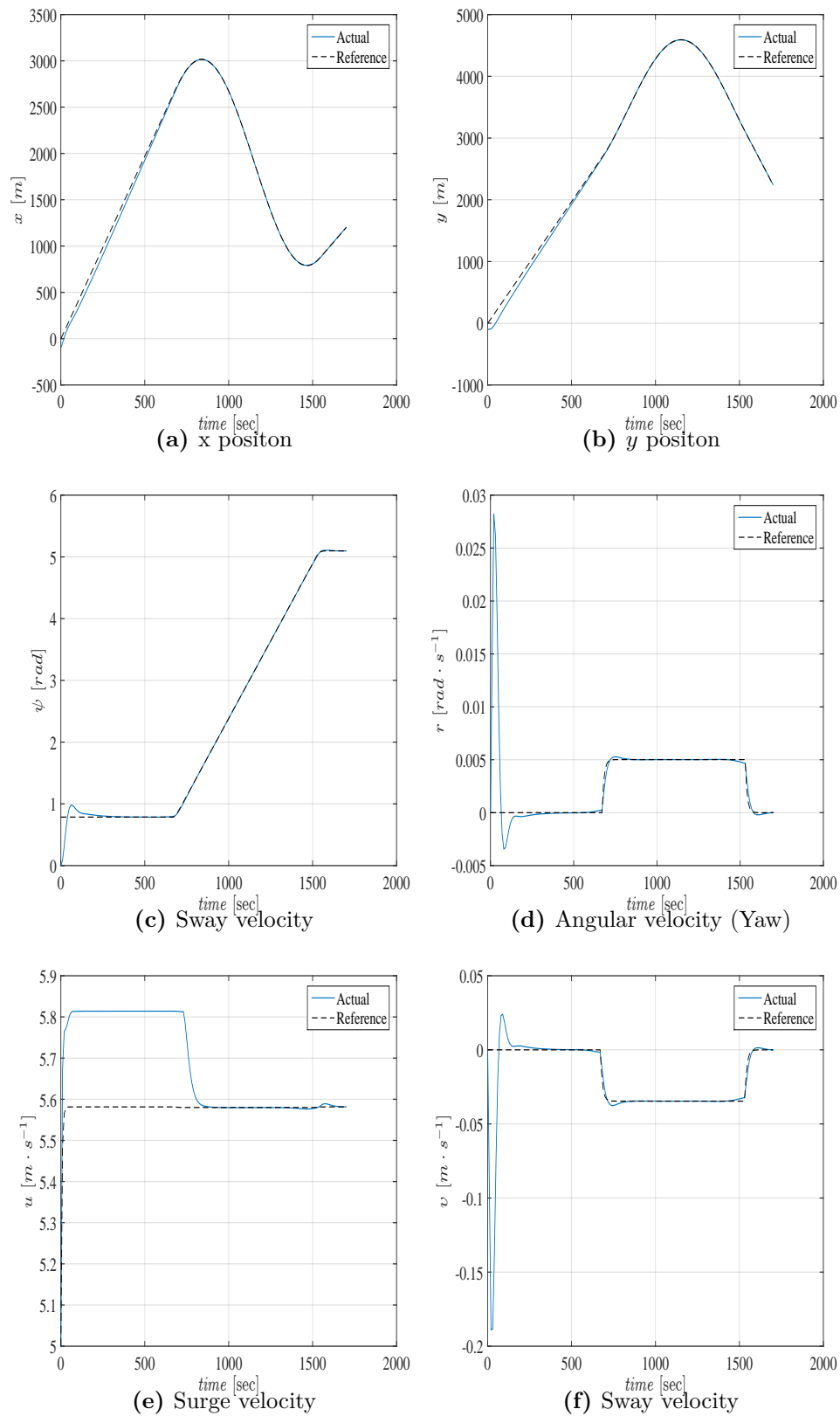


**Figure 6.5:** NMPC simulation results of the states for scenario 2.

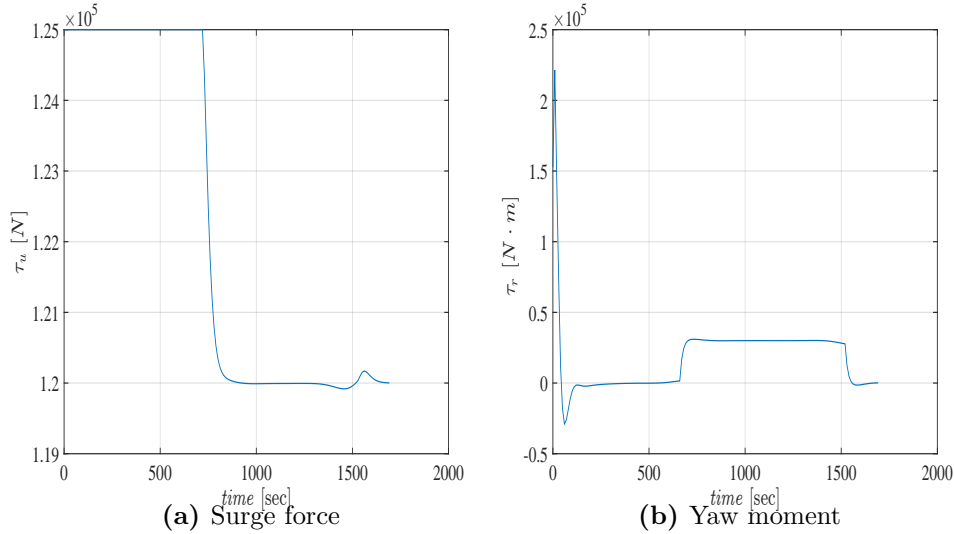


**Figure 6.6:** NMPC simulation results of the control input for scenario 2.

sway and yaw velocities are depicted in Figures 6.5e, 6.5f and 6.5d, respectively. The positions and heading are shown in Figures 6.5e, 6.5f and 6.5d, respectively. The surge force and yaw moments are demonstrated in Figures 6.6a and 6.6b. The controller shows a great ability to follow curved paths while satisfying the maximum surge force and yaw moment.

As the vessel starts from an initial condition different from the reference in both scenarios, the surge speed reference is violated until the position error is around zero, which is achieved by increasing the position factors of the weighing matrix  $Q$  over the velocity factors. The worst-case execution time of the generated code on the aforementioned computer are  $1.4867$  ms and  $1.9896$  ms for scenarios one and two, respectively, which are extremely small compared to our 10.0 seconds sampling interval and taking into consideration the selected long prediction and control horizon of 30 samples.

### 6.3 Disturbances Counteraction

The Nominal NMPC presented in Section 6.2 for solving the trajectory tracking problem of surface vessels does not take into account the external environmental

disturbance  $\mathbf{b}(t)$  which is not measured in real-time and degrades the controller performance, and does not have an integral component (like traditional linear MPC) that can compensate the disturbances.

As discussed in Chapter 5, there are two main categories that could be used to handle the disturbance in the NMPC algorithm: Passive Anti-Disturbance Control (PADC) and Active Anti-Disturbance Control (AADC). Due to the advantages of AADC mentioned there, a disturbance observer in the Disturbance Observer Based Control (DOBC) framework will be used as presented in Section 5.2.

Knowing the disturbance value, it can be compensated by adding an appropriate canceling signal that has the disturbance magnitude but in the opposite sign or equivalently, in the case of MPC, including it in the prediction model. Putting it differently, the environmental disturbances of the ship are considered as a known input for the NMPC prediction model. The combined structure of NMPC with disturbance observer is demonstrated in Figure 6.7.

Based on that, the prediction model (6.1) will be replaced by:

$$\dot{\mathbf{x}} = \mathcal{F}(\mathbf{x}) + g\mathbf{u} + g_b(\mathbf{x})\hat{\mathbf{b}} \quad (6.6)$$

where  $\hat{\mathbf{b}}$  is obtained from the nonlinear disturbance observer (5.5). The optimal control problem formulation for trajectory tracking will be similar to  $\mathbb{OCP}_{T_p}^t$ :

$$\mathbb{OCP}_{T_p, t}^{t_1} : \min_{\mathbf{u}(\cdot)} V_{T_p}(t, \mathbf{x}_{t_k}, \mathbf{u}(\cdot)) = \int_{\tau=t_k}^{t_k+T_p} \ell(\tau, \mathbf{x}(\tau), \mathbf{u}(\tau)) d\tau$$

subject to :

$$\begin{aligned} \dot{\mathbf{x}}(t) &= f(\mathbf{x}, \mathbf{u}, \hat{\mathbf{b}}) = \mathcal{F}(\mathbf{x}) + g\mathbf{u} + g_b(\mathbf{x})\hat{\mathbf{b}} \text{ with } \mathbf{x}(t_k) = \mathbf{x}_{t_k} \\ \mathbf{u}(t) &\in \mathbb{U}, \forall t \in [t_k, t_k + T_p) \end{aligned}$$

where the stage cost function and the feasible control set  $\mathbb{U}$  remain as (6.4) and (6.5), respectively. The NDO gain  $l(\mathbf{x})$  and the design matrix  $p(\mathbf{x})$  are designed according to (5.21) and (5.22), respectively.

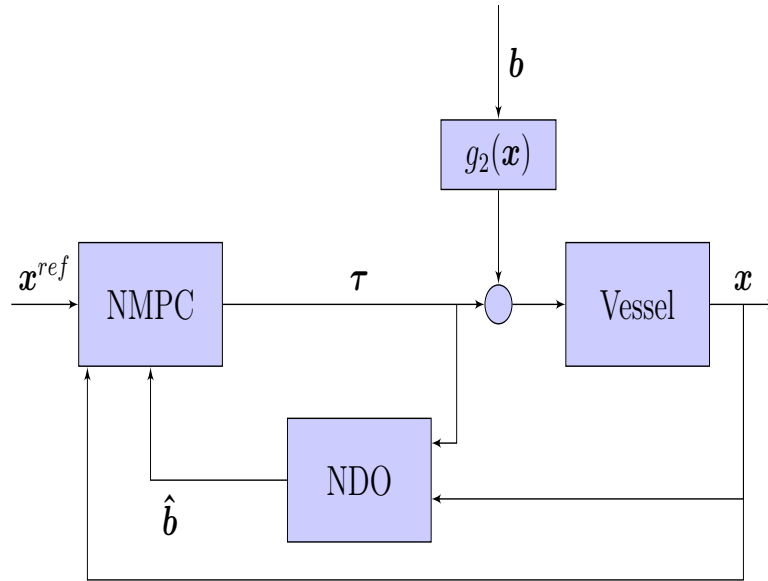


**Figure 6.7:** NMPC-NDO scheme

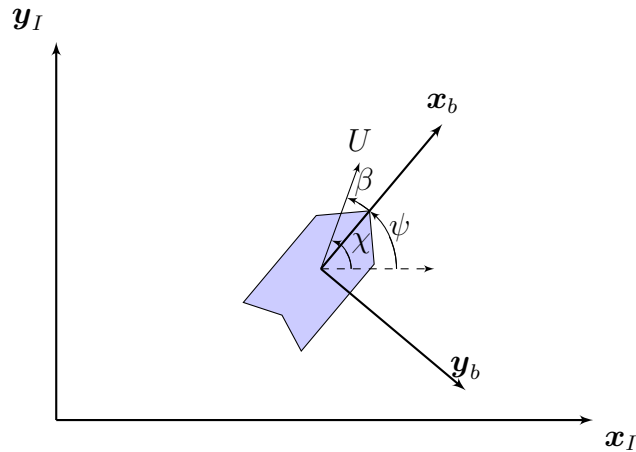


**Figure 6.8:** The geometrical relationship between course  $\chi$ , heading angle  $\psi$  and sideslip angle  $\beta$ .

### 6.3.1 Sideslip Angle Compensation

In the case of undereducated vessels, the controller can not reject the disturbance force component in the sway direction as there is no sway control force generated by the actuators of the vessel, even if the disturbance value is known.

Although the terms course and heading are used interchangeably in much of the literature on guidance, navigation and control of marine craft [11], they

are not equivalent and this leads to confusion. Here, they are going to be used differently, hence the following definitions, adopted from [11, 109], are required to avoid this confusion (see Figure 6.8):

**Definition 6.5** (Velocity Vector). *It is the specification of the vessel's speed  $U = \sqrt{u^2 + v^2}$ , and orientation  $\beta = \tan^{-1}(\frac{v}{u})$  with respect to the vessel's body reference frame.*

**Definition 6.6** (Sideslip (Drift) Angle  $\beta$ ). *The angle from  $x_B$ -axis to the velocity vector of the vessel, positive rotation about the  $z_I$ -axis by the right-hand screw convention.*

**Definition 6.7** (Heading (Yaw) Angle  $\psi$ ). *The angle from  $x_I$ -axis to the  $x_B$  axis, positive rotation about the  $z_I$ -axis by the right-hand screw convention.*

**Definition 6.8** (Course Angle  $\chi$ ). *The angle from  $x_I$ -axis to the velocity vector of the vessel, positive rotation about the  $z_I$ -axis by the right-hand screw convention.*

By these definitions, it is clear that  $\chi = \psi + \beta$ , and in case of straight line motion, the sideslip angle  $\beta$  will be zero and both heading and course angles will be equal except in case of external disturbance acting on the transverse direction. In this case, the sway velocity will not be zero, and hence heading and course angle are not equal, even for straight line motion.

In order to overcome the aforementioned limitation due to the absence of sway control force, the heading angle  $\psi$  in the stage cost function (4.6) is going to be replaced with the course angle  $\chi$ , as the vessel will not be able to achieve zero tracking error for the heading angle in case of external disturbance in the sway direction. This will lead to a non-zero sideslip angle, even if the ship is moving in straight line, but will create a force component that rejects the sway disturbance occurred in the zero-sideslip angle case. Based on that, the control objective will be steering the vessel states to track the reference states, except for the heading angle

$\psi$ , and the vessel course angle  $\chi$  to track the reference course angle  $\chi^{ref}$  where

$\chi^{ref} = \psi^{ref} + \beta^{ref}$ . Therefore, the stage cost function will be modified to:

$$\bar{\ell}(t, \mathbf{x}(t), \mathbf{u}(t)) = \|\bar{\mathbf{x}}(t) - \bar{\mathbf{x}}^{ref}(t)\|_Q + \|\mathbf{u}(t) - \mathbf{u}^{ref}(t)\|_R \quad (6.7)$$

where  $\bar{\mathbf{x}} = [x \ y \ \chi \ u \ v \ r]^T$  and  $\bar{\mathbf{x}}^{ref}(t) = [x^{ref} \ y^{ref} \ \chi^{ref} \ u^{ref} \ v^{ref} \ r^{ref}]^T$ . This is

motivated by the research done in [110] where sideslip angle is taken into account to

cope with high wind and tide conditions and achieve higher tracking accuracy even

for smaller ship speeds. The optimization problem  $\text{OC}\mathbb{P}_{T_p, t}^{t1}$  will be modified to be:

$$\text{OC}\mathbb{P}_{T_p, t}^{t2} : \min_{\mathbf{u}(\cdot)} V_{T_p}(t, \mathbf{x}_{t_k}, \mathbf{u}(\cdot)) = \int_{\tau=t_k}^{t_k+T_p} \bar{\ell}(\tau, \mathbf{x}(\tau), \mathbf{u}(\tau)) d\tau$$

subject to :

$$\begin{aligned} \dot{\mathbf{x}}(t) &= f(\mathbf{x}, \mathbf{u}, \hat{\mathbf{b}}) = \mathcal{F}(\mathbf{x}) + g\mathbf{u} + g_b(\mathbf{x})\hat{\mathbf{b}} \text{ with } \mathbf{x}(t_k) = \mathbf{x}_{t_k} \\ \mathbf{u}(t) &\in \mathbb{U}, \forall t \in [t_k, t_k + T_p) \end{aligned}$$

The algorithm for integrating NDO into the NMPC to counteract external disturbances and add integrator action into the NMPC is as follows:

**Algorithm 6.1** NMPC-NDO Algorithm for Trajectory Tracking

- 
- 1: Set the time index  $t = t_0$ , the prediction horizon  $T_p$ , sampling interval  $T_s$ , weight matrices  $Q$  and  $R$ , the observer convergence rate  $K_w$ , and the disturbance initial value  $\hat{\mathbf{b}}(t_0) = \mathbf{0}$ .
  - 2: Measure the values of the states  $\mathbf{x}(t_k)$  or estimate them.
  - 3: Solve the discretized form of the optimization problem  $\mathbb{OCP}_{T_p,t}^{t_1}$  over the discrete time instants  $T_d$  and get the optimal control sequence  $[\mathbf{u}(t_k) \cdots \mathbf{u}(t_{k+N-1})]$  and the corresponding predicted states  $[\mathbf{x}(t_k) \cdots \mathbf{x}(t_{k+N})]$ .
  - 4: Apply only the first control element  $\mathbf{u}(t_k)$ .
  - 5: Solve the NDO equations (5.5) to get the estimated value for the disturbance  $\hat{\mathbf{b}}(t + T_s)$ , and assume that it is constant over the prediction horizon.
  - 6: wait for the next sample and set the time index  $k = k + 1$ , then go to step 2.
- 

**6.3.2 Simulation Results**

To assess the performance of this algorithm, two simulation scenarios are presented using MATLAB with the aid of ACADO toolkit and qpOASES solver. These results have been obtained on 3.3 GHz core i5 CPU with 8 GB RAM. The NMPC-NDO parameters are presented in Table 6.3.

**Table 6.3:** NMPC-NDO Parameters for Trajectory Tracking

Parameter	Value
$T_p$	200.0 <i>sec</i>
$T_s$	5.0 <i>sec</i>
$N$	40
$Q$	$diag(5, 5, 5, 0.2, 0.2, 0.2)$
$R$	$diag(0.001, 0.001)$
$K_w$	$diag(0.1, 0.1, 0.1)$

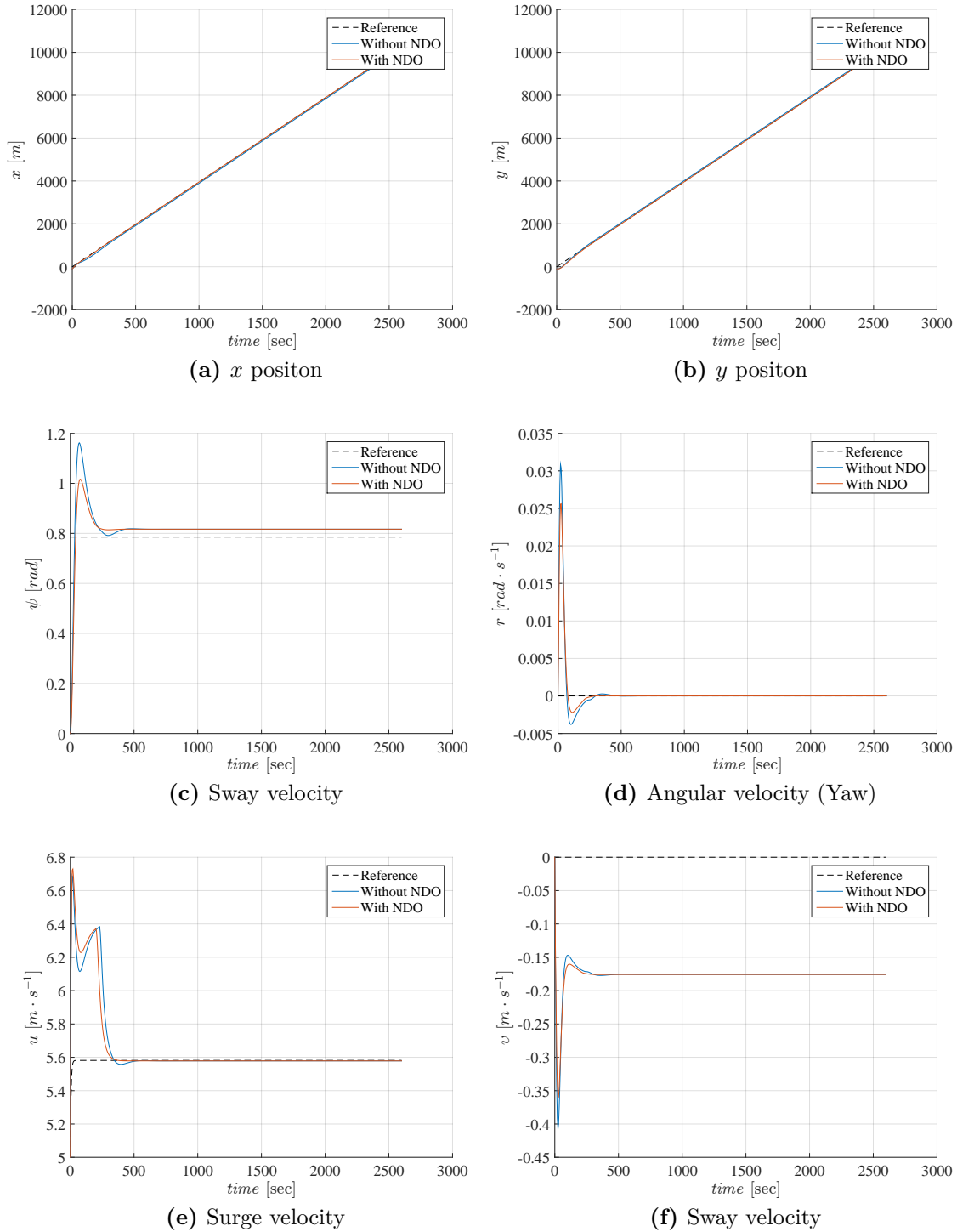


**Figure 6.9:** NMPC-NDO simulation results of the states for scenario 1.



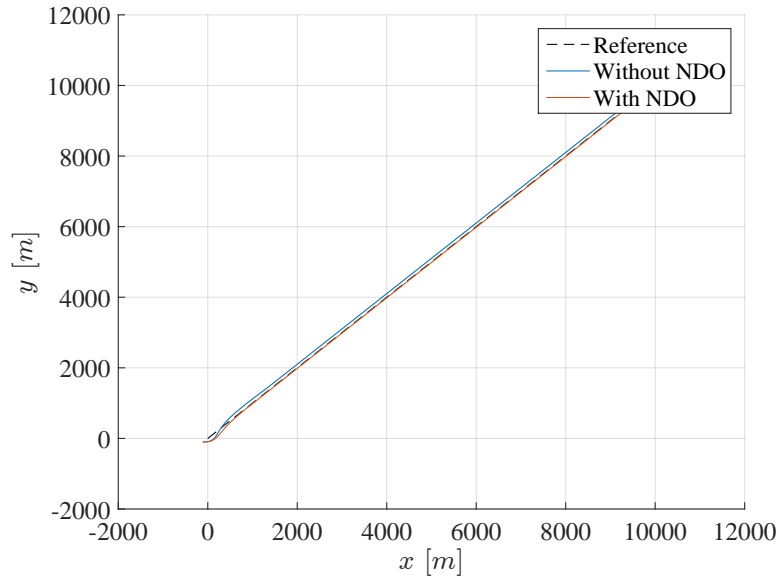


**Figure 6.10:** NMPC-NDO simulation results of the trajectory for scenario 1.

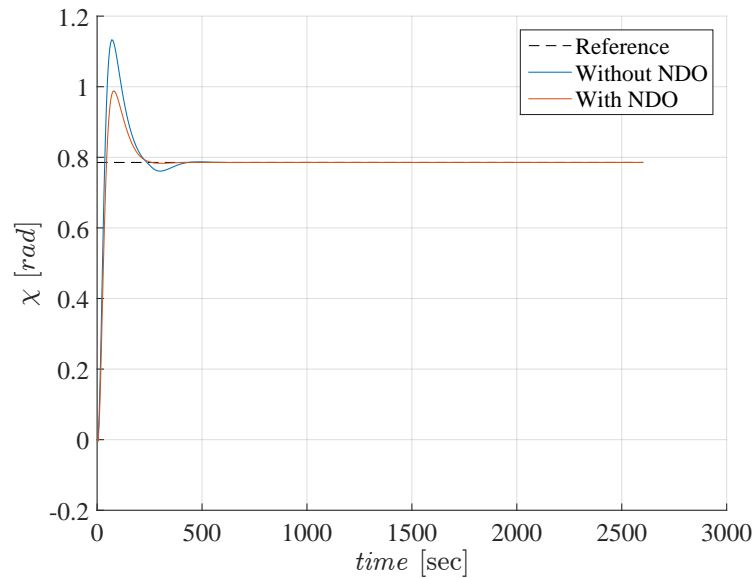


**Figure 6.11:** NMPC-NDO simulation results of the Course angle for scenario 1.

### Scenario 1

In this scenario, the NMPC-NDO algorithm is evaluated for a straight line reference trajectory that is generated by applying  $\tau_u^{ref}(t) = 120.0kN$  and  $\tau_r^{ref}(t) = 0.0N.m$  to the reference model. The reference and the actual ship initial conditions are give in Table 6.4. The vessel is subjected to a constant disturbance of

$\mathbf{b} = [14kN \ -10kN \ 5kN.m]$ . The NMPC-NDO algorithm is compared to the NMPC without disturbance estimation.

**Table 6.4:** Initial conditions for NMPC-NDO scenarios

Reference Initial Condition	Value	Actual Initial Condition	Value
$x_r$	0.0 m	$x$	-100.0 m
$y_r$	0.0 m	$y$	-100.0 m
$\psi_r$	$\frac{\pi}{4}$ rad	$\psi$	0.0 rad
$u_r$	5.0 m/sec	$u$	5.0 m/sec
$v_r$	0.0 m/sec	$v$	0.0 m/sec
$r_r$	0.0 rad/sec	$r$	0.0 rad/sec

The surge, sway and yaw velocities and positions are depicted in Figure 6.9 for the NMPC and the NMPC-NDO schemes. The surge force and yaw moment are shown in Figure 6.12. It is shown in Figure 6.13 that NDO could estimate the actual disturbance applied to the vessel. It is clear from the vessel trajectory presented in Figure 6.10 that the vessel, governed by the the NMPC-NDO, can follow the straight line reference trajectory without the need to sway velocity ( $v$ ) excitation, which can not be achieved in many backstepping techniques such as [108]. The NMPC scheme leads to a larger tracking error compared to the NMPC-NDO scheme.

It is clear in Figure 6.9c and 6.11 that the heading and course angles are not equal due to the transverse component of the environmental forces, and the controller can not lead to zero tracking error for the heading angle but almost zero for the course angle. In order to quantify the tracking performance, the integral of the tracking error performance index  $\int \|\mathbf{x}(t) - \mathbf{x}(t)^{ref}\|$  is used for both schemes. The integral tracking error for the NMPC-NDO is  $7.35 \times 10^5$ , while the NMPC leads to  $3.27 \times 10^6$ , which show how the integration of the NMPC and NDO leads to a better tracking performance.

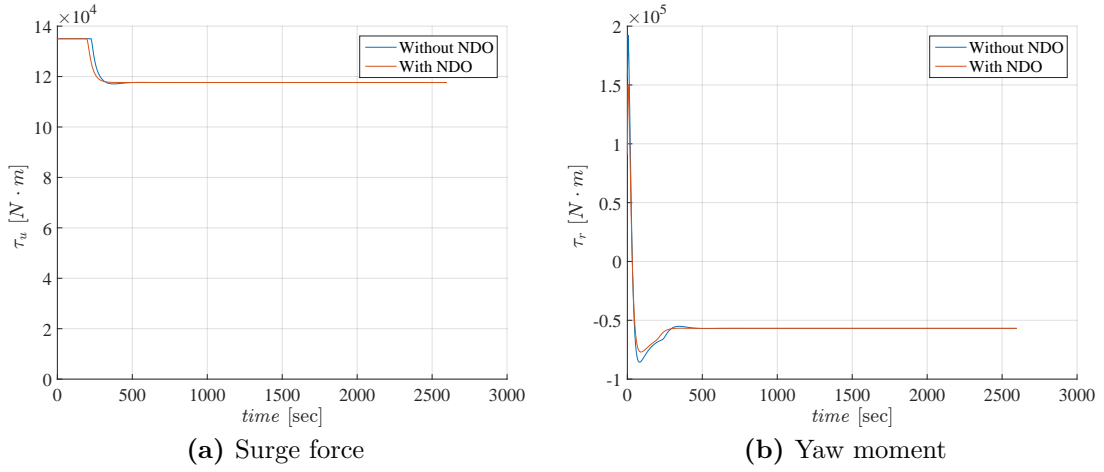


**Figure 6.12:** NMPC-NDO simulation results of the control input for scenario 1.

## Scenario 2

In this scenario, the NMPC-NDO algorithm is evaluated for a circular reference trajectory that is generated by applying  $\tau_{u_r}(t) = 120.0kN$  and  $\tau_{r_r}(t) = 10.0kN.m$  to the reference model. The reference initial conditions and the actual ship initial condition are give in Table 6.4. A constant disturbance  $\mathbf{b} = [14kN \ -10kN \ 5kN.m]$  is applied to the vessel.

The velocity and position states of the vessel are depicted in Figure6.15 for the NMPC and the NMPC-NDO schemes. The input force and moment are shown in Figure6.17. It is clear from the vessel trajectory presented in Figure6.14 that the vessel, governed by the the NMPC-NDO, can follow the circular trajectory with smaller tracking error compared to the NMPC scheme.

The integral of the tracking error performance index  $f \left\| \mathbf{x}(t) - \mathbf{x}(t)^{ref} \right\|$  for the NMPC-NDO is  $8.91 \times 10^5$ , while the NMPC leads to an error of  $2.7 \times 10^6$ , which show how the integration of the NMPC and NDO leads to a better tracking performance for the circular reference trajectory.

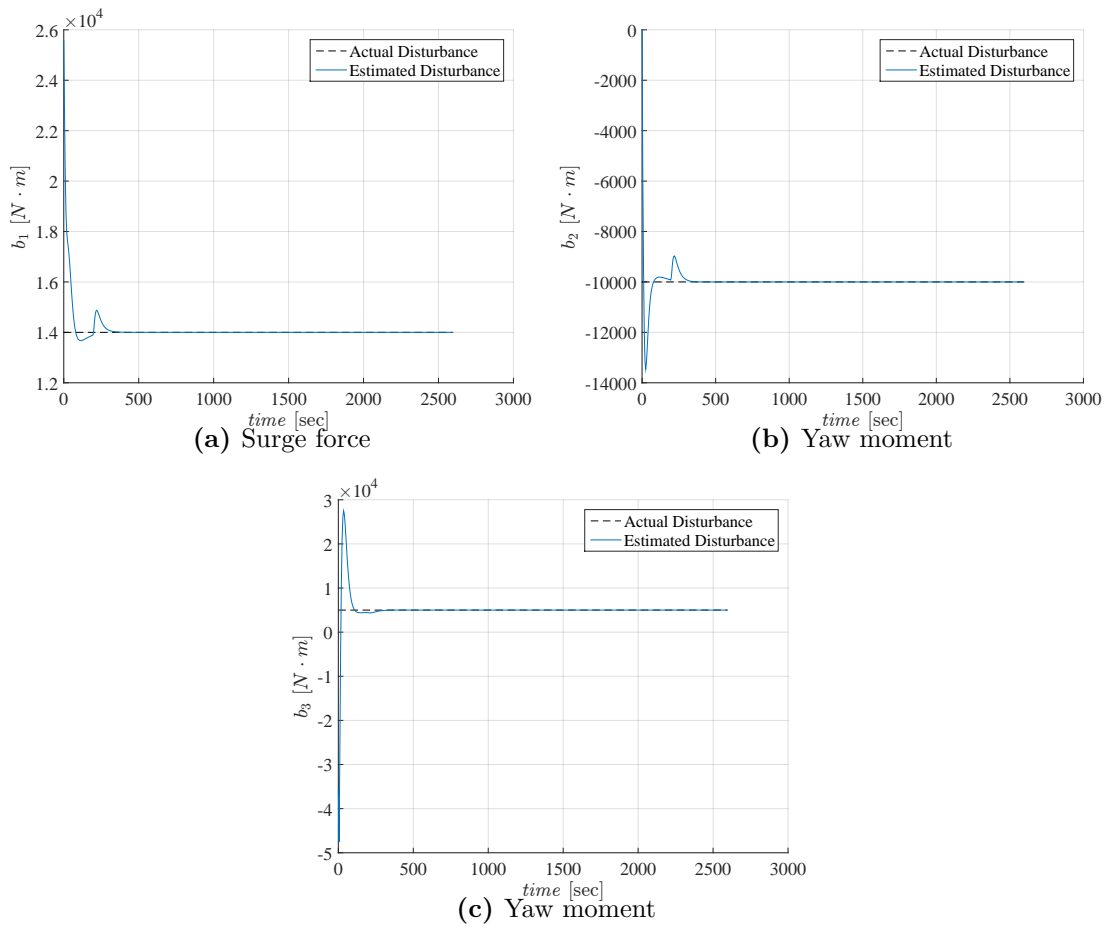


**Figure 6.13:** NMPC-NDO simulation results of the disturbance estimation  $\hat{\mathbf{b}}$  for scenario 1.

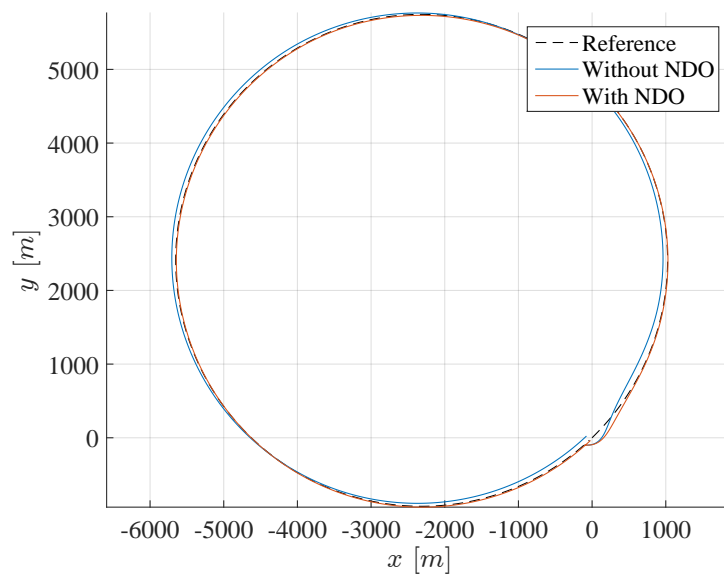


**Figure 6.14:** NMPC-NDO simulation results of the trajectory for scenario 2.

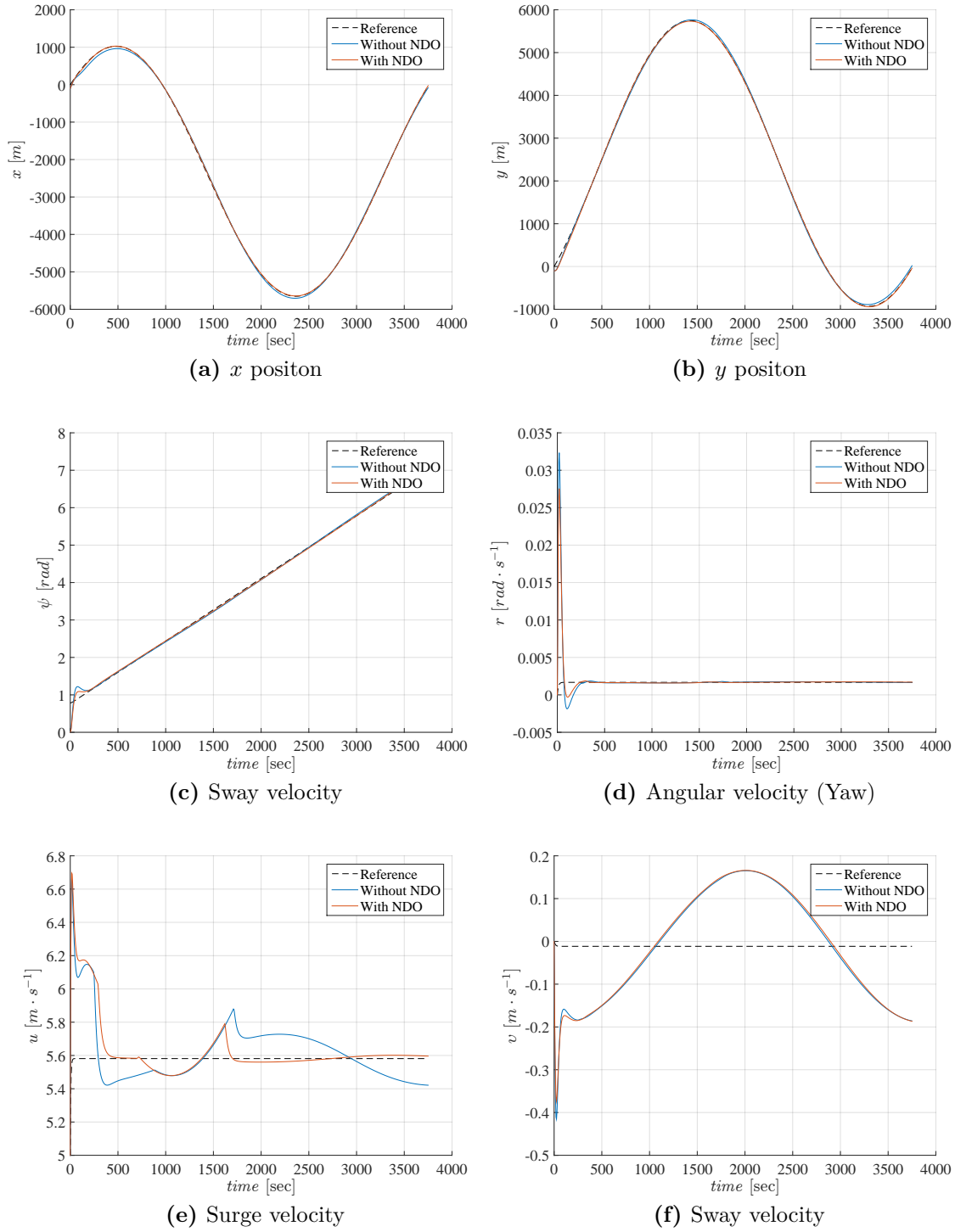
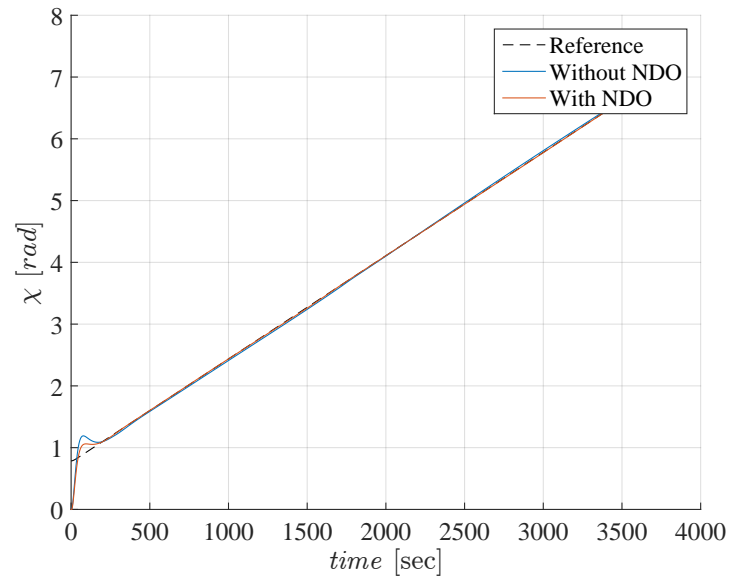
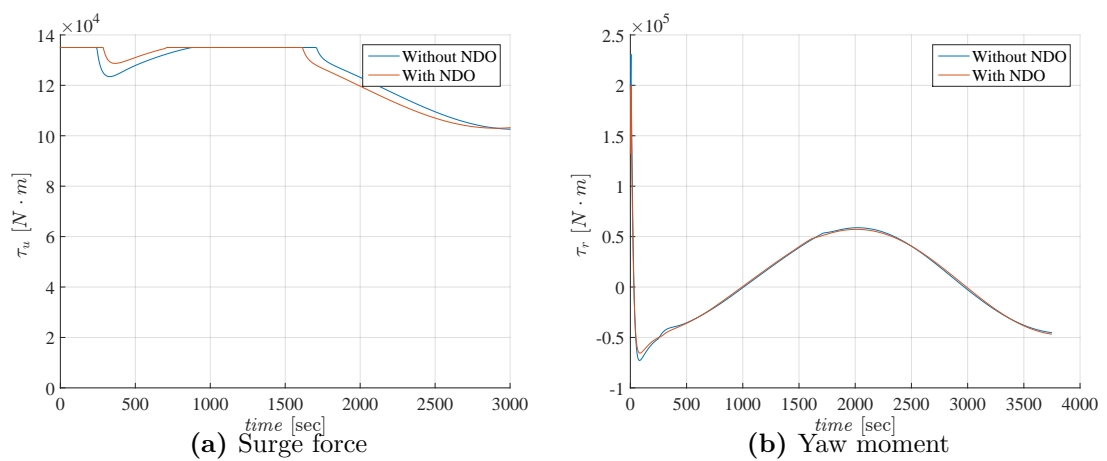


Figure 6.15: NMPC-NDO simulation results of the states for scenario 2.



**Figure 6.16:** NMPC-NDO simulation results of the course angle for scenario 2.



**Figure 6.17:** NMPC-NDO simulation results of the control input for scenario 2.





# 7

## Last-line of Defense Collision Avoidance of Surface Vessels

### 7.1 Introduction

Recently, collision avoidance systems have become essential from the viewpoint of maneuvering ships safely in crowded or crossing areas due to the increasing number of collision accidents[111]. In the maritime industry, ship collisions have always been a concern to the public because of their resulting loss of human life, assets and/or damage to the environment. Collisions between ships happen due to different reasons, often as a consequence of human error, as it was established in the past through thorough investigations, unfortunately often in the aftermath of severe disasters [112].

A collision avoidance system is a safety system designed to prevent or reduce the severity of a collision among ships and obstacles. In case of a collision risk, the collision avoidance system sends alerts to the navigators suggesting necessary actions or (in case of autonomous vessels) overrides the ship controller and sends necessary signals to the ship actuators. It is composed of two main components: obstacles

detection (not addressed in this thesis) and optimum collision-free trajectory finder which is the main focus of this chapter.

Collision avoidance is handled usually as a trajectory planning problem that generates the optimum collision-free trajectory. This trajectory is used as a reference to the trajectory tracking controller of the ship which generates the necessary forces and moments to track the reference trajectory. In this chapter, the collision avoidance problem is handled differently by integrating both the trajectory tracking and collision avoidance into one scheme. The main advantage of this scheme is the ability to include the ship dynamics in the collision avoidance design which qualify it to be a last-line of defense.

### 7.1.1 Ship Domain

The ship domain is defined by the two-dimensional area surrounding a ship that should be free from other ships or obstacles[113]. There are wide variations of ship domain models and new ones are being continuously proposed, either based on theoretical analyses or real data [114]. They are used in marine traffic engineering, e.g. for determining the capacity of traffic lanes and assessing collision risk [115, 116], as well as in collision avoidance for determining safe manoeuvres [117]. The shape and size of a ship domain are usually dependent on ship's length and speed [118] though parameters of other ships may also be taken into account [115]. Ship domains are often given explicitly as geometrical figures but, especially in case of restricted waters, they may also be given as functions proposed on the basis of safety parameters defined in the ECDIS [119]. The differences between different shapes are sometimes very subtle[118], but those small differences actually lead to different navigational decisions (collision avoidance manoeuvres).

Various ship domains have been presented by many researchers who have taken into account different shapes and sizes. The determination of ship domains strongly depends on the statistical data and operators experiences. The circular ship domain

is one of the common and simple shapes with its center located at the center of the ship and its radius determined according to the ship length. Another circular ship domain is proposed by [120] where the circle is divided into three sectors:

$$\begin{array}{ll} \text{Sector 1, starboard sector:} & 0.0^\circ < \theta < 112.5^\circ \\ \text{Sector 2, astern sector:} & 112.5^\circ < \theta < 247.5^\circ \\ \text{Sector 3, port sector:} & 247.5^\circ < \theta < 360^\circ \end{array}$$

which is smoothed in [121] to be one circle whose area is the sum of the three sectors and the center of the ship is located at lower left quarter of the smoothed circle in order to retain the same characteristics.

Elliptic ship domain is another famous design which is widely used and was firstly introduced in [122]. It is an elliptic disk whose center is the position of the ship center, major semi-axis is along the fore-aft of the ship, and minor semi-axis is along the port-starboard of the ship. This shape is better in representing the ship geometry and is very suitable for ships in narrow channel. The two radii of the ellipse are determined according to many empirical rules which, sometimes, take into consideration the collision situation. In some cases, the ship position is shifted with respect to the ellipse center (e.g. move it backward to make the aft area bigger specially in head-on situation). Some famous ship domains are presented in Figure 7.1. The information needed for safe navigation is currently obtained by combining radar data with information obtained visually. However, misjudgments accompanying visual observations comprise a major cause of ship collisions.

In this thesis, neither the effect of the ship domain geometry nor the dimension on the collision avoidance system are investigated, rather the main focus on designing a collision avoidance system that respect the ship domain geometry given its geometry and dimension. The circular and elliptical ship domains are used at the following section whose centers coincide with the center of the ship. Shifting the ship center w.r.t the center of the circle or the ellipse could be achieved easily by shifting the position data used as an input for the collision avoidance algorithm.

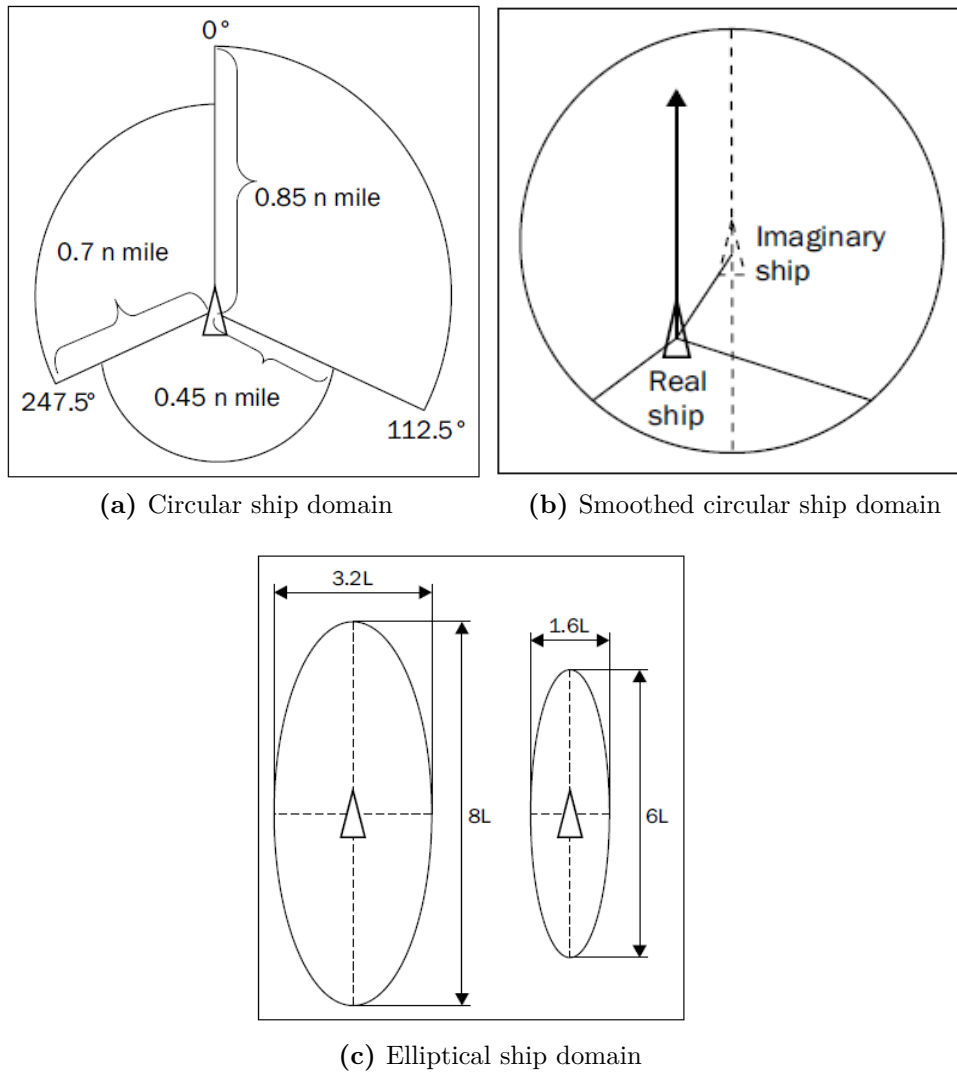


**Figure 7.1:** Different famous ship domains[123].

### 7.1.2 Navigation Information System

In addition to the GPS, IMU and Log devices that are fused together to give full states measurement of the ship, other devices must be onboard of the ship in order to give information about the encountered vessels.

The radar is the main device used for automatic collision avoidance. Currently, it is used with an Automatic Radar Plotting Aid (ARPA) that converts radar contact into objects' tracks. The system can calculate the tracked objects' course,

speed and Closest Point of Approach (CPA), thereby knowing if there is a danger of collision with other ships or landmasses. ARPA-enabled radars are now available even for small yachts.

All ships over 300 gross tons and passenger ships must have an Automatic Identification System (AIS). AIS is an automatic tracking system that supports the marine radar, which continues to be the primary method of collision avoidance. The ships that have AIS transceivers broadcast their information through a VHF radio frequency link so that they can be tracked by other vessels. The AIS transponders on each vessel broadcast three types of information: Static Information, such as the call sign and name of vessel, IMO Number, type of ship, length and beam, and location of position-fixing antenna; Dynamic Information, automatically updated from connected ship sensors, such as the ship's position, course over ground, speed over ground and navigational status, for example, at anchor, underway by engines or engaged in fishing; and finally, Voyage Information, manually entered by the crew, such as ship's draught, destination and ETA and the nature of any hazardous cargo.

In order for the collision avoidance system to function properly, a prediction of the encountered vessels motion is required. Some researchers focus mainly on the prediction problem using extended Kalman filter[124], neural networks and time series as in [125], and other artificial intelligence techniques.

In this thesis, the motion prediction of encountered vessels is predicted using the Constant Velocity (CV) model presented in [126]. In this model, the vessel is assumed to move in straight line with constant velocity. The direction of motion is used as the course angle of the vessel. Suppose that there exists  $N_o$  encountered

ships or obstacles. The CV states prediction of the  $i^{\text{th}}$  ship of obstacle  $\hat{\mathbf{x}}_o^i$  is given by:

$$\hat{\mathbf{x}}_o^i(t) = \begin{bmatrix} x_o^i(t_k) + \dot{x}_o^i \cdot \Delta t \\ y_o^i(t_k) + \dot{y}_o^i \cdot \Delta t \\ \arctan\left(\frac{\dot{y}_o^i}{\dot{x}_o^i}\right) \\ \dot{x}_o^i(t_k) \\ \dot{y}_o^i(t_k) \\ 0 \end{bmatrix}, \quad t \geq t_k \quad (7.1)$$

where  $x_o^i(t_k)$  and  $y_o^i(t_k)$  are the current position of the encountered vessel,  $t_k$  is the current time slot, and  $\Delta t = t_{k+1} - t_k$ .

## 7.2 NMPC for Collision Avoidance

In this section, the collision avoidance problem formulation is presented as an NMPC controller. The NMPC objective function of minimizing the tracking error and the control constraint for physical limitation will be the same, and the state constraints set  $\mathbb{X}$  is used for the operational constraints, i.e. collision avoidance. For static obstacles avoidance, the state constraints  $\mathbb{X}$  will be fixed during the dynamic optimization problem, but in case of collision avoidance with moving objects (i.e. ships), the state constraint will be time varying over the prediction horizon (i.e.  $\mathbb{X}(t)$ ).

The NMPC formulation as a dynamic optimization problem satisfies the solution optimality requirements **R1** and that leads to a minimum deviation from the planned trajectory, while the differential equation equality constraint satisfies the dynamic collision avoidance requirement **R4**. The time varying state constraints makes the encountered vessel prediction component independent from the collision avoidance component which satisfies the flexibility requirement **R5**. Including the NDO in the prediction model of the NMPC satisfies the disturbance counteraction requirement **R2** and leads to less tracking error.

In the following, the formulation of the state constraints to achieve a separation condition among the controlled prediction of the ship domain of the own ship and the uncontrolled prediction of the ship domain of the encountered ships is presented.

### 7.2.1 Circular Ship Domain

In this subsection, the ships are assumed to have a circular ship domain. Therefore, the collision avoidance constraint, between the own vessel and the  $i^{th}$  encountered ship, is formulated as:

$$D_o^i(t) := \sqrt{(x(t) - x_o^i(t))^2 + (y(t) - y_o^i(t))^2} \geq R^i \quad (7.2)$$

where  $x(t)$  and  $y(t)$  are the prediction of the position for own vessel over the prediction horizon,  $\hat{x}_o^i(t)$  and  $\hat{y}_o^i(t)$  are the prediction of the position for the  $i^{th}$  ship or obstacle,  $R^i$  is the safety radius measured from the center of own ship to the center of the ship or the obstacle,  $i \in \{1, 2, \dots, N_o\}$ , and  $N_o$  is the number of obstacles that are fed to the algorithm. The safety radius is selected according to the own ship and obstacles dimensions as follows:

$$R^i = R_o^i + D_s^i + \frac{L}{2} \quad (7.3)$$

where  $R_o^i$  is the radius of the circular envelop for the  $i^{th}$  obstacle,  $L$  is the length of our vessel, and  $D_s^i$  is the safety distance required between the vessel and the  $i^{th}$  obstacle. If the obstacle is a ship, the radius of its circular envelope will be selected to be half of its length. This is illustrated for a prediction horizon  $N = 2$  in Figure 7.2.

Define the position states vector  $\mathbf{x}_p \in \mathbb{R}^2$  to be  $\mathbf{x}_p := S\mathbf{x}$ , where  $S = \begin{bmatrix} 1 & 0 & 0 & 0 & 0 & 0 \\ 0 & 1 & 0 & 0 & 0 & 0 \end{bmatrix} \in \mathbb{R}^2 \times \mathbb{R}^6$ , and the estimated position vector of center of the  $i^{th}$  ship or obstacle is  $\hat{\mathbf{x}}_{po}^i = [\hat{x}_o^i \ \hat{y}_o^i]^T \in \mathbb{R}^2$ . The state constraint set  $\mathbb{X}(t)$  is defined as:

$$\mathbb{X}(t) := \bigcap_{i=1}^{N_o} \mathbb{X}^i(t) \quad (7.4)$$

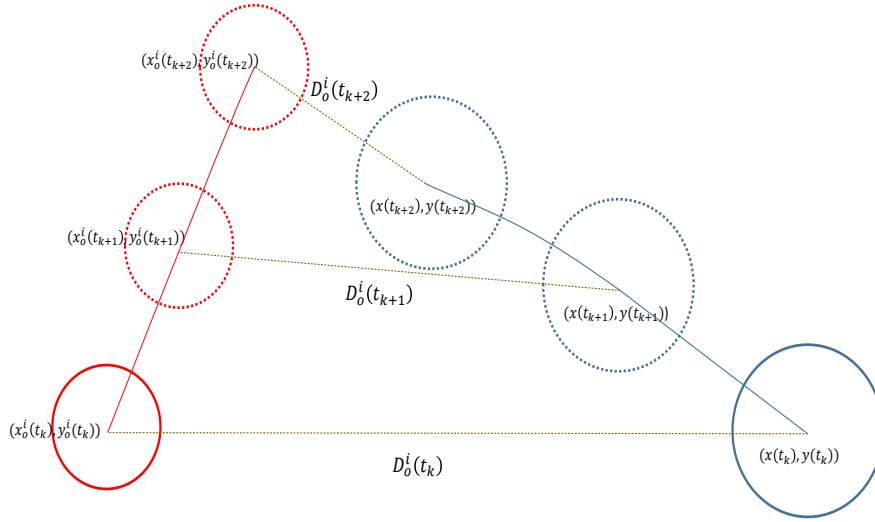


**Figure 7.2:** Collision avoidance for circular ship domains.

where  $\mathbb{X}^i(t)$  defines the state constraint set between the own ship and each obstacle or encountered ship as follows:

$$\mathbb{X}^i(t) := \{\mathbf{x}_p \in \mathbb{R}^2 \mid \|\mathbf{x}_p - \hat{\mathbf{x}}_{po}^i\| \geq R^i\}. \quad (7.5)$$

Therefore, the dynamic optimization problem for collision avoidance with circular ship domain is formulated as follows:

$$\min_{\mathbf{u}(\cdot)} V_{T_p}(t, \mathbf{x}_{t_k}, \mathbf{u}(\cdot)) = \int_{\tau=t_k}^{t_k+T_p} \bar{\ell}(\tau, \mathbf{x}(\tau), \mathbf{u}(\tau)) d\tau$$

subject to :

$$\dot{\mathbf{x}}(t) = f(\mathbf{x}, \mathbf{u}, \hat{\mathbf{b}}) = \mathcal{F}(\mathbf{x}) + g\mathbf{u} + g_b(\mathbf{x})\hat{\mathbf{b}} \text{ with } \mathbf{x}(t_k) = \mathbf{x}_{t_k}$$

$$\mathbf{u}(t) \in \mathbb{U}.,$$

$$\mathbf{x}(t) \in \mathbb{X}(t) = \bigcap_{i=1}^{N_o} \mathbb{X}^i(t) \forall t \in [t_k, t_k + T_p).$$



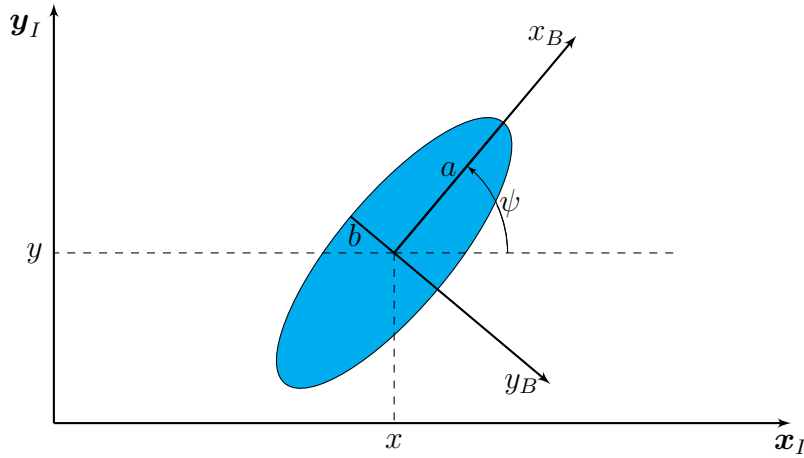


**Figure 7.3:** Elliptic Disk.

### 7.2.2 Elliptical Ship Domain

The circular ships domain are suitable for ships in open seas, but when it comes to narrow channels, it will not be preferable due to the skinny design of the ship, i.e. its width is much shorter than its length. One of the ship domains that suits better narrow channels is the elliptical one which will be used for collision avoidance throughout this subsection.

Similar to the circular ship domain formulation, the collision avoidance for elliptical ship domain is formulated as a separation condition between elliptic disks. This condition is then reformulated to suit the NMPC dynamic optimization problem.

The elliptic disk ship domain is depicted in Figure 7.3 and is parameterized by its position  $(x, y)$ , orientation or heading angle  $\psi$ , semi-major radius  $a$ , and semi-minor radius  $b$ . The elliptic disk is the closed type of conic section results from the intersection of a cone by a plane, and is expressed in the plane with respect to an inertial frame as:

$$\bar{\mathcal{A}} \equiv \{(x_c, y_c) \mid Ax_c^2 - 2Bx_cy_c + Cy_c^2 + (2By - 2Ax)x_c + (2Bx - 2Cy)y_c + (Ax^2 - 2Bx_py + Cy^2 - 1) \leq 0\} \quad (7.6)$$

where  $A = \left(\frac{\cos(\psi)^2}{a^2} + \frac{\sin(\psi)^2}{b^2}\right)$ ,  $B = \frac{\sin(2\psi)}{2} \left(\frac{1}{a^2} - \frac{1}{b^2}\right)$  and  $C = \left(\frac{\sin(\psi)^2}{a^2} + \frac{\cos(\psi)^2}{b^2}\right)$ .

The elliptic disk can be represented by a  $3 \times 3$  matrix  $\mathcal{A} = [a_{i,j}]$  as:

$$\bar{\mathcal{A}} \equiv \{X \mid X^T \mathcal{A} X \leq 0\} \quad (7.7)$$

where  $X = [x_c \ y_c \ 1]^T$  is the 3-D column vector containing the homogeneous coordinates and

$$\mathcal{A} = \begin{bmatrix} A & -B & By - Ax \\ -B & C & Bx - Cy \\ By - Ax & Bx - Cy & Ax^2 - 2Bxy + Cy^2 - 1 \end{bmatrix}. \quad (7.8)$$

By elementary math, the matrix  $\mathcal{A}$  satisfies the condition that  $\det(\mathcal{A}) < 0$ .

Suppose that our vessel, represented by the moving elliptic disk  $\bar{\mathcal{A}}(t)$ , encounters  $N_o$  other vessels indexed by the superscript  $[i]$  and represented by the moving elliptic disks  $\bar{\mathcal{B}}^{[i]}(t)$ , then the motion of our vessel is collision-free if every pair of elliptic disks  $\{\bar{\mathcal{A}}(t), \bar{\mathcal{B}}^{[i]}(t)\}$  is separate for all  $t \in [t_k, t_{k+N}]$ . Otherwise, one of these pairs collides, i.e.  $\bar{\mathcal{A}}(t)$  and  $\bar{\mathcal{B}}^{[i]}(t)$  are touching or overlapping for some  $t \in [t_k, t_{k+N}]$ . The characteristic polynomial between every pair  $\{\bar{\mathcal{A}}(t), \bar{\mathcal{B}}^{[i]}(t)\}$  is

$$\mathcal{P}^{[i]}(\lambda, t) = \det(\lambda \mathcal{A}(t) - \mathcal{B}^{[i]}(t)) \quad (7.9)$$

and can be expanded as

$$\mathcal{P}^{[i]}(\lambda, t) = C_3^{[i]}(t)\lambda^3 + C_2^{[i]}(t)\lambda^2 + C_1^{[i]}(t)\lambda + C_0^{[i]}(t) = 0, \quad (7.10)$$

where:

$$\begin{aligned} C_3^{[i]}(t) &= a_{11}M^{[i]}_{11} - a_{12}M^{[i]}_{21} + a_{13}M^{[i]}_{31}, \\ C_2^{[i]}(t) &= a_{11}M^{[i]}_{12} - a_{12}M^{[i]}_{22} + a_{13}M^{[i]}_{32} - b^{[i]}_{11}M^{[i]}_{11} \\ &\quad + b^{[i]}_{12}M^{[i]}_{21} - b^{[i]}_{13}M^{[i]}_{31}, \\ C_1^{[i]}(t) &= a_{11}M^{[i]}_{13} - a_{12}M^{[i]}_{23} + a_{13}M^{[i]}_{33} - b^{[i]}_{11}M^{[i]}_{12} \\ &\quad + b^{[i]}_{12}M^{[i]}_{22} - b^{[i]}_{13}M^{[i]}_{32}, \\ C_0^{[i]}(t) &= -b^{[i]}_{11}M^{[i]}_{13} + b^{[i]}_{12}M^{[i]}_{23} - b^{[i]}_{13}M^{[i]}_{33}, \end{aligned}$$

$$\begin{aligned}
M^{[i]}_{11} &= a_{22}a_{33} - a_{23}a_{32}, \\
M^{[i]}_{12} &= a_{32}b^{[i]}_{23} + b^{[i]}_{32}a_{23} - b^{[i]}_{22}a_{33} - a_{22}b^{[i]}_{33}, \\
M^{[i]}_{13} &= b^{[i]}_{22}b^{[i]}_{33} - b^{[i]}_{23}b^{[i]}_{32}, \\
M^{[i]}_{21} &= a_{21}a_{33} - a_{23}a_{31}, \\
M^{[i]}_{22} &= a_{31}b^{[i]}_{23} + b^{[i]}_{31}a_{23} - a_{21}b^{[i]}_{33} - b^{[i]}_{21}a_{33}, \\
M^{[i]}_{23} &= b^{[i]}_{21}b^{[i]}_{33} - b^{[i]}_{23}b^{[i]}_{31}, \\
M^{[i]}_{31} &= a_{21}a_{32} - a_{22}a_{31}, \\
M^{[i]}_{32} &= a_{31}b^{[i]}_{22} + b^{[i]}_{31}a_{22} - a_{32}b^{[i]}_{21} - b^{[i]}_{32}a_{21}, \\
M^{[i]}_{33} &= b^{[i]}_{21}b^{[i]}_{32} - b^{[i]}_{22}b^{[i]}_{31}.
\end{aligned}$$

The discriminant of  $\mathcal{P}^{[i]}(\lambda, t)$  with respect to  $\lambda$ , as a function of  $t$ , is

$$\begin{aligned}
\Delta^{[i]}(t) &= 18C_3^{[i]}C_2^{[i]}C_1^{[i]}C_0^{[i]} - 4C_2^{[i]3}C_0^{[i]} + C_2^{[i]2}C_1^{[i]2} \\
&\quad - 4C_3^{[i]}C_1^{[i]3} - 27C_3^{[i]2}C_0^{[i]2}
\end{aligned} \tag{7.11}$$

**Proposition 7.1.** *Consider a pair of moving elliptic disks  $\{\bar{\mathcal{A}}(t), \bar{\mathcal{B}}^{[i]}(t)\}$  in the Euclidean plane  $\mathbf{E}^2$  represented by the matrices  $\mathcal{A}$  and  $\mathcal{B}^{[i]}(t)$ , respectively. Let  $\mathcal{P}^{[i]}(\lambda, t) = C_3^{[i]}(t)\lambda^3 + C_2^{[i]}(t)\lambda^2 + C_1^{[i]}(t)\lambda + C_0^{[i]}(t)$  be their characteristic polynomial and  $\Delta^{[i]}(t)$  denotes the discriminant of  $\mathcal{P}^{[i]}(\lambda, t)$  with respect to  $\lambda$ . Suppose that every pair  $\{\bar{\mathcal{A}}(T_0), \bar{\mathcal{B}}^{[i]}(T_0)\}$  is separate, then the motions of them are collision-free for all  $t \in [T_k, T_{k+N}]$  if*

1.  $C_2^{[i]}(t) < 0$
2.  $\Delta^{[i]}(t) > 0, \forall t \in [T_k, T_{k+N}]$ .

*Proof.* we will show that the conditions  $C_2^{[i]}(t) < 0$  and  $\Delta^{[i]}(t) > 0$  are sufficient for the condition in Theorem B.1 to be satisfied.

First, we provide the condition for  $\mathcal{P}^{[i]}(\lambda, t) = 0$  to be real. From Theorem B.2, the third order characteristic polynomial has three real roots, if the discriminant  $\Delta^{[i]}(t) > 0$  for all  $t \in [T_k, T_{k+N}]$ .

Second, we develop a condition for negative roots. From the elliptic disk matrix properties, it is simple to show that  $C_3^{[i]} = \det(\mathcal{A}) < 0$  and  $C_0^{[i]} = -\det(\mathcal{B}^{[i]}) > 0$ . By constructing the following Routh-Hurwitz table for  $\mathcal{P}^{[i]}(\lambda, t)$

$$\begin{array}{c|cc} \lambda^3 & C_3^{[i]} & C_1^{[i]} \\ \lambda^2 & C_2^{[i]} & C_0^{[i]} \\ \lambda & \frac{C_2^{[i]}C_1^{[i]} - C_3^{[i]}C_0^{[i]}}{C_2^{[i]}} & \\ \lambda^0 & C_0^{[i]} & \end{array},$$

if we constrain  $C_2^{[i]}(t)$  to be less than zero, we have only one sign change for the first column elements of Routh table regardless of the undetermined sign of the third element  $\frac{C_2^{[i]}C_1^{[i]} - C_3^{[i]}C_0^{[i]}}{C_2^{[i]}}$ . That results in at least two negative roots.  $\square$

This formulation satisfies the proper ship domain requirement **R3** as the minor radius  $b$  can be chosen to suit either open seas by increasing it or narrow channels by decreasing it. The state constraint set  $\mathbb{X}(t)$  of the NMPC is defined as:

$$\mathbb{X}(t) := \bigcap_{i=1}^{N_o} \mathbb{X}^i(t) \quad (7.12)$$

where  $\mathbb{X}^i(t)$  defines the state constraint set between the own ship and each obstacle or encountered ship.

$$\mathbb{X}^i(t) := \{\mathbf{x} \in \mathbb{R}^6 \mid C_2^{[i]}(t) < 0 \wedge \Delta^{[i]}(t) > 0\}. \quad (7.13)$$

Therefore, the dynamic optimization problem for collision avoidance with elliptical ship domain is formulated as follows:

$$\min_{\mathbf{u}(\cdot)} V_{T_p}(t, \mathbf{x}_{t_k}, \mathbf{u}(\cdot)) = \int_{\tau=t_k}^{t_k+T_p} \bar{\ell}(\tau, \mathbf{x}(\tau), \mathbf{u}(\tau)) d\tau$$

subject to :

$$\dot{\mathbf{x}}(t) = f(\mathbf{x}, \mathbf{u}, \hat{\mathbf{b}}) = \mathcal{F}(\mathbf{x}) + g\mathbf{u} + g_b(\mathbf{x})\hat{\mathbf{b}} \text{ with } \mathbf{x}(t_k) = \mathbf{x}_{t_k}$$

$$\mathbf{u}(t) \in \mathbb{U},$$

$$\mathbf{x}(t) \in \mathbb{X}(t) = \bigcap_{i=1}^{N_o} \mathbb{X}^i(t) \forall t \in [t_k, t_{k+N}).$$

### 7.2.3 COLREGs Compliance

The maneuvering, occurred due to the optimal solution of the NMPC-NDO problem with the collision avoidance constraint (7.2) for circular ship domains or (7.13) for elliptical ship domains, might be random in the sense of maneuvering direction and not necessarily compliant to the International Regulations for Preventing Collisions at Sea (COLREGs)[12] that set rules for the actions a vessel should follow when encountering other vessels at sea. We will focus on the three typical situations; head-on, overtaking and crossing, which are described in rules number 13,14 and 15 of section II of COLREGs in order to satisfy the action to avoid collision requirement **R6**.

In a head-on situation between two vessels, both vessels must turn to the starboard side so that they pass on the port side of each other. In an overtaking situation, the overtaking vessel can turn to either starboard or port side according to the situation, and starboard is chosen for our algorithm. When two vessels are crossing each other, the vessel which has the other on the starboard side must give way and avoid crossing ahead of her. We here conclude that the vessel should prioritize its maneuvering to the starboard side. To integrate COLREGs into our NMPC approach, we impose another nonlinear state constraint into the NMPC dynamic optimization problem that forces the encounter vessel to be on the left side of the straight line generated by our vessel's position  $(x(t_k), y(t_k))$  and heading angle  $\psi(t_k)$ . It takes the form:

$$\sin(\psi)(x(t) - \hat{x}_o^i(t)) - \cos(\psi(t))(y(t) - \hat{y}_o^i(t)) \geq 0 \quad (7.14)$$

This constraint can not be added as a hard constraint to the optimization problem as it is quite often to be infeasible over the prediction horizon. As discussed in Section 1.3 the COLREGs constraints are not hard, and the stand-on and the give-way vessels shall do any necessary action to avoid the collision. Therefore,

the COLREGs compliance constraint (7.14) is softened using slack variables. The softened constraint of (7.14) becomes:

$$\sin(\psi)(x(t) - \hat{x}_o^i(t)) - \cos(\psi(t))(y(t) - \hat{y}_o^i(t)) + slk^i \geq 0 \quad (7.15)$$

where  $slk^i$  is a positive slack variable which is handled as a control input in the optimization problem. Therefore, an extra control constraint is added for the slack variables as follows:

$$\mathbf{slk} := [slk^1 slk^2 \dots slk^{N_o}]^T \geq \mathbf{0} \quad (7.16)$$

The state constraint for the circular ship domain becomes:

$$\mathbb{X}(t) := \bigcap_{i=1}^{N_o} \mathbb{X}^i(t) = \{\mathbf{x}_p \in \mathbb{R}^2 \mid \|\mathbf{x}_p - \hat{\mathbf{x}}_{po}^i\|^2 \geq R^i \wedge (7.15)\}, \quad (7.17)$$

and for the elliptical ship domain becomes:

$$\mathbb{X}(t) := \bigcap_{i=1}^{N_o} \mathbb{X}^i(t) = \{\mathbf{x}_p \in \mathbb{R}^6 \mid C_2^{[i]}(t) < 0 \wedge \Delta^{[i]}(t) > 0 \wedge (7.15)\}. \quad (7.18)$$

The stage cost function (6.7) is modified to account for the slack variables as follows:

$$\bar{\ell}(t, \mathbf{x}(t), \mathbf{u}(t), \mathbf{slk}(t)) = \|\bar{\mathbf{x}}(t) - \bar{\mathbf{x}}_r(t)\|_Q + \|\mathbf{u}(t) - \mathbf{u}_r(t)\|_R + \|\mathbf{slk}\|_S \quad (7.19)$$

The COLREGs collision avoidance constraints (7.17) or (7.18) can only be imposed when there is risk of collision for the vessel that must do the maneuvering according to the situation. Hence, the rule-based decision support system presented in [127] is adapted to identify the collision risk and detect which vessel will stand on its course and which one must do the maneuvering (give-away). The rule-based system is checked over the whole prediction horizon  $T_p$ . In case of circular ship domain, the decision support system is as follows:

- The USV is in overtaking situation if:
  - $\|\mathbf{x}_p - \hat{\mathbf{x}}_{po}^i\| \leq R^i \wedge |\psi(t) - \psi_o^i(t)| \leq \frac{\pi}{4}$
- The USV is in head-on situation if:
  - $\|\mathbf{x}_p - \hat{\mathbf{x}}_{po}^i\| \leq R^i \wedge |\psi(t) - \psi_o^i(t) + \pi| \leq \frac{\pi}{4}$

- The USV is in crossing from the right situation if:

$$- \left\| \mathbf{x}_p - \hat{\mathbf{x}}_{po}^i \right\| \leq R^i \wedge \frac{\pi}{4} \leq \psi_o^i(t) - \psi(t) \leq \frac{3\pi}{4}$$

- The USV is in crossing from the left situation if:

$$- \left\| \mathbf{x}_p - \hat{\mathbf{x}}_{po}^i \right\| \leq R^i \wedge \frac{5\pi}{4} \leq \psi_o^i(t) - \psi(t) \leq \frac{7\pi}{4}$$

In case of elliptical ship domain, the decision support system is as follows:

- The USV is in overtaking situation if:

$$- C_2^{[i]}(t) < 0 \wedge \Delta^{[i]}(t) > 0 \wedge |\psi(t) - \psi_o^i(t)| \leq \frac{\pi}{4}$$

- The USV is in head-on situation if:

$$- C_2^{[i]}(t) < 0 \wedge \Delta^{[i]}(t) > 0 \wedge |\psi(t) - \psi_o^i(t) + \pi| \leq \frac{\pi}{4}$$

- The USV is in crossing from the right situation if:

$$- C_2^{[i]}(t) < 0 \wedge \Delta^{[i]}(t) > 0 \wedge \frac{\pi}{4} \leq \psi_o^i(t) - \psi(t) \leq \frac{3\pi}{4}$$

- The USV is in crossing from the left situation if:

$$- C_2^{[i]}(t) < 0 \wedge \Delta^{[i]}(t) > 0 \wedge \frac{5\pi}{4} \leq \psi_o^i(t) - \psi(t) \leq \frac{7\pi}{4}$$

The algorithm of the NDO-NMPC collision avoidance scheme with circular ship domain and COLREGs compliance is:

---

**Algorithm 7.1** NMPC-NDO Algorithm for Trajectory Tracking and Collision Avoidance for Circular Ship Domains

---

- 1: Set the time index  $t = t_0$ , the prediction horizon  $T_p$ , sampling interval  $T_s$ , weight matrices  $Q$  and  $R$ , the observer convergence rate  $K_w$ , and the disturbance initial value  $\hat{\mathbf{b}}(t_0) = \mathbf{0}$ .
- 2: Measure the value of the states  $\mathbf{x}(t_k)$  or estimate them.
- 3: Get the position, velocity and heading of the nearby vessels using a communication media or via radar and predict the position over the prediction horizon  $T_p$  using constant velocity (CV) model.
- 4: Execute the rule-based decision support system.
- 5: **if** the USV is in overtaking, head-on or crossing from the right **then**
- 6:   Execute the following NMPC problem:

$$\min_{\mathbf{u}(\cdot)} V_{T_p}(t, \mathbf{x}_{t_k}, \mathbf{u}(\cdot)) = \int_{\tau=t_k}^{t_k+T_p} \bar{\ell}(t, \mathbf{x}(t), \mathbf{u}(t), \mathbf{slk}(t)) d\tau$$

subject to :

$$\dot{\mathbf{x}}(t) = f(\mathbf{x}, \mathbf{u}, \hat{\mathbf{b}}) = \mathcal{F}(\mathbf{x}) + g\mathbf{u} + g_b(\mathbf{x})\hat{\mathbf{b}} \text{ with } \mathbf{x}(t_k) = \mathbf{x}_{t_k}$$

$$\mathbf{u}(t) \in \mathbb{U},$$

(7.17) and (7.16)

- 7: **else**
- 8:   Execute the following NMPC problem:

$$\min_{\mathbf{u}(\cdot)} V_{T_p}(t, \mathbf{x}_{t_k}, \mathbf{u}(\cdot)) = \int_{\tau=t_k}^{t_k+T_p} \bar{\ell}(t, \mathbf{x}(t), \mathbf{u}(t), \mathbf{slk}(t)) d\tau$$

subject to :

$$\dot{\mathbf{x}}(t) = f(\mathbf{x}, \mathbf{u}, \hat{\mathbf{b}}) = \mathcal{F}(\mathbf{x}) + g\mathbf{u} + g_b(\mathbf{x})\hat{\mathbf{b}} \text{ with } \mathbf{x}(t_k) = \mathbf{x}_{t_k}$$

$$\mathbf{u}(t) \in \mathbb{U},$$

- 9: **end if**
  - 10: Get the optimal control sequence  $[\mathbf{u}(t_k) \cdots \mathbf{u}(t_{k+N-1})]$  and the corresponding predicted states  $[\mathbf{x}(t_k) \cdots \mathbf{x}(t_{k+N})]$ .
  - 11: Apply only the first control element  $\mathbf{u}(t_k)$ .
  - 12: Solve the NDO equations (5.5) to get the estimated value for the disturbance  $\hat{\mathbf{b}}(t + T_s)$ , and assume that it is constant over the prediction horizon.
  - 13: wait for the next sample and set the time index  $k = k + 1$ , then go to step 2.
- 

The algorithm of the NDO-NMPC collision avoidance scheme with elliptical ship domain and COLREGs compliance is:



---

**Algorithm 7.2** NMPC-NDO Algorithm for Trajectory Tracking and Collision Avoidance for Elliptical Ship Domains
 

---

- 1: Set the time index  $t = t_0$ , the prediction horizon  $T_p$ , sampling interval  $T_s$ , weight matrices  $Q$  and  $R$ , the observer convergence rate  $K_w$ , and the disturbance initial value  $\hat{\mathbf{b}}(t_0) = \mathbf{0}$ .
- 2: Measure the value of the states  $\mathbf{x}(t_k)$  or estimate them.
- 3: Get the position, velocity and heading of the nearby vessels using a communication media or via radar and predict the position over the prediction horizon  $T_p$  using constant velocity (CV) model.
- 4: Execute the rule-based decision support system.
- 5: **if** the USV is in overtaking, head-on or crossing from the right **then**
- 6:   Execute the following NMPC problem:

$$\min_{\mathbf{u}(\cdot)} V_{T_p}(t, \mathbf{x}_{t_k}, \mathbf{u}(\cdot)) = \int_{\tau=t_k}^{t_k+T_p} \bar{\ell}(t, \mathbf{x}(t), \mathbf{u}(t), \mathbf{slk}(t)) d\tau$$

subject to :

$$\dot{\mathbf{x}}(t) = f(\mathbf{x}, \mathbf{u}, \hat{\mathbf{b}}) = \mathcal{F}(\mathbf{x}) + g\mathbf{u} + g_b(\mathbf{x})\hat{\mathbf{b}} \text{ with } \mathbf{x}(t_k) = \mathbf{x}_{t_k}$$

$$\mathbf{u}(t) \in \mathbb{U},$$

(7.18) **and** (7.16)

- 7: **else**
- 8:   Execute the following NMPC problem:

$$\min_{\mathbf{u}(\cdot)} V_{T_p}(t, \mathbf{x}_{t_k}, \mathbf{u}(\cdot)) = \int_{\tau=t_k}^{t_k+T_p} \bar{\ell}(t, \mathbf{x}(t), \mathbf{u}(t), \mathbf{slk}(t)) d\tau$$

subject to :

$$\dot{\mathbf{x}}(t) = f(\mathbf{x}, \mathbf{u}, \hat{\mathbf{b}}) = \mathcal{F}(\mathbf{x}) + g\mathbf{u} + g_b(\mathbf{x})\hat{\mathbf{b}} \text{ with } \mathbf{x}(t_k) = \mathbf{x}_{t_k}$$

$$\mathbf{u}(t) \in \mathbb{U},$$

- 9: **end if**
  - 10: Get the optimal control sequence  $[\mathbf{u}(t_k) \cdots \mathbf{u}(t_{k+N-1})]$  and the corresponding predicted states  $[\mathbf{x}(t_k) \cdots \mathbf{x}(t_{k+N})]$ .
  - 11: Apply only the first control element  $\mathbf{u}(t_k)$ .
  - 12: Solve the NDO equations (5.5) to get the estimated value for the disturbance  $\hat{\mathbf{b}}(t + T_s)$ , and assume that it is constant over the prediction horizon.
  - 13: wait for the next sample and set the time index  $k = k + 1$ , then go to step 2.
- 

**Remark:** All the state constraints are included in the code generation of the optimization problem and can be deactivated by relaxing the upper and lower

limits of the inequalities during the execution.

## 7.3 Simulation Results

In this section, the usage of NMPC for collision avoidance is evaluated for both circular and elliptical ship domains. For each case, three typical collision scenarios; head-on, overtaking and crossing are demonstrated between two vessels. MATLAB with the aid of ACADO toolkit and qpOASES solver is used for obtaining the simulation results on a 3.3 GHz core i5 CPU with 8 GB RAM. The ship model presented in appendix A is used for both own and encountered vessel.

### 7.3.1 Circular Ship Domain

The NMPC-NDO simulation results for the circular ship domain collision avoidance scheme is presented in this subsection. The simulation parameters are given in Table 7.1. Both vessels are assumed to have a circular ship domain of 40 *m* radius, and the safety distance between them is 20 *m*. The encountered vessel is assumed to have the NMPC-NDO scheme and its position and velocity are assumed to be measured or exchanged via a communication link, and its predicted trajectory is calculated using the constant velocity model (7.1).

**Table 7.1:** NMPC-NDO Parameters for Circular Ship Domain Collision Avoidance

Parameter	Value
$T_p$	200.0 <i>sec</i>
$T_s$	5.0 <i>sec</i>
$N$	40
$Q$	$diag(5, 5, 5, 0.2, 0.2, 0.2)$
$R$	$diag(0.001, 0.001)$
$S$	0.001
$K_w$	$diag(0.1, 0.1, 0.1)$
$R^1$	100

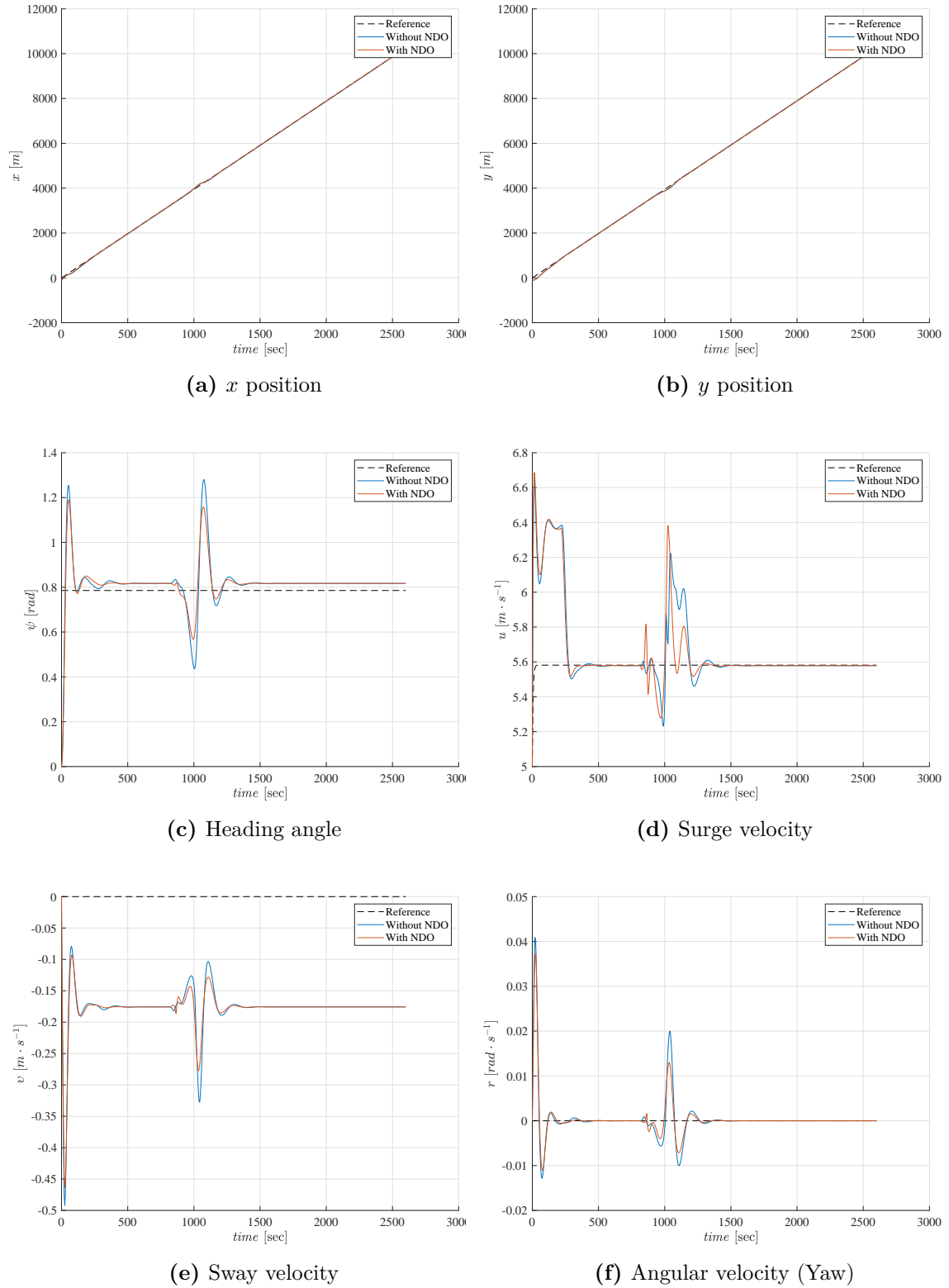


**Figure 7.4:** Simulation results of the states for the circular scheme head-on scenario.

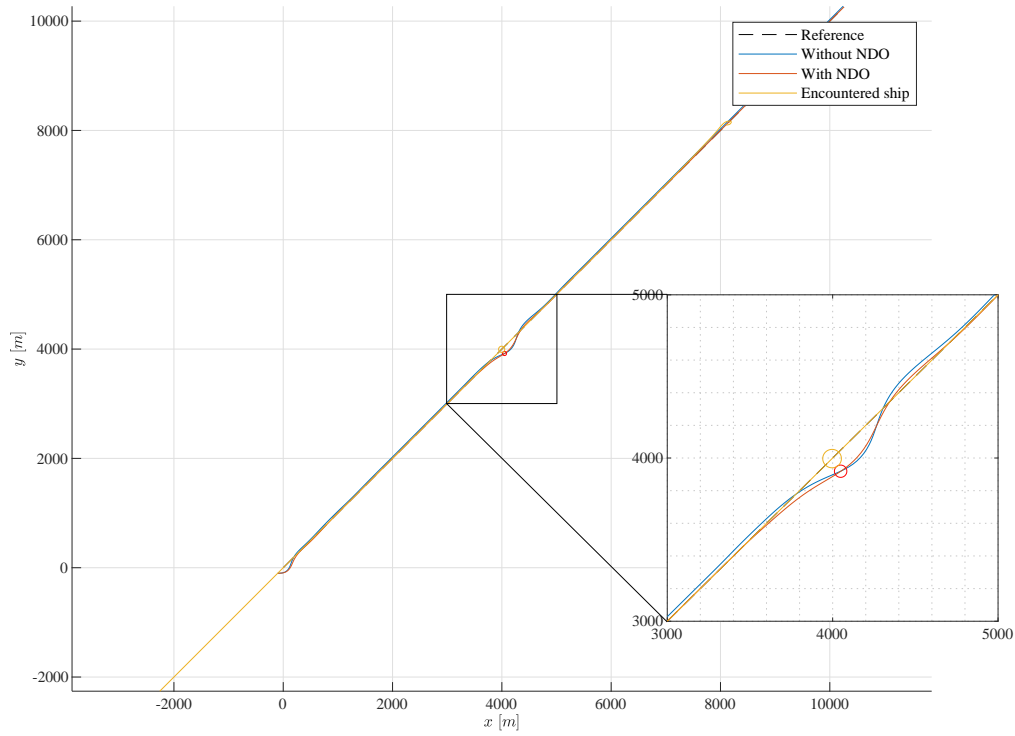


**Figure 7.5:** Trajectory for scenario 2 for the circular scheme head-on scenario.

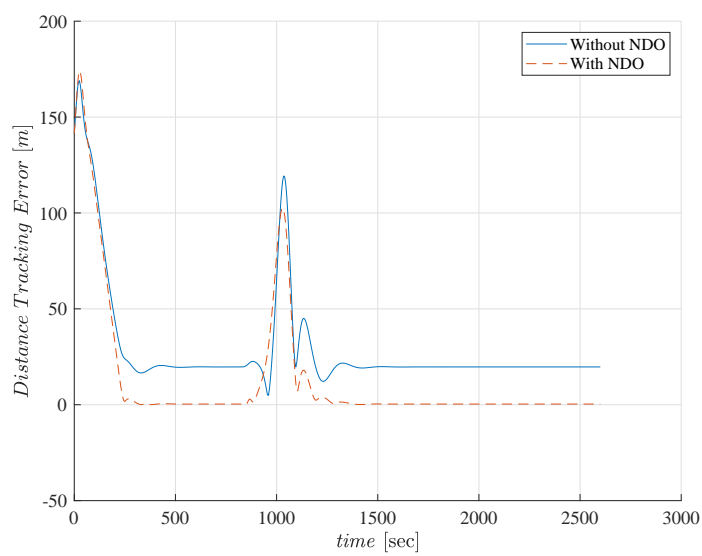


**Figure 7.6:** Distance tracking error for the circular scheme head-on scenario.

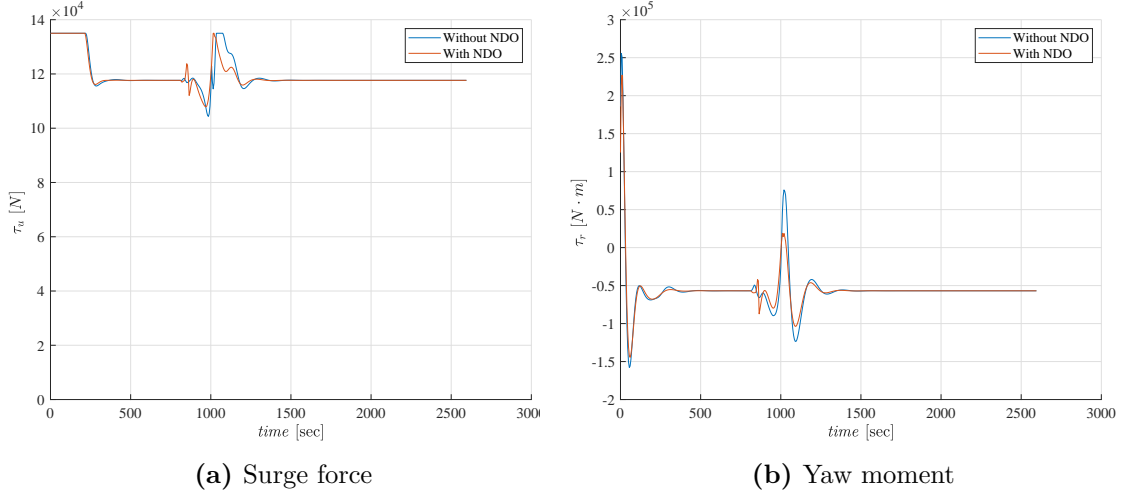


**Figure 7.7:** Simulation results of the control input for for the circular scheme head-on scenario.

### Head-on Scenario

In this scenario, our vessel is assumed to confront another vessel in a head-on situation. The encountered vessel is assumed here to have no collision avoidance to give the worst case scenario. The position and heading angle are presented in Figures 7.4a, 7.4b and 7.4c , respectively. The surge, sway and yaw velocities are presented in Figures 7.4d, 7.4e and 7.4f, respectively. The surge force and yaw moments are presented in Figure7.7a and 7.7b.

It is shown from the trajectory of the vessel presented in Figure7.5 that the own vessel could follow the reference trajectory and maneuver to the starboard side in order to avoid the collision with the encountered vessel. The trajectory tracking error of the NMPC-NDO scheme is close to zero except during the collision avoidance maneuver which leads to a deviation of about  $115\text{ m}$  as shown in Figure7.6. On the other side, the case of not using NDO leads to a maximum distance tracking error of  $125\text{m}$  and  $84\text{m}$  while collision constraint is active and not active, respectively. In both cases, collision avoidance constraints and surge force and yaw moment constraints are respected. Regardless of using NDO, the collision avoidance constraint in both

schemes leads to a new collision-free trajectory, as close as possible to the reference trajectory. The minimum distance between the centers of both vessels is about 102  $m$  which demonstrates the ability to use our scheme as a last line of defense as this distance is slightly greater than the 100  $m$  safety distance. In order to quantify the tracking performance, the integral of the tracking error performance index  $\int \|\mathbf{x}(t) - \mathbf{x}(t)^{ref}\|$  is used for both schemes. The integral tracking error for the NMPC-NDO is  $7.61 \times 10^5$ , while the NMPC leads to  $9.8 \times 10^5$ , which shows how the integration of the NMPC and NDO leads to a better tracking performance.

### Overtaking Scenario

In this scenario, the overtaking situation is assessed by bringing the encountered vessel on the same path of own vessel but at a lower speed with the same simulation parameters as in the head-on situation. As shown in Figure 7.9, the own vessel maneuvers to the starboard side, according to rule 13 of COLREGs, then maneuvers back to the original trajectory after overtaking the other vessel. The position and the heading angle are presented in Figures 7.8a, 7.8b and 7.8c, respectively, while Figures 7.8d, 7.8e and 7.8f show the surge, sway and yaw velocities. In Figures 7.11a and 7.11b, the surge force and yaw moment generated by our NMPC scheme are shown.

The trajectory tracking error of the NMPC-NDO scheme is close to zero except during the collision avoidance maneuver which leads to a deviation of about 115  $m$  for the NDO case, as shown in Figure 7.10. On the other side, the case of not using NDO leads to a maximum distance tracking error of 125 $m$  and 84 $m$  while collision constraint is active and not active, respectively. In both cases, collision avoidance constraints and surge force and yaw moment constraints are respected. Regardless of using NDO, the collision avoidance constraint in both schemes leads to a new collision-free trajectory, as close as possible to the reference trajectory. The minimum distance between the centers of both vessels is about 101  $m$  which demonstrates the ability to use our scheme as a last line of defense as this distance

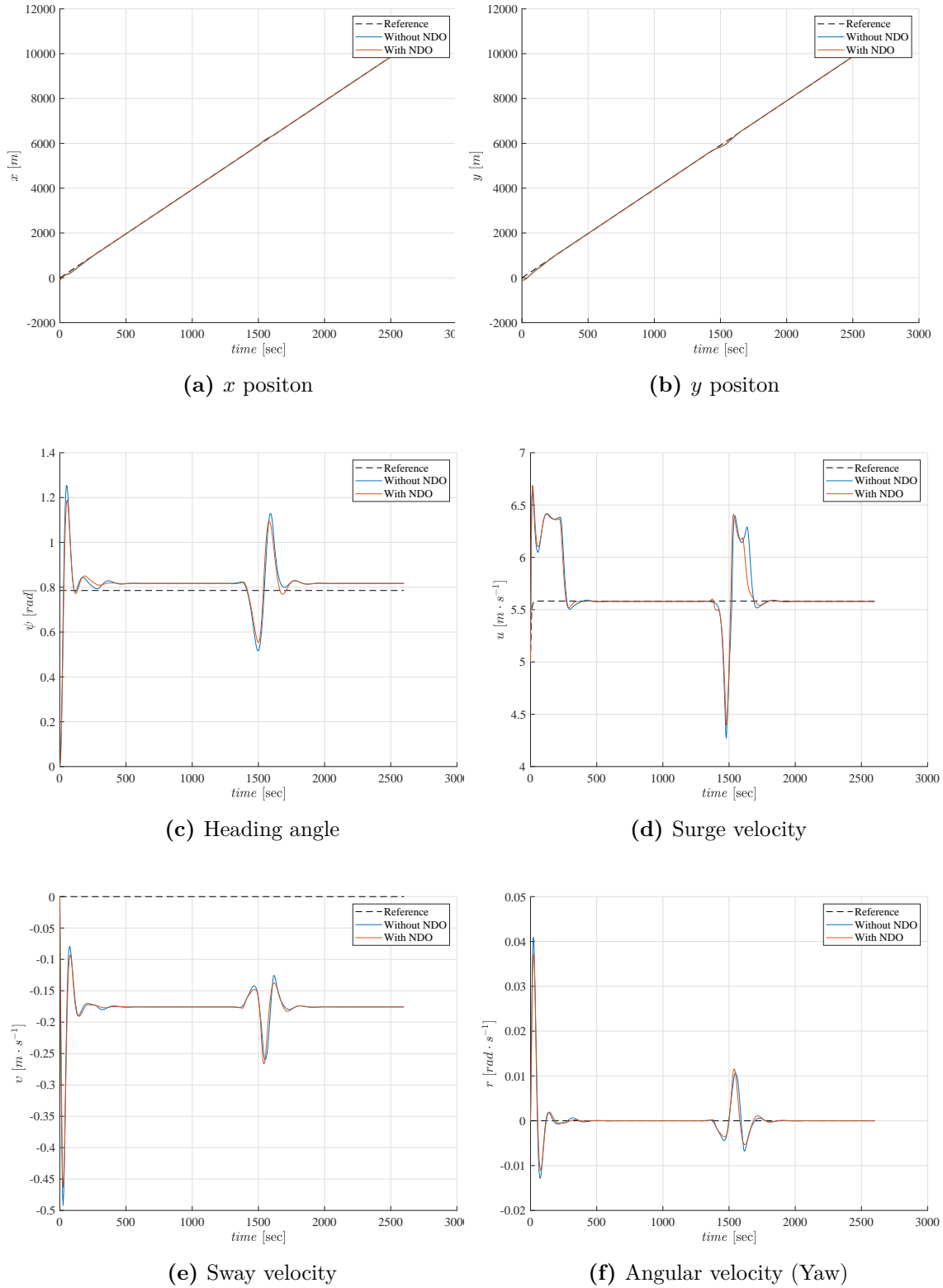


**Figure 7.8:** Simulation results of the states for the circular scheme overtaking scenario.

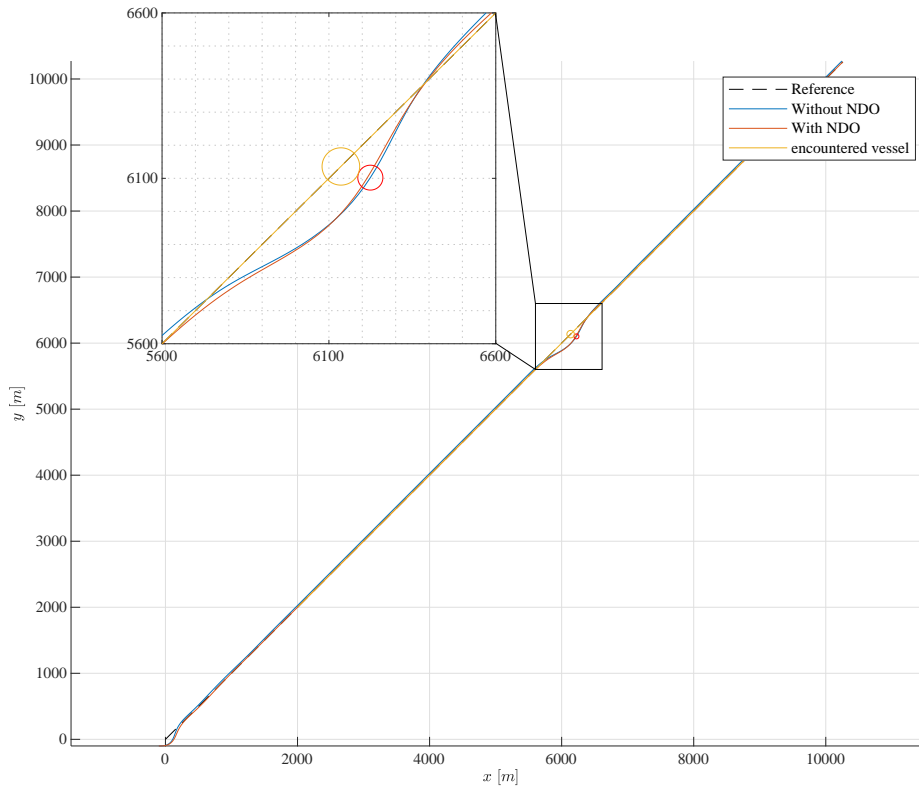


**Figure 7.9:** Trajectory for the circular scheme overtaking scenario.

is slightly greater than the 100  $m$  safety distance. The integral tracking error  $\int \|\mathbf{x}(t) - \mathbf{x}(t)^{ref}\|$ , used as performance index, is  $7.203 \times 10^5$  for the NMPC-NDO case, while for the not using the NDO is  $9.35 \times 10^5$ , which shows how the integration of the NMPC and NDO leads to a better tracking performance.

### Crossing Scenario

To give a comprehensive evaluation for the NMPC-NDO scheme for collision avoidance, the typical crossing situation between two vessels is evaluated. The scenario is designed such that both vessels collide at the position  $(x, y) = (4000m, 4000m)$ . Figure7.12 shows the states for the own vessel while Figure7.14 shows the control input. It is shown in Figure7.13 that own ship obeys rule 15 of COLREGs by turning to the starboard side and passing at aft of the encountered vessel keeping a



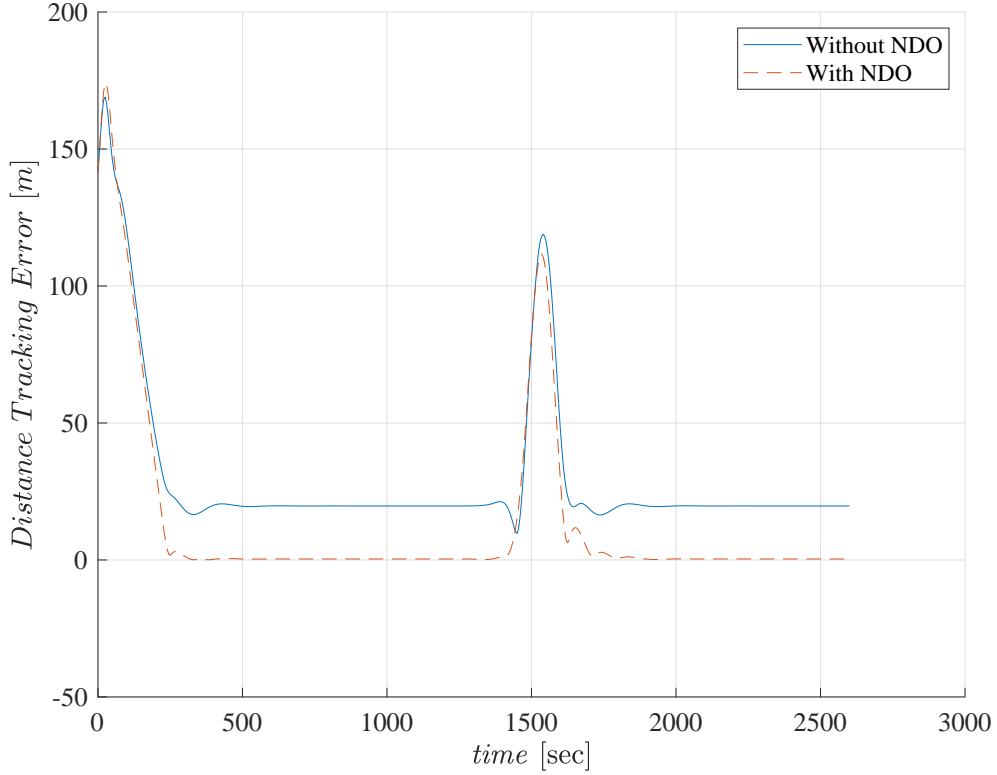


**Figure 7.10:** Distance tracking error for the circular scheme overtaking scenario.

minimum distance of about  $123m$  and then tracks the generated trajectory when the collision risk is over. The integral tracking error  $\int \|\mathbf{x}(t) - \mathbf{x}(t)^{ref}\|$  is  $8.108 \times 10^5$  for the NMPC-NDO case while for the not using the NDO is  $1.004 \times 10^6$ , which show the benefit of integrating NDO with the NMPC. The maximum execution time of this scheme is about  $15ms$  which is very small compared to the sampling interval and which guarantee a fast reaction of the ship in case of collision risk.

### 7.3.2 Elliptical Ship Domain

The NMPC-NDO simulation results for the elliptical ship domain collision avoidance scheme is presented in this subsection. The simulation parameters are similar to the circular one except for the ship domain geometry parameters, and are given in

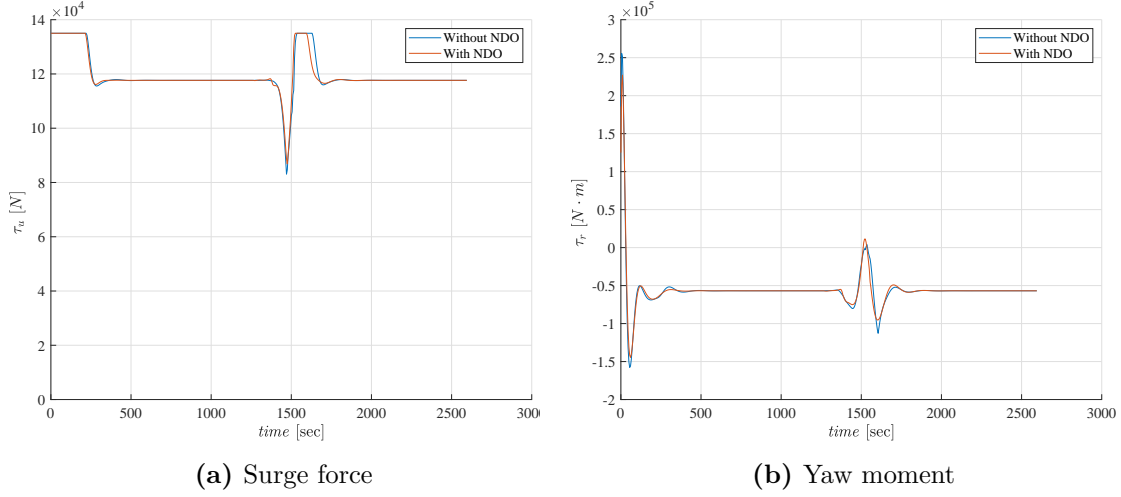


**Figure 7.11:** Simulation results of the control input for the circular scheme overtaking scenario.

Table 7.2. Both vessels are assumed to have an elliptical ship domain with radii of  $96m$  and  $13.5m$ . The encountered vessel is assumed also to have no collision avoidance scheme and its position and velocity are assumed to be measured or exchanged via a communication link, and its predicted trajectory is calculated using the constant velocity model (7.1).

**Table 7.2:** NMPC-NDO Parameters for Circular Ship Domain Collision Avoidance

Parameter	Value
$T_p$	200.0 sec
$T_s$	5.0 sec
$N$	40
$Q$	$diag(5, 5, 5, 0.2, 0.2, 0.2)$
$R$	$diag(0.001, 0.001)$
$S$	0.001
$K_w$	$diag(0.1, 0.1, 0.1)$
$a = a^1$	96m
$b = b^1$	13.5m

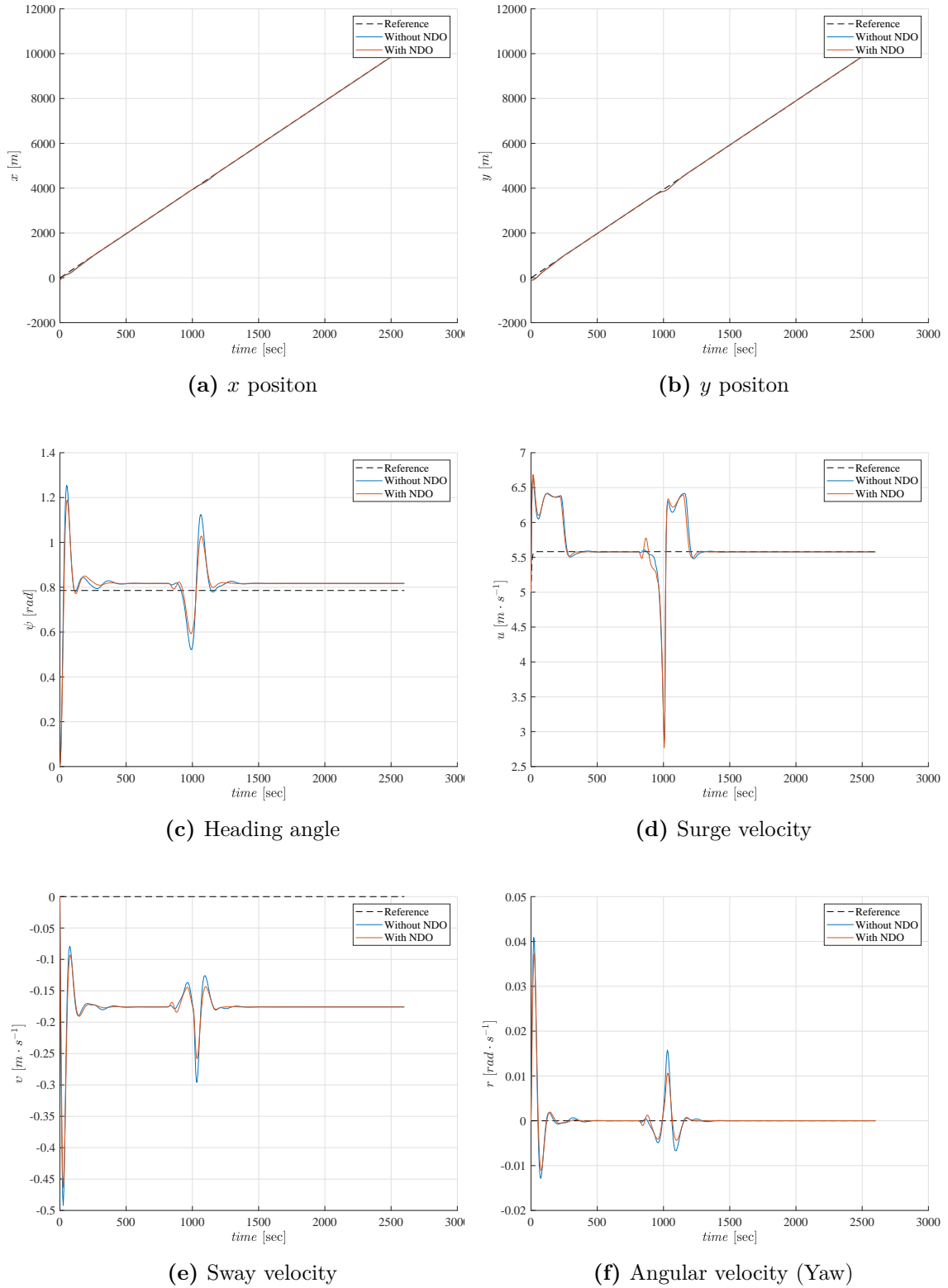


**Figure 7.12:** Simulation results of the states for the circular scheme crossing scenario.

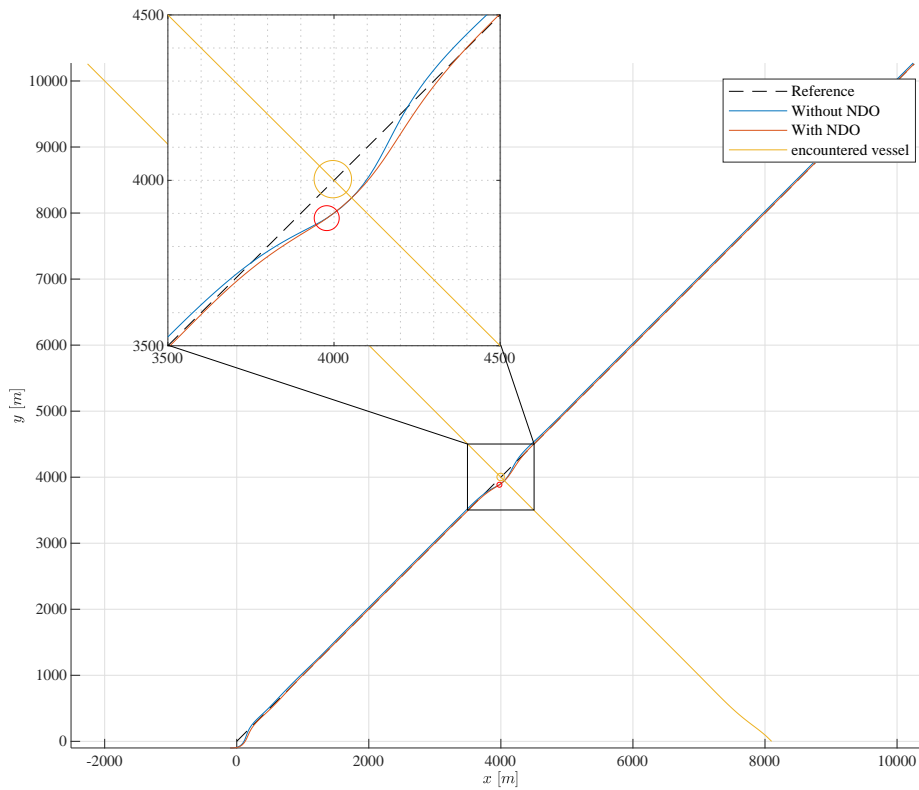


**Figure 7.13:** Trajectory for the circular scheme crossing scenario.

### Head-on Scenario

In this scenario, our vessel is assumed to confront another vessel in a head-on situation. The states of the own vessel is depicted in the six sub-figures of Figure7.15. It is shown from the trajectory of the vessel presented in Figure7.16 that the own vessel can follow the reference trajectory and maneuver to the starboard side in order to avoid the collision with the encountered vessel while keeping a minimum distance of  $60m$  which is much less than the  $100m$  achieved by the circular scheme. This justifies the ability of the elliptical ship domain formulation for dense traffic areas or in narrow rivers. As shown in Figure7.17, the surge force and yaw moment constraints are respected over the simulation time.

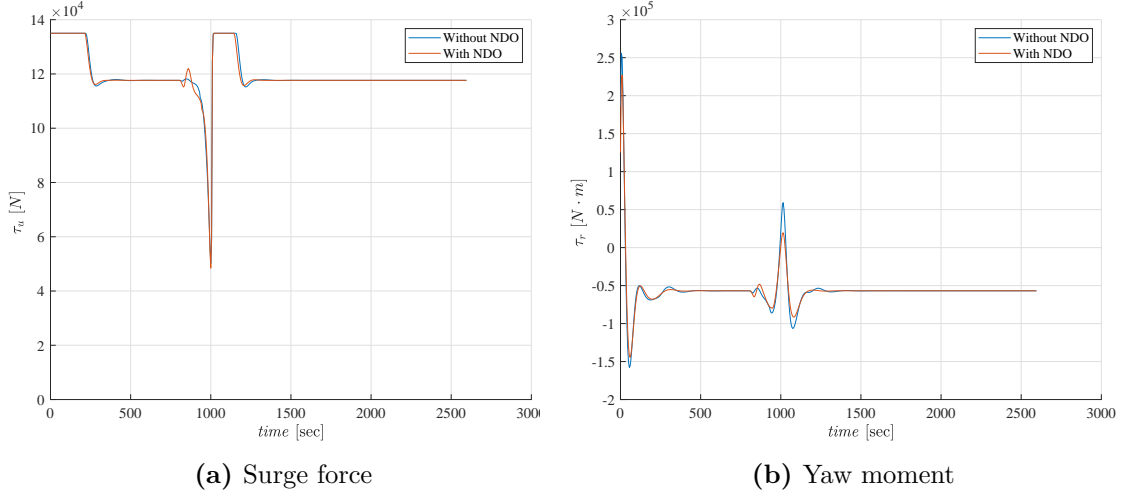


**Figure 7.14:** Simulation results of the control input for the circular scheme crossing scenario.

### Overtaking Scenario

The overtaking situation between two ships is assessed by having a slow encountered vessel on the path of the own ship, with the same simulation parameters as in Table 7.2. As shown in Figure 7.19, the own vessel maneuvers to the starboard side, according to rule 13 of COLREGs, then maneuvers back to the original trajectory after overtaking the other vessel. The position and the heading angle are presented in Figures 7.18a, 7.18b and 7.18c, respectively, while Figures 7.18e, 7.18f and 7.18d show the surge, sway and yaw velocities. In Figures 7.20a and 7.20b, the surge force and yaw moment which are generated by our NMPC scheme, are shown.

### Crossing Scenario

In this scenario, the crossing situation between two vessels is evaluated by having two ships with a  $\frac{\pi}{2}$  bearing. The scenario is designed such that both vessels collide at the position  $(x, y) = (4000m, 4000m)$ . Figure 7.21e shows the states for the own vessel, while Figure 7.23 shows the control input. It is shown in Figure 7.13 that own ship obeys rule 15 of COLREGs by turning to the starboard side and passing

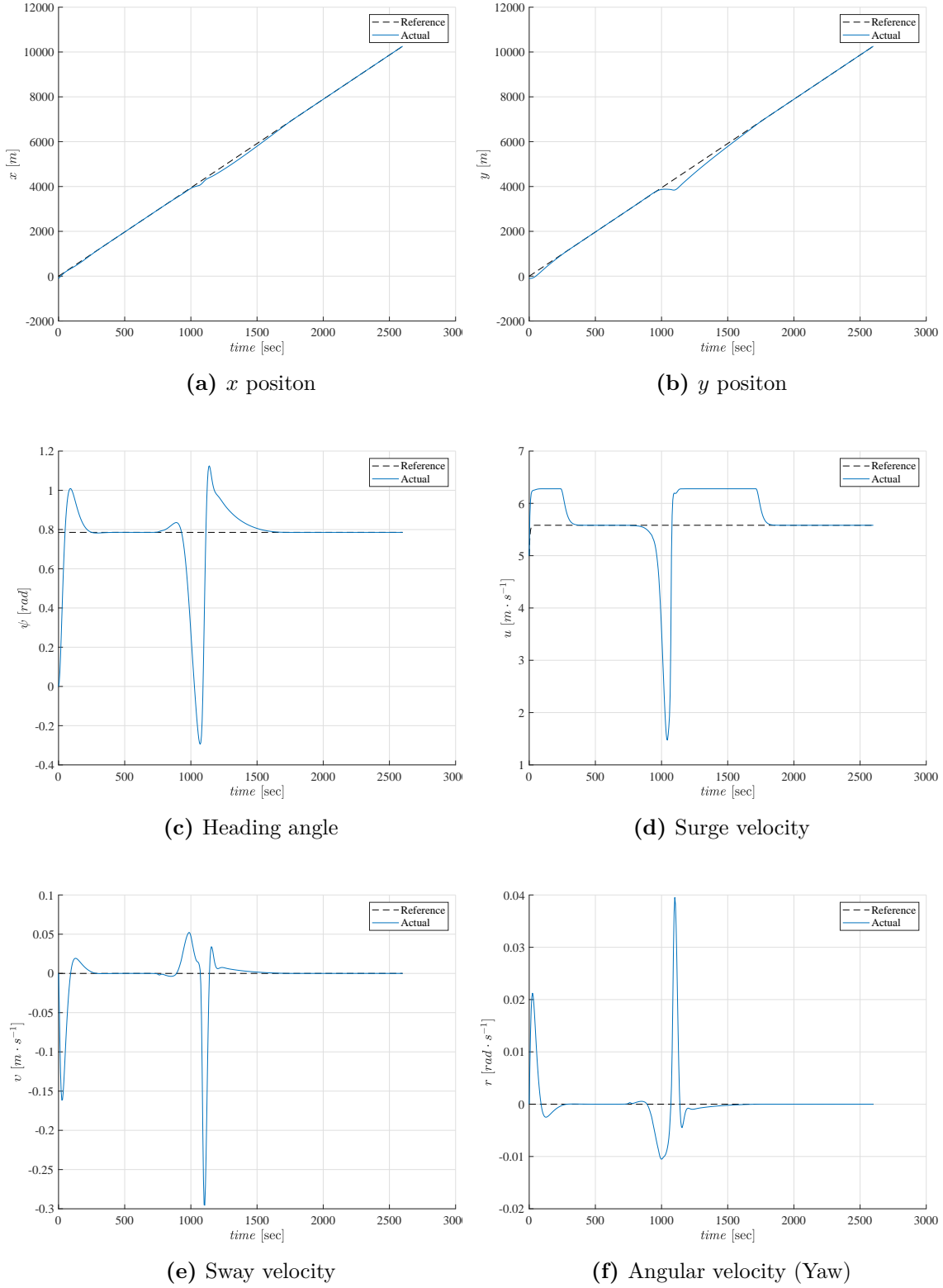


**Figure 7.15:** Simulation results of the states for the elliptical scheme head-on scenario.

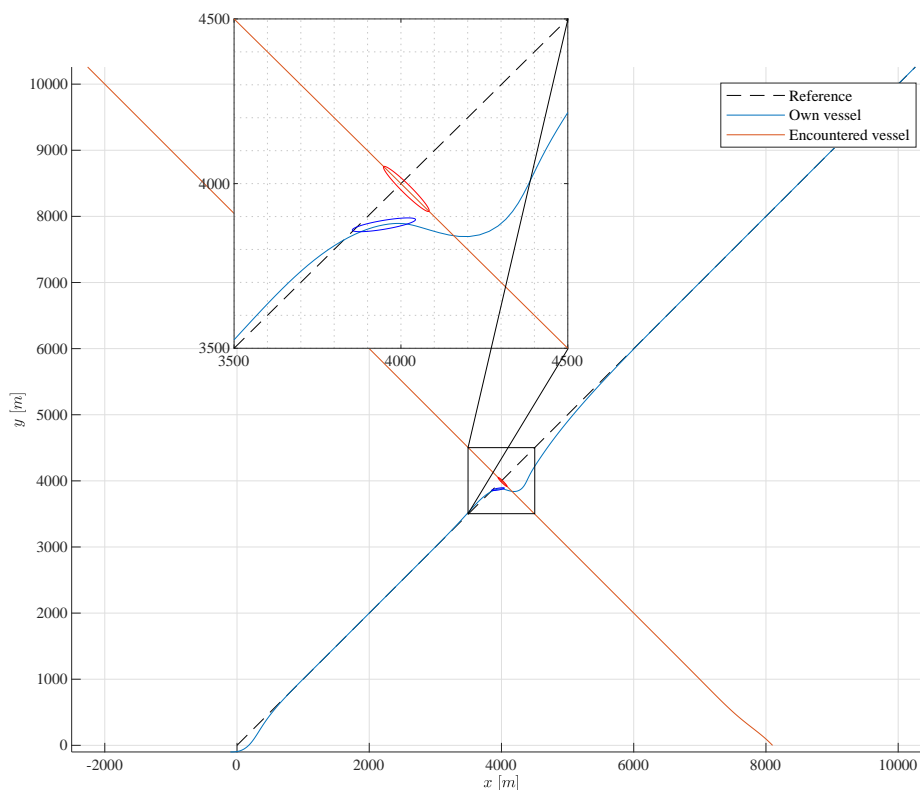


**Figure 7.16:** Trajectory for the elliptical scheme head-on scenario.

at aft of the encountered vessel keeping a minimum distance of about  $127m$  and then tracks the generated trajectory when the collision risk is over. The maximum execution time of elliptical ship domain scheme is about  $25ms$  which is still fast for the collision avoidance decision and much shorter than the sampling interval.

## 7.4 Discussion

In this section, a discussion about the circular and elliptical ship domain NMPC schemes is given to show that the requirements in section 2.1 are met. The design of the trajectory tracking and collision avoidance as a Nonlinear Model Predictive Control problem, which is solved using nonlinear programming, leads to a minimum deviation from the planned trajectory. Moreover, including the control forces and

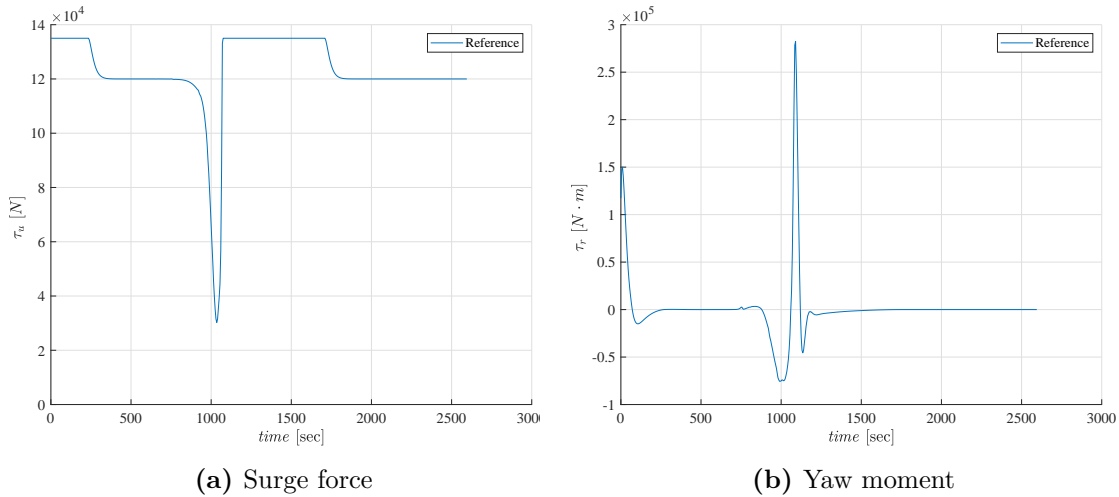


**Figure 7.17:** Simulation results of the control input for the elliptical scheme head-on scenario.

moments in the optimization problem achieves that with the minimum energy. The steady state position tracking error is less than  $0.4 \text{ m}$  which is about  $4.5\%$  of the ship width. Therefore, solution optimality requirement **R1** is met with respect to the prediction model.

The prediction model and the optimization problem are formulated as time-varying which adds the possibility to compensate for the external environmental disturbance if it is measured, estimated or it has a model. In our scheme a Nonlinear Disturbance Observer is used to estimate the external disturbance which leads to more accurate tracking demonstrated by the smaller integral tracking error as a performance index, and therefore, environmental disturbance counteraction requirement **R2** is satisfied.

The presented NMPC collision avoidance scheme is mainly motivated by employing the nonlinear motion model of the vessel, i.e. kinematics and kinetics, instead of just using the kinematics. This leads to a more accurate maneuvering specially in critical situations and shows that control system techniques can be used for collision avoidance. Moreover, the geometry of the ship and the safety area around it are included in the design. They are represented by either a circular



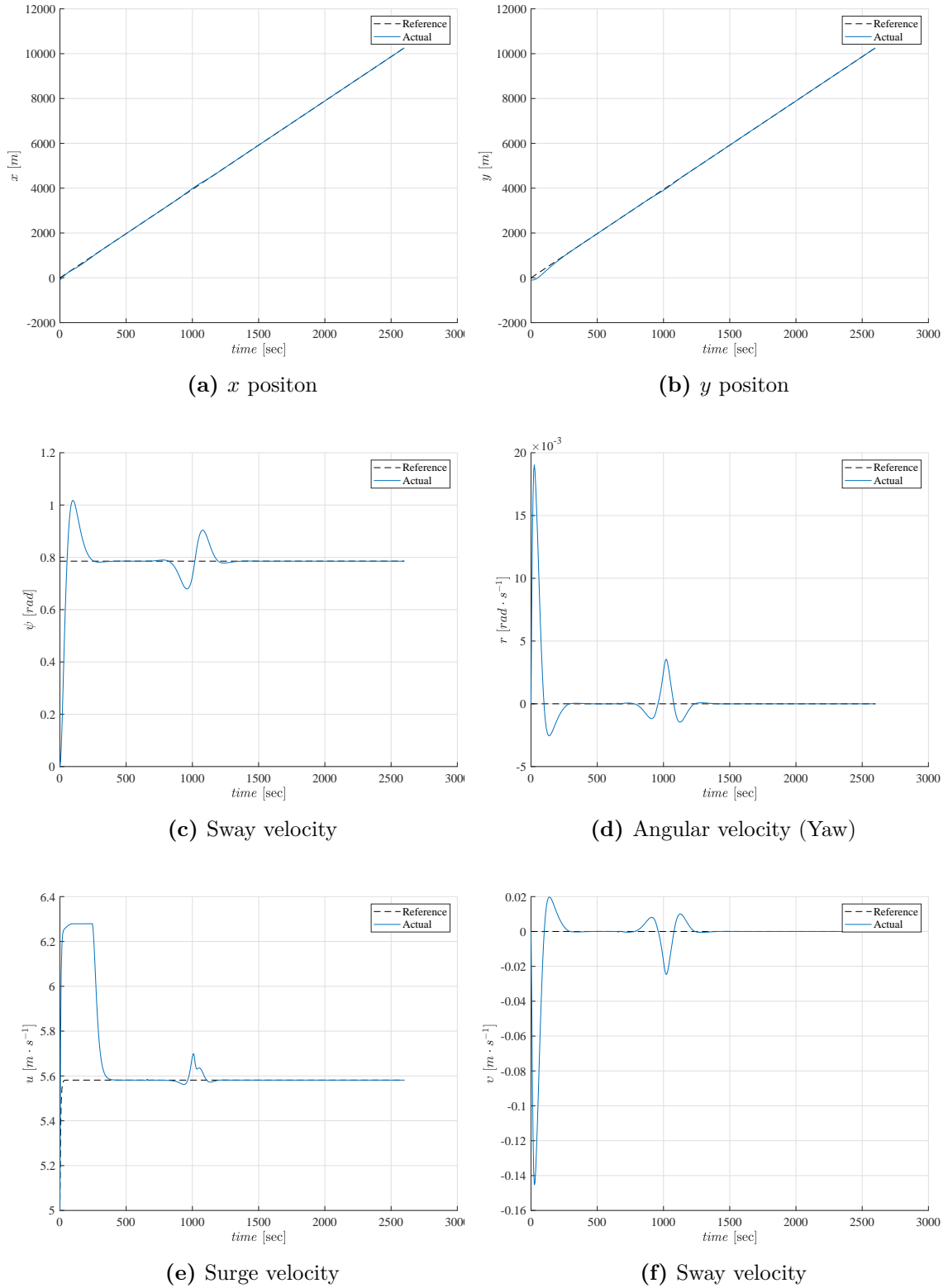


**Figure 7.18:** Simulation results of the states for the elliptical scheme overtaking scenario.

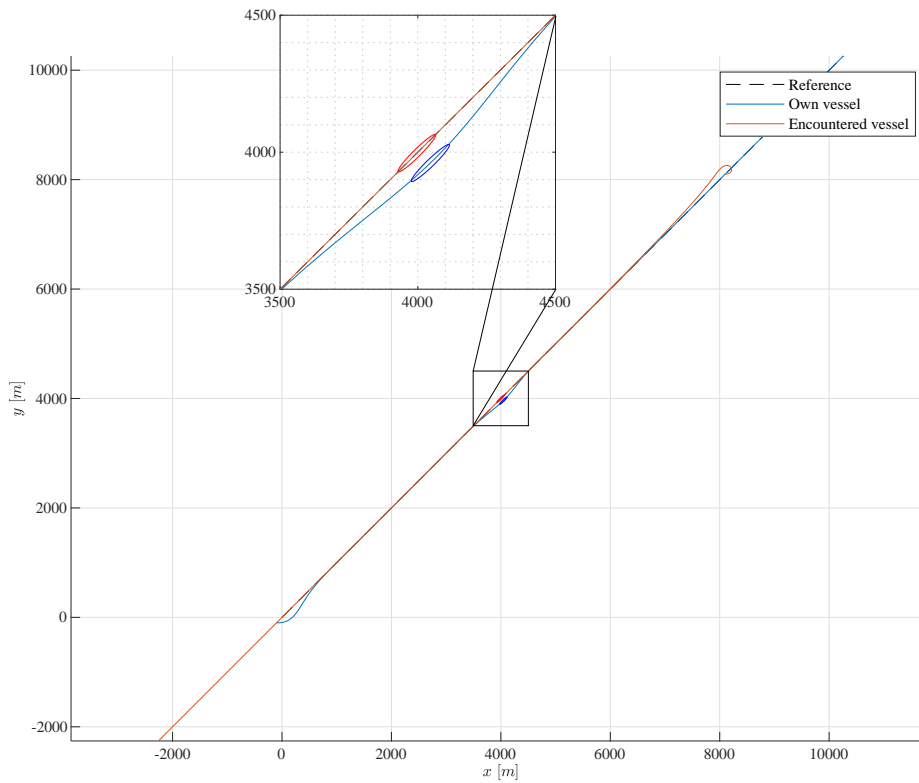


**Figure 7.19:** Trajectory for the elliptical scheme overtaking scenario.

disk or an elliptic disk, and the collision avoidance is formulated as a separation condition. The accurate collision avoidance maneuvering is clear from the small distances achieved between the two ship domain. For example, the circular ship domain case leads to a minimum distance between both circular disks of about  $2.0m$  and  $1.0m$  for the head-on and overtaking situations. The crossing situation has a minimum distance of  $23.0m$  which is still considered acceptable considering that the encountered ship cut a distance of  $25.0m$  during the  $5.0s$  sampling interval. Based on that, both the dynamics-based collision avoidance and the ship domain requirements, **R3** and **R4**, are satisfied, and the presented algorithms can be utilized to act as a last line of defense collision avoidance system.

The state constraints that are used for collision avoidance are formulated as a

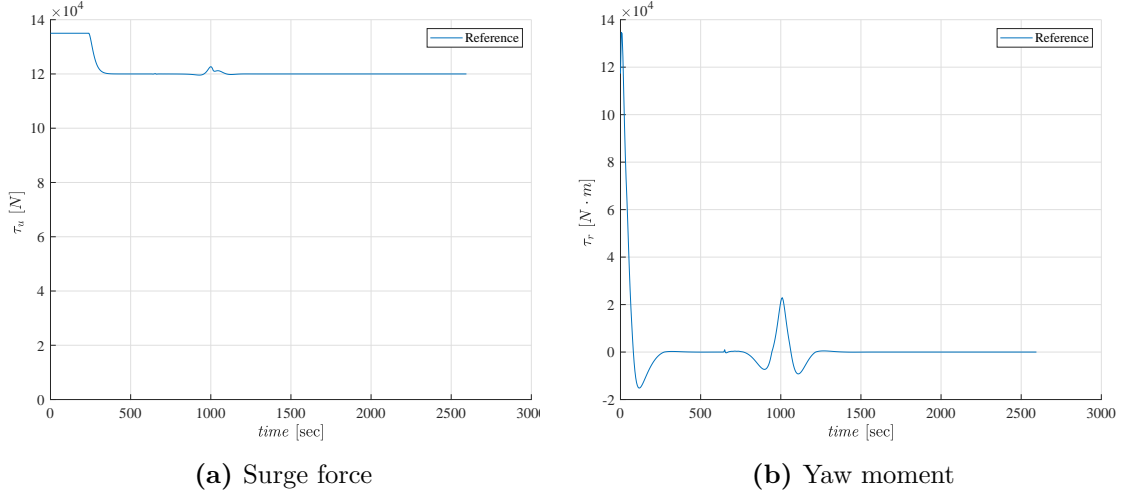
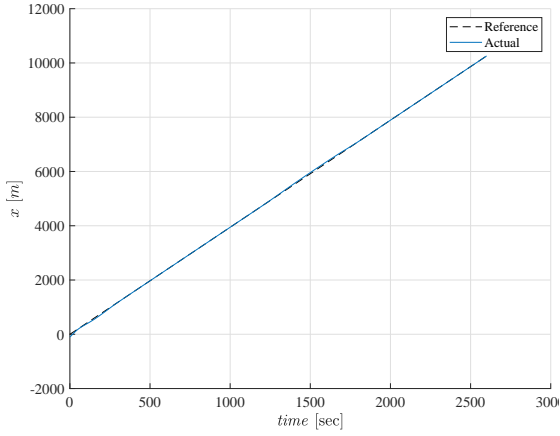


**Figure 7.20:** Simulation results of the control input for the elliptical scheme overtaking scenario.

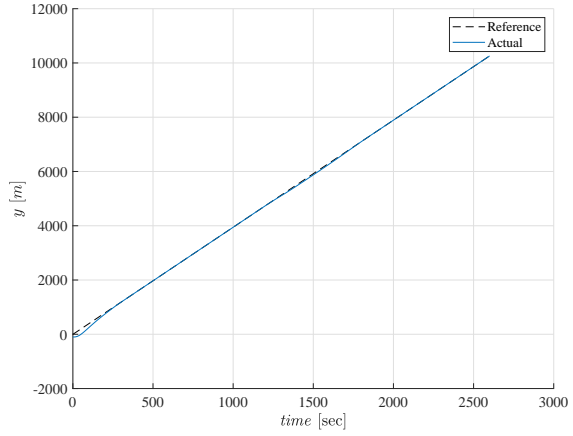
time varying constraints where the prediction of the encountered vessel are treated as an input to the algorithm. This satisfies the requirement of common intention knowledge **R5** as the prediction component is totally independence from tracking and collision avoidance algorithm, and therefore, other sophisticated prediction techniques can be integrated in a modular way.

All the maneuvering achieved by the NMPC algorithm in case of collision risk for the three scenarios presented in this thesis; head-on, overtaking and crossing, either with circular or elliptical ship domain are compliant with the action to avoid collision rules, rules 13, 14 and 15, of COLREGs.

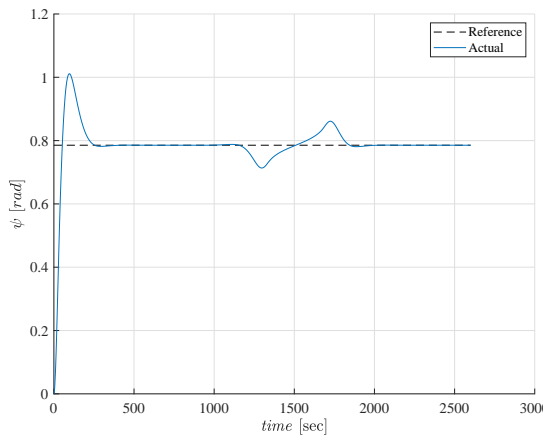
The maximum computation time of the algorithm is about  $15ms$  for the circular ship domain scheme and  $25ms$  for the elliptical ship domain scheme, which is in the range of 0.3% to 0.5% of the sampling interval ( $T_s = 5s$ ) selected for our ship, that has a length of  $32m$ , and therefore requirement **R7** is satisfied and the computation delay can be neglected. It is about 8.3% of the maximum computation time of the Fast Evasive Trajectory Planner presented in [17] on almost the same computer specifications. It is clear from the dynamic model of the ship that larger ship size, or equivalently mass, leads to slower response time and vice versa. Therefore,



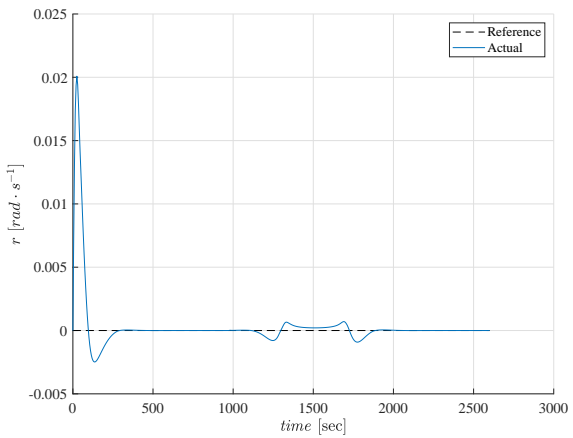
(a)  $x$  position



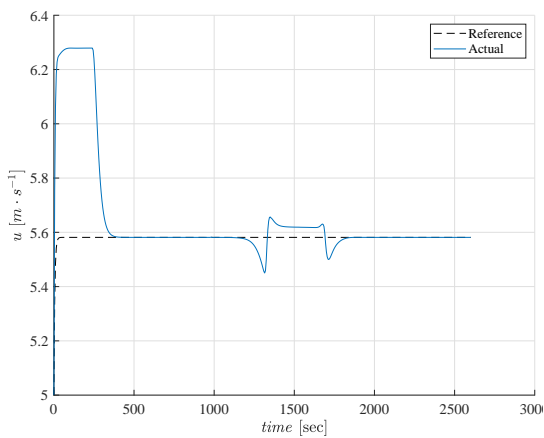
(b)  $y$  position



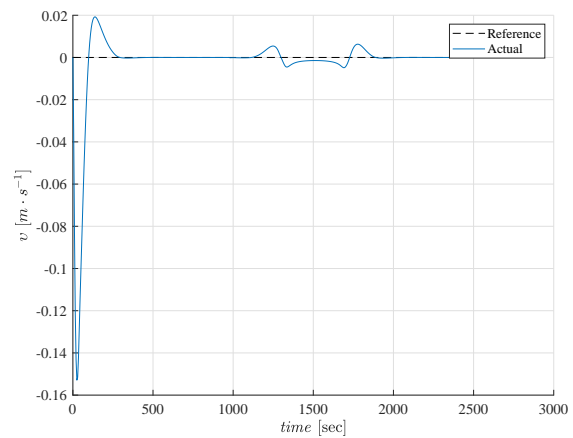
(c) Sway velocity



(d) Angular velocity (Yaw)

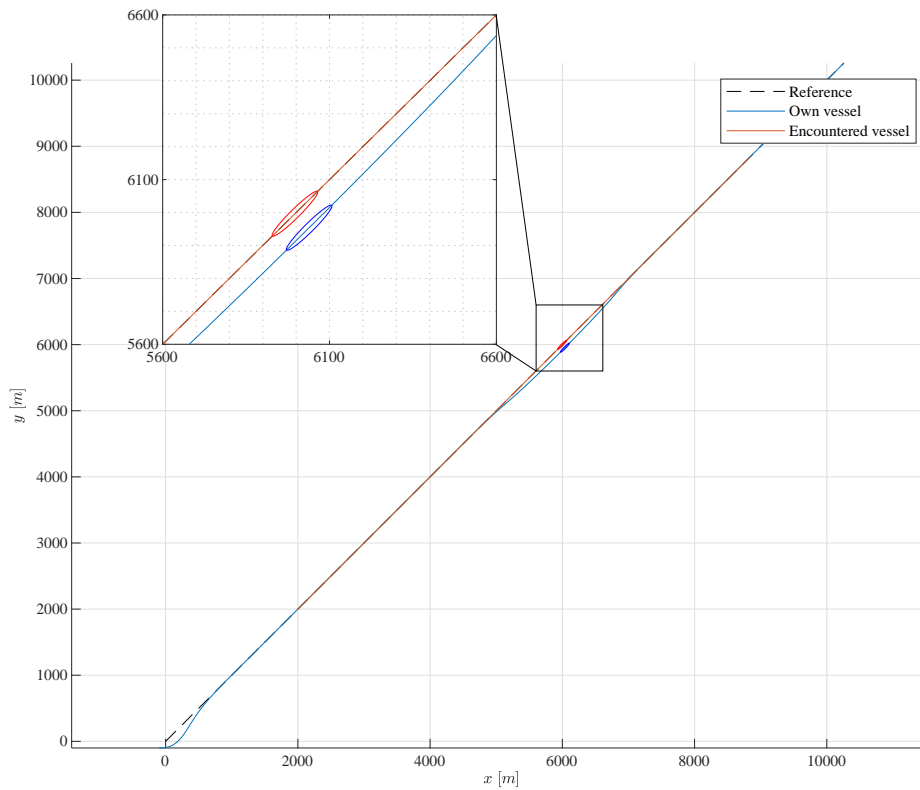


(e) Surge velocity



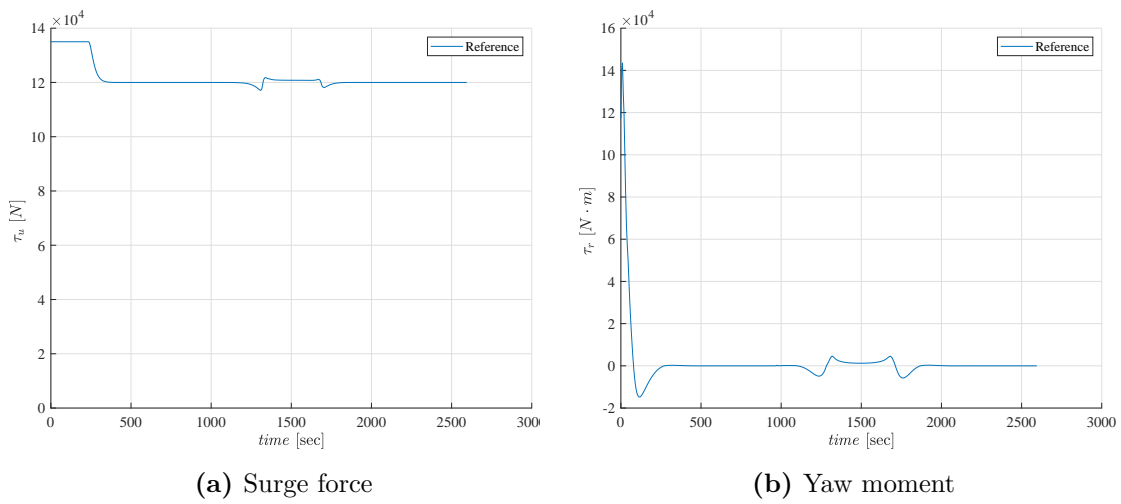
(f) Sway velocity

Figure 7.21: Simulation results of the states for the elliptical scheme crossing scenario.



**Figure 7.22:** Trajectory for the elliptical scheme crossing scenario.

our algorithm can be used for any bigger ship that has a sampling interval larger than  $5sec$ , and for smaller ships with a minimum sampling interval of  $0.5sec$  in order to satisfy the requirement **R7**.



**Figure 7.23:** Simulation results of the control input for the elliptical scheme crossing scenario.

# 8

## Conclusion and Future Work

### 8.1 Conclusion

This thesis proposes an NMPC approach for trajectory tracking of underactuated surface vessels with controller-embedded collisions avoidance technique based on circular and elliptical ship domain representations. A 3-DOF nonlinear model of a 32m length ship is used with only two control variables; surge force and yaw moment. The NMPC is considered as a dynamic optimization problem with an objective to minimize the tracking, and subject to control constraint to respect the maximum force and moment of the ship, and time-varying state constraints which are utilized for collision avoidance. Circular ship domain collision avoidance is formulated as simple Euclidean distance between every two ships, while elliptical ship domain collision avoidance is formulated based on the separation condition between two elliptic disks. In order to add robustness to the NMPC approach, a nonlinear disturbance observer is designed to estimate constant or slowly time varying disturbance. The estimated disturbance is then used as a known input of the prediction model and leads to less tracking error. To avoid the possible random behavior of the solver and to follow the International Regulations for Preventing

Collisions at Sea (COLREGs) that set rules for the actions a vessel should follow when encountering other vessels at sea, head-on, overtaking and crossing rules are included in the optimization problem as an extra state constraint that gives a priority to the ship to turn to the starboard side.

This algorithm is exported as a static memory C code using ACADO toolkit that facilitates real-time implementation due to the efficient computation. MATLAB simulations are used to assess the validity of the proposed technique after compiling the exported code into mex files. The effectiveness of this algorithm is evaluated for three typical collision scenarios; head-on, overtaking and crossing.

## 8.2 Future Work

Open topics for future research are as follows:

**Distributed MPC:** Handling the collision avoidance problem among ships as a cooperative multi-agent networked control system problem using Distributed Model Predictive Control techniques. In this case, a full communication among the vessels is assumed to exchange their intentions.

**Robust MPC:** In order to achieve a higher levels of safety, extension of the work presented in this thesis using Robust MPC techniques is considered as a future research to account for the uncertainties in the measurements, the ship model and the estimated disturbances.

**Time-delay Effect:** Analyze the effect of data loss and time delay in the communication link among vessels on the collision avoidance problem. Include the time-delay in the NMPC optimization problem and achieve robustness against unknown, but bounded, time-delay.

**Studying Other Obstacles Geometry:** This thesis considers only two geometric shapes for the ship or the obstacles, circular and elliptical. Including other shapes will be of a great interest for being able to handle geometrically complex obstacles.



**Supervisory Control:** In order to utilize the schemes presented in this thesis, it is necessary to have a supervisory control component which formulates the static obstacles from the digital maps in to the shapes handled by the schemes. It also should have a fail-safe behavior in case of infeasible solution.



# Appendices



# A

## Vessels Parameters

The ship chosen for simulation is a monohull ship with a length of  $L = 32m$ , a width of about  $W = 9 m$ , a mass of  $118 \times 10^3 kg$  and other parameters calculated by using Vessel RESponse (VERES)—a program that calculates the added mass and damping matrices for surface ships, see [128]. The model of the ship is as follow:

$$M\dot{\mathbf{v}} + C(\mathbf{v})\mathbf{v} + D\mathbf{v} = \boldsymbol{\tau} + R(\psi)^T\mathbf{b} + \mathbf{w}(t) \quad (\text{A.1})$$

where:

$$M = \begin{bmatrix} m_{11} & 0 & 0 \\ 0 & m_{22} & 0 \\ 0 & 0 & m_{33} \end{bmatrix},$$
$$D = \begin{bmatrix} d_{11} & 0 & 0 \\ 0 & d_{22} & 0 \\ 0 & 0 & d_{33} \end{bmatrix}, \text{ and } C(\mathbf{v}) = \begin{bmatrix} 0 & 0 & -m_{22}v \\ 0 & 0 & m_{11}u \\ m_{22}v & -m_{11}u & 0 \end{bmatrix}.$$

The vessel parameters are taken from [129] and are presented in Table A.1. The ship is underactuated and has only actuation in the surge and yaw direction, i.e. no sway force.

**Table A.1:** Surface Vessel Parameters

Parameter	Value	Unit
$m_11$	$120.0 \times 10^3$	kg
$m_22$	$172.9 \times 10^3$	kg
$m_33$	$636.0 \times 10^5$	kg
$d_11$	$215.0 \times 10^2$	$\text{kg} \cdot \text{s}^{-1}$
$d_22$	$97.0 \times 10^3$	$\text{kg} \cdot \text{s}^{-1}$
$d_33$	$802.0 \times 10^4$	$\text{kg} \cdot \text{m}^2 \cdot \text{s}^{-1}$

# B

## Mathematical Preliminaries

### B.1 Young's Inequality

In mathematics, Young's inequality for products is a mathematical inequality about the product of two numbers. The inequality is named after William Henry Young. Young's inequality for products can be used to prove Hölder's inequality. It is also widely used to estimate the norm of nonlinear terms in PDE theory, since it allows one to estimate a product of two terms by a sum of the same terms raised to a power and scaled.

In its standard form, the inequality states that if  $a$  and  $b$  are nonnegative real numbers and  $p$  and  $q$  are positive real numbers such that  $\frac{1}{p} + \frac{1}{q} = 1$ , then

$$ab \leq \frac{a^p}{p} + \frac{b^q}{q} \tag{B.1}$$

. A common case of Young's inequality is when  $p = q = 2$  which is useful in robust control and estimation:

$$ab \leq \frac{a^2}{2} + \frac{b^2}{2} \tag{B.2}$$

.

## B.2 Separation Condition between Two Elliptic Disks

In this section, a theorem for the separation condition between two elliptic disks, i.e. the condition that they are not intersecting, is presented. The elliptic disk is depicted in Figure 7.3 and is parameterized by its position  $(x, y)$ , orientation or heading angle  $\psi$ , semi-major radius  $a$ , and semi-minor radius  $b$ . It is expressed as:

$$\bar{\mathcal{A}} \equiv \{(x_c, y_c) \mid Ax_c^2 - 2Bx_cy_c + Cy_c^2 + (2By - 2Ax)x_c + (2Bx - 2Cy)y_c + (Ax^2 - 2Bxy + Cy^2 - 1) \leq 0\} \quad (\text{B.3})$$

where  $A = \left(\frac{\cos(\psi)^2}{a^2} + \frac{\sin(\psi)^2}{b^2}\right)$ ,  $B = \frac{\sin(2\psi)}{2} \left(\frac{1}{a^2} - \frac{1}{b^2}\right)$  and  $C = \left(\frac{\sin(\psi)^2}{a^2} + \frac{\cos(\psi)^2}{b^2}\right)$ . The elliptic disk can be represented by a  $3 \times 3$  matrix  $\mathcal{A} = [a_{i,j}]$  as:

$$\bar{\mathcal{A}} \equiv \{X \mid X^T \mathcal{A} X \leq 0\} \quad (\text{B.4})$$

where  $X = [x_c \ y_c \ 1]^T$  is the 3-D column vector containing the homogeneous coordinates and

$$\mathcal{A} = \begin{bmatrix} A & -B & By - Ax \\ -B & C & Bx - Cy \\ By - Ax & Bx - Cy & Ax^2 - 2Bxy + Cy^2 - 1 \end{bmatrix}. \quad (\text{B.5})$$

The separation theorem is as follow:

**Theorem B.1.** *Given two elliptic disks  $(\bar{\mathcal{A}}, \bar{\mathcal{B}})$  represented by the matrices  $\mathcal{A} = [a_{i,j}]$  and  $\mathcal{B} = [b_{i,j}]$  respectively:*

1.  $\bar{\mathcal{A}}$  and  $\bar{\mathcal{B}}$  touch externally iff  $\mathcal{P}(\lambda) = \det(\lambda\mathcal{A} - \mathcal{B}) = 0$  has two repeated real negative roots.
2.  $\bar{\mathcal{A}}$  and  $\bar{\mathcal{B}}$  are separate iff  $\mathcal{P}(\lambda) = 0$  has two distinct real negative roots.

*Proof.* see reference [130] □



### B.3 Cubic Polynomial

In this section we present the result about the nature of the cubic polynomial roots without solving it.

**Theorem B.2.** Consider a cubic polynomial  $\mathcal{P}(\lambda) = C_3\lambda^3 + C_2\lambda^2 + C_1\lambda + C_0$ . Let  $\Delta = 18C_3C_2C_1C_0 - 4C_2^3C_0 + C_2^2C_1^2 - 4C_3C_1^3 - 27C_3^2C_0^2$  be the discriminant of  $\mathcal{P}(\lambda)$ .  $\Delta$  can be positive, negative, or zero depending on the roots nature as follow:

1. If  $\Delta > 0$ , then  $\mathcal{P}(\lambda)$  has three distinct real roots;
2. if  $\Delta = 0$ , then  $\mathcal{P}(\lambda)$  has a multiple root and all its roots are real;
3. if  $\Delta < 0$ , then  $\mathcal{P}(\lambda)$  has one real root and two complex conjugate roots.

*Proof.* See chapter 10 in [131].

□



## References

- [1] T. Statheros, W.G.J. Howells, and K.D. McDonald-Maier. “Autonomous Ship Collision Avoidance Navigation Concepts, Technologies and Techniques”. In: (2008), pp. 129–142.
- [2] Eliopoulou Eleftheria, Papanikolaou Apostolos, and Voulgarellis Markos. “Statistical analysis of ship accidents and review of safety level”. In: *Safety Science* 85.October 2017 (2016), pp. 282–292.
- [3] Tor Arne Johansen, Tristan Perez, and Andrea Cristofaro. “Ship collision avoidance and COLREGS compliance using simulation-based control behavior selection with predictive hazard assessment”. In: *IEEE Transactions on Intelligent Transportation Systems* 17.12 (2016), pp. 3407–3422.
- [4] Xin Wang, Zhengjiang Liu, and Yao Cai. “The ship maneuverability based collision avoidance dynamic support system in close-quarters situation”. In: *Ocean Engineering* August (2017), pp. 1–12.
- [5] Paul Ryan. “The Titanic Tale”. In: *Oceanus* (1985).
- [6] John P. Eaton and Charles A. Haas. *Titanic: Triumph and Tragedy*. Norton, 1995.
- [7] Lewis Collins. *Titanic’s Final Manoeuvre*. Tech. rep. 2013, pp. 1–4.
- [8] Robert Rylander. “Autonomous safety on vessels”. In: (2016).
- [9] Morten Breivik. *Topics in Guided Motion Control of Marine Vehicles*. June. 2010.
- [10] Ørnulf Jan Rødseth and Håvard Nordahl. *Definitions for Autonomous Merchant Ships*. Tech. rep. Norwegian Forum for Autonomous Ships, 2017, p. 22.
- [11] Thor I. Fossen. *Handbook of Marine Craft Hydrodynamics and Motion Control*. 1st. 1. John Wiley & Sons Ltd., 2011, p. 575.
- [12] “COLREGS - International Regulations for Preventing Collisions at Sea”. In: *Convention on the International Regulations for Preventing Collisions at Sea, 1972* (1972), pp. 1–74.
- [13] Sascha Hornauer. “Maritime Trajectory Negotiation for n-Vessel Collision Avoidance”. PhD thesis. University of Oldenburg, 2016, p. 141.
- [14] M.R. Benjamin and J.a. Curcio. “COLREGS-based navigation of autonomous marine vehicles”. In: *2004 IEEE/OES Autonomous Underwater Vehicles (IEEE Cat. No.04CH37578)* June 2014 (2004), pp. 32–39.

- [15] S. Campbell, M. Abu-Tair, and W. Naeem. “An automatic COLREGs-compliant obstacle avoidance system for an unmanned surface vehicle”. In: *Proceedings of the Institution of Mechanical Engineers, Part M: Journal of Engineering for the Maritime Environment* 228.2 (2013), pp. 108–121.
- [16] Zhiwei Zhang and Xiao Ming Li. “Global ship accidents and ocean swell-related sea states”. In: *Natural Hazards and Earth System Sciences* (2017).
- [17] Michael Blaich. “Path Planning and Collision Avoidance for Safe Autonomous Vessel Navigation in Dynamic Environments”. PhD thesis. University of Oldenburg, 2016, p. 168.
- [18] Roger Skjetne. “The Maneuvering Problem”. PhD thesis. NTNU, 2005.
- [19] Shihua Li et al. *Disturbance Observer-Based Control :Methods and Applications*. Taylor & Francis Group, 2014.
- [20] Ammar Aljuhne, Axel Hahn, and Oliver Zielinski. “Noise characteristics in extreme shallow water with relation to ship maneuvering parameters”. In: *2017 IEEE International Symposium on Signal Processing and Information Technology (ISSPIT)*. 2017.
- [21] Christian Denker et al. “E-Navigation based cooperative collision avoidance at sea: The MTCAS approach”. In: *2016 European Navigation Conference, ENC 2016* (2016).
- [22] Vincent Léchappé et al. “Predictive control of disturbed systems with input delay: Experimental validation on a DC motor”. In: *12th Time Delay Systems Workshop*. Vol. 48. 12. Ann Arbor, United States, 2016.
- [23] Dongkyoung Chwa. “Global tracking control of underactuated ships with input and velocity constraints using dynamic surface control method”. In: *IEEE Transactions on Control Systems Technology* 19.6 (2011), pp. 1357–1370.
- [24] Z H Peng et al. “Adaptive Dynamic Surface Control for Formations of Autonomous Surface Vehicles With Uncertain Dynamics”. In: *IEEE Transactions on Control Systems Technology* 21.2 (2013), pp. 513–520.
- [25] Hao Wang, Dan Wang, and Zhouhua Peng. “Adaptive dynamic surface control for cooperative path following of marine surface vehicles with input saturation”. In: *Nonlinear Dynamics* 77.1 (2014), pp. 107–117.
- [26] Tieshan Li, Bo Yu, and Biguang Hong. “A novel adaptive fuzzy design for path following for underactuated ships with actuator dynamics”. In: *2009 4th IEEE Conference on Industrial Electronics and Applications, ICIEA 2009* (2009), pp. 2796–2800.
- [27] Xin Hu, Jialu Du, and Yuqing Sun. “Robust Adaptive Control for Dynamic Positioning of Ships”. In: (2017), pp. 1–10.
- [28] Khac Duc Do. “Path-tracking control of underactuated ships under tracking error constraints”. In: *Journal of Marine Science and Application* 14.4 (2015), pp. 343–354.

- [29] Nazli E. Kahveci and Petros a. Ioannou. “Adaptive steering control for uncertain ship dynamics and stability analysis”. In: *Automatica* 49.3 (2013), pp. 685–697.
- [30] Zaopeng Dong et al. “Trajectory tracking control of underactuated USV based on modified backstepping approach”. In: *International journal of naval architecture and ocean engineering* 7.5 (2015), pp. 817–832.
- [31] Zhong Ping Jiang and Henk Nijmeijer. “A recursive technique for tracking control of nonholonomic systems in chained form”. In: *IEEE Transactions on Automatic Control* 44.2 (1999), pp. 265–279.
- [32] K. D. Do and J. Pan. “State- and output-feedback robust path-following controllers for underactuated ships using Serret-Frenet frame”. In: *Ocean Engineering* 31.5-6 (2004), pp. 587–613.
- [33] F Kühne, J Gomes, and W Fetter. “Mobile robot trajectory tracking using model predictive control”. In: *II IEEE latin-american robotics symposium*. 2005, pp. 1–7.
- [34] Bruno J Guerreiro et al. “Trajectory Tracking Nonlinear Model Predictive Control for Autonomous Surface Craft”. In: *IEEE Transaction on Control Systems Technology* 22.6 (2014), pp. 3006–3011.
- [35] Alexey Pavlov, Håvard Nordahl, and Morten Breivik. “MPC-based optimal path following for underactuated vessels”. In: *IFAC Proceedings Volumes (IFAC-PapersOnline)* (2009), pp. 340–345.
- [36] So-Ryeok Oh and Jing Sun. “Path following of underactuated marine surface vessels using line-of-sight based model predictive control”. In: *Ocean Engineering* 37.2-3 (2010), pp. 289–295.
- [37] Zheng Yan and Jun Wang. “Model Predictive Control for Tracking of Underactuated Vessels Based on Recurrent Neural Networks”. In: *IEEE Journal of Oceanic Engineering* 37.4 (2012), pp. 717–726.
- [38] David Q. Mayne. “Model predictive control: Recent developments and future promise”. In: *Automatica* (2014).
- [39] Mohamed Abdelaal, Martin Fränzle, and Axel Hahn. “Nonlinear Model Predictive Control for Tracking of Underactuated Vessels under Input Constraints”. In: *2015 IEEE European Modelling Symposium on Mathematical Modelling and Computer Simulation*. 2015, pp. 313–318.
- [40] J. M. Quero, E. F. Camacho, and L. G. Franquelo. “Neural Network for Constrained Predictive Control”. In: *IEEE TRANSACTIONS ON CIRCUITS AND SYSTEMS* 40.9 (1993), pp. 621–626.
- [41] Li-xin Wang and Feng Wan. “Structured neural networks for constrained model predictive control”. In: *Automatica* 37 (2001), pp. 1235–1243.
- [42] Long Cheng and Æ Zeng-guang Hou Æ Min. “Constrained multi-variable generalized predictive control using a dual neural network”. In: *Neural Comput & Applic* 16 (2007), pp. 505–512.
- [43] Yunpeng Pan and Jun Wang. “Two Neural Network Approaches to Model Predictive Control”. In: *American Control Conference*. 2008, pp. 1685–1690.

- [44] Yunpeng Pan and Jun Wang. “Model Predictive Control of Unknown Nonlinear Dynamical Systems Based on Recurrent Neural Networks”. In: *IEEE TRANSACTIONS ON INDUSTRIAL ELECTRONICS* 59.8 (2012), pp. 3089–3101.
- [45] Zheng Yan and Jun Wang. “Robust model predictive control of nonlinear affine systems based on a two-layer recurrent neural network”. In: *The 2011 International Joint Conference on Neural Networks* (2011), pp. 24–29.
- [46] Mingming Wang, Jianjun Luo, and Ulrich Walter. “A non-linear model predictive controller with obstacle avoidance for a space robot”. In: *Advances in Space Research* (2015).
- [47] Roman Smierzchalski. “Evolutionary trajectory planning of ships in navigation traffic areas”. In: *Journal of Marine Science and Technology* 4 (1999), pp. 1–6.
- [48] Rafal Szlapczynski. “Evolutionary Sets Of Safe Ship Trajectories : A New Approach To Collision Avoidance”. In: *THE JOURNAL OF NAVIGATION* 64 (2011), pp. 169–181.
- [49] Rafal Szlapczynski and Joanna Szlapczynska. “On evolutionary computing in multi-ship trajectory planning”. In: *Applied Intelligence* 37 (2012), pp. 155–174.
- [50] R. Szlapczynski. “Evolutionary Sets of Safe Ship Trajectories : Evaluation of Individuals”. In: *International Journal on Marine Navigation and Safety of Sea Transportation* 6.3 (2012), pp. 345–353.
- [51] Yongqiang Zhuo. “Intelligent Collision Avoidance Control for Large Ships”. In: *International Conference on Information Science, Electronics and Electrical Engineering (ISEEE)*. 2014, pp. 1887–1891.
- [52] Yu-hong Liu and Chao-jian Shi. “A Fuzzy-Neural Inference Network for Ship Collision Avoidance”. In: *International Conference on Machine Learning and Cybernetics*. 1. Guangzhou, 2005, pp. 4754–4759.
- [53] Ibrahim Ari et al. “Optimal ship navigation with safety distance and realistic turn constraints”. In: *European Journal of Operational Research* 229.3 (2013), pp. 707–717.
- [54] Peng Wang and Baocang Ding. “A synthesis approach of distributed model predictive control for homogeneous multi-agent system with collision avoidance”. In: *International Journal of Control* 87.1 (2014), pp. 52–63.
- [55] Bassam Alrifaae, Masoumeh Ghanbarpour Mamaghani, and Dirk Abel. “Centralized Non-Convex Model Predictive Control for Cooperative Collision Avoidance of Networked Vehicles”. In: *IEEE International Symposium on Intelligent Control (ISIC)*. 2014, pp. 1583–1588.
- [56] Khac Duc Do and Jie Pan. *Control of Ships and Underwater Vehicles: Design for Underactuated and Nonlinear Marine Systems*. Springer, 2009.
- [57] SNAME The Society of Naval Architects and Marine Engineers. *Nomenclature for Treating the Motion of a Submerged Body Through a Fluid*. 1950.

- [58] Roger Skjetne, yvind N. Smogeli, and Thor I. Fossen. “A Nonlinear Ship Manoeuvring Model: Identification and adaptive control with experiments for a model ship”. In: *Modeling, Identification and Control* 25.1 (2004), pp. 3–27.
- [59] Thor I Fossen. *Guidance and Control of Ocean Vehicles*. 1994. arXiv: 9809069v1 [arXiv:gr-qc].
- [60] Thor I. Fossen. *Marine Control Systems: Guidance, Navigation, and Control of Ships, Rigs and Underwater Vehicles*. Trondheim: Springer, 2002.
- [61] A. J. Sørensen, S. I. Sagatun, and T. I. Fossen. “Design of a dynamic positioning system using model-based control”. In: *Control Engineering Practice* 4.3 (1996), pp. 359–368.
- [62] Asgeir J. Sørensen. “Kompendium: Marine Cybernetics: Modelling and Control”. In: *Marine Technology Centre, Trondheim, Norway* (2002).
- [63] M A Abkowitz. *Lectures on ship hydrodynamics—steering and manoeuvrability*. Tech. rep. Lyngby, Denmark: Hydro-Og Laboratorium, 1964.
- [64] K K Fedyayevsky and G V Sobolev. *Control and Stability in Ship Design*. State Union Shipbuilding Industry Publishing House, 1964.
- [65] N. H. Norrbin. “Theory and observations on the use of a mathematical model for ship manoeuvring in deep and confined waters”. In: *8th Symp. Naval Hydrodynamics*. Pasadena, California, USA, 1970.
- [66] Thor I Fossen and Jann Peter Strand. “Passive nonlinear observer design for ships using lyapunov methods: full-scale experiments with a supply vessel”. In: *Automatica* 35.1 (1999), pp. 3–16.
- [67] A. I. Propoi. “Application of linear programming methods for the synthesis of automatic sampled-data systems”. In: *Avtomat. i Telemekh.*, 24.7 (1963), pp. 912–920.
- [68] Flavio Manenti. “Considerations on nonlinear model predictive control techniques”. In: *Computers and Chemical Engineering* 35.11 (2011), pp. 2491–2509.
- [69] Lars Gruene. *Nominal Model Predictive Control*. Tech. rep. Bayreuth, Germany: Mathematical Institute, University of Bayreuth, 2013.
- [70] C. R. Cutler and B.L. Ramaker. “Dynamic matrix control– A computer control algorithm”. In: *AIChE 86th National Meeting*. Houston, TX, 1979.
- [71] C. R. Cutler and B.L. Ramaker. “Dynamic matrix control– A computer control algorithm”. In: *Joint Automatic Control Conference*. San Francisco, California, 1980.
- [72] D.W. Clarke, C. Mohtadi, and P.S. Tuffs. “Generalized predictive control—Part I. The basic algorithm”. In: *Automatica* 23.2 (1987), pp. 137–148.
- [73] D.W. Clarke, C. Mohtadi, and P.S. Tuffs. “Generalized predictive control– II. Extensions and interpretations”. In: *Automatica* 23 (1987), pp. 149–160.

- [74] F. Borrelli, A. Bemporad, and M. Morari. *Explicit Nonlinear Model Predictive Control: Theory and Applications*. 2012.
- [75] J.B. Rawlings and D.Q. Mayne. *Model Predictive Control : Theory and Design*. 1st. Nob Hill Publishing, LLC, 2009, pp. 1–11.
- [76] Michael Athans and Peter Falb. *Optimal Control: An Introduction to the Theory and Its Applications*. New York, NY: McGraw-Hill Book Company, 1966.
- [77] Richard E. Bellman. *Dynamic Programming*. Rand Corporation, 1957.
- [78] Jun Yang and Wei Xing Zheng. “Offset-Free Nonlinear MPC for Mismatched Disturbance Attenuation With Application to a Static Var Compensator”. In: *IEEE Transaction on Circuits and Systems* 61.1 (2014), pp. 49–53.
- [79] Lars Grüne and Jürgen Pannek. *Nonlinear Model Predictive Control Theory and Algorithms*. Springer, 2011.
- [80] Lars Grüne and Jürgen Pannek. *Nonlinear Model Predictive Control Theory and Algorithms*. 2011.
- [81] Lalo Magni et al. “A stabilizing model-based predictive control algorithm for nonlinear systems”. In: *Automatica* 37.9 (2001), pp. 1351–1362.
- [82] D.Q. Mayne et al. “Constrained model predictive control: Stability and optimality”. In: *Automatica* 36 (2000), pp. 789–814.
- [83] C.J. Ong, D. Sui, and E.G. Gilbert. “Enlarging the terminal region of nonlinear model predictive control using the support vector machine method”. In: *Automatica* 42.6 (2006), pp. 1011–1016.
- [84] H Chen and Frank Allgöwer. “A quasi-infinite horizon nonlinear model predictive control scheme with guaranteed stability”. In: *Automatica* 34.10 (1998), pp. 1205–1217.
- [85] Lalo Magni and R. Scattolini. “Stabilizing model predictive control of nonlinear continuous time systems”. In: *Annual Reviews in Control* 28.1 (2004), pp. 1–11.
- [86] S. S. Keerthi and E. G. Gilbert. “Optimal infinite-horizon feedback laws for a general class of constrained discrete-time systems: Stability and moving-horizon approximations”. In: *Journal of Optimization Theory and Applications* 57.2 (1988), pp. 265–293.
- [87] D.Q. Mayne and H. Michalska. “Receding horizon control of nonlinear systems”. In: *IEEE Transactions on Automatic Control* 35.7 (1990), pp. 814–824.
- [88] G. De Nicolao, L. Magni, and R. Scattolini. “Stabilizing receding-horizon control of nonlinear time-varying systems”. In: *IEEE Transactions on Automatic Control* 43.7 (1998), pp. 1030–1036.
- [89] Ali Jadbabaie and John Hauser. “On the Stability of Receding Horizon Control With a General Terminal Cost”. In: *IEEE Transactions on Automatic Control* 50.5 (2005), pp. 674–678.
- [90] Moritz Diehl, Hans Joachim Ferreau, and Niels Haverbeke. “Efficient Numerical Methods for Nonlinear MPC and Moving Horizon Estimation”. In: *Nonlinear Model Predictive Control*. 2009, pp. 391–417.



- [91] G. A. Ray and W. H. Hicks. "Approximation methods for optimal control synthesis". In: *The Canadian Journal Chemical Engineering* 49 (1971), pp. 522–528.
- [92] R.W.H. Sargent and G.R. Sullivan. "The Development of an Efficient Optimal Control Package". In: *Proceedings of the 8th IFIP Conference on Optimization Techniques*. Heidelberg: Springer, 1977.
- [93] D. Kraft. "On converting optimal control problems into nonlinear programming problems". In: *Computational Mathematical Programming*. Springer, 1985, pp. 261–280.
- [94] P Deuffhard. "A Modified Newton Method for the Solution of Ill-Conditioned Systems of Nonlinear Equations with Application to Multiple Shooting". In: *Numerische Mathematik* 22 (1974), pp. 289–315.
- [95] H. G. Bock and K. J. Plitt. "A multiple shooting algorithm for direct solution of optimal control problems". In: *Proc. IFAC World Congress Budapest*. Budapest, 1984, pp. 243–247.
- [96] C Kirches et al. "Efficient Direct Multiple Shooting for Nonlinear Model Predictive Control on Long Horizons". In: *Journal of Process Control* 22.3 (2012), pp. 540–550.
- [97] D.B. Leineweber et al. "An efficient multiple shooting based reduced SQP strategy for large-scale dynamic process optimization. Part I: Theoretical aspects". In: *Computers & Chemical Engineering* 27.2 (2003), pp. 157–166.
- [98] T.H. Tsang, D.M. Himmelblau, and T.F. Edgar. "Optimal control via collocation and nonlinear programming". In: *International Journal of Control* 21 (1975), pp. 763–768.
- [99] L.T. Biegler. "Solution of dynamic optimization problems by successive quadratic programming and orthogonal collocation". In: *Computers and Chemical Engineering* 8 (1984), pp. 243–248.
- [100] Oskar von Stryk. "Numerical Solution of Optimal Control Problems by Direct Collocation". In: *International Series in Numerical Mathematics* 111 (1993), pp. 129–143.
- [101] Boris Houska and Hans Joachim. *ACADO Toolkit User's Manual*. 2014.
- [102] Thor I. Fossen. *Nonlinear passive control and observer design for ships*. 2000.
- [103] Mohamed E Abdelaal, Hassan M Emara, and A Bahgat. "Interval Type 2 Fuzzy Sliding Mode Control With Application to Inverted Pendulum on a Cart". In: *ICIT2013*. 2013, pp. 100–105.
- [104] W.-H. Chen. "Disturbance Observer Based Control for Nonlinear Systems". In: *IEEE/ASME Transactions on Mechatronics* 9.4 (2004), pp. 706–710.
- [105] Jialu Du et al. "Robust dynamic positioning of ships with disturbances under input saturation". In: *Automatica* 73 (2016), pp. 207–214.

- [106] Harald Aschemann and Andreas Rauh. “Nonlinear control and disturbance compensation for underactuated ships using extended linearisation techniques”. In: *IFAC Proceedings Volumes (IFAC-PapersOnline)*. Rostock-Warnemünde: IFAC, 2010, pp. 167–172.
- [107] A Pedro Aguiar. “Trajectory-Tracking and Path-Following of Underactuated Autonomous Vehicles With Parametric Modeling Uncertainty”. In: 52.8 (2007), pp. 1362–1379.
- [108] K. Y. Pettersen and H. Nijmeijer. “Underactuated ship tracking control: Theory and experiments”. In: *International Journal of Control* 74.14 (2001), pp. 1435–1446.
- [109] M Breivik and TI Fossen. “Path following of straight lines and circles for marine surface vessels”. In: *Proc. of the IFAC CAMS* (2004), pp. 65–70.
- [110] Thor I. Fossen, Kristin Y. Pettersen, and Roberto Galeazzi. “Line-of-Sight Path Following for Dubins Paths With Adaptive Sideslip Compensation of Drift Forces”. In: *IEEE Transactions on Control Systems Technology* 23 (2014), pp. 820–827.
- [111] Yuji Sato and Hiromitsu Ishii. “Study of a collision-avoidance system for ships”. In: *Control Engineering Practice* 6.9 (1998), pp. 1141–1149.
- [112] Catherine Hetherington, Rhona Flin, and Kathryn Mearns. “Safety in shipping: The human element”. In: *Journal of Safety Research* 37.4 (2006), pp. 401–411.
- [113] T. G. Coldwell. “Marine Traffic Behaviour in Restricted Waters”. In: *Journal of Navigation* 36.3 (1983), pp. 430–444.
- [114] Martin Gamborg Hansen et al. “Empirical ship domain based on AIS data”. In: *Journal of Navigation* 66.6 (2013), pp. 931–940.
- [115] Zbigniew Pietrzykowski and Janusz Uriasz. “The ship domain - A criterion of navigational safety assessment in an open sea area”. In: *Journal of Navigation* 62.1 (2009), pp. 93–108.
- [116] Zhe Xiang, Qinyou Hu, and Chaojian Shi. “A Clustering Analysis for Identifying Areas of Collision Risk in Restricted Waters”. In: *TransNav, the International Journal on Marine Navigation and Safety of Sea Transportation* 7.2 (2013), pp. 101–105.
- [117] TengFei Wang et al. “Ship Domain Model for Multi-ship Collision Avoidance Decision-making with COLREGs Based on Artificial Potential Field”. In: *TransNav, the International Journal on Marine Navigation and Safety of Sea Transportation* 11.1 (2017), pp. 85–92.
- [118] Rafal Szlapczynski and Joanna Szlapczynska. “A Simulative Comparison of Ship Domains and Their Polygonal Approximations”. In: *TransNav* 9 (2015), pp. 135–141.
- [119] Z Pietrzykowski and M Wielgosz. “Navigation Safety Assessment in the Restricted Area with the Use of ECDIS”. In: *The International Journal on Marine Navigation and Safety of Sea Transportation* 5.1 (2011), pp. 29–35.

- [120] Elisabeth M Goodwin. “A Statistical Study of Ship Domains.pdf”. In: *The Journal of Navigation* 28.3 (1975), pp. 328–344.
- [121] P. V. Davis, M. J. Dove, and C. T. Stockel. “A Computer Simulation of Multi-Ship Encounters”. In: *Journal of Navigation* 35.2 (1982), pp. 347–352.
- [122] Yahei Fujii and Kenichi Tanaka. “Traffic Capacity”. In: *Journal of Navigation* 24.4 (1971), pp. 543–552.
- [123] Qingyang Xu and Ning Wang. “A survey on ship collision risk evaluation”. In: *Promet - Traffic & Transportation* 26.6 (2014), pp. 475–486.
- [124] Dominik Petrich et al. “Map-based long term motion prediction for vehicles in traffic environments”. In: *IEEE Conference on Intelligent Transportation Systems, Proceedings, ITSC Itsc* (2013), pp. 2166–2172.
- [125] Guoyuan Li et al. “Neural-network-based modelling and analysis for time series prediction of ship motion”. In: *Ship Technology Research* 64.1 (2017), pp. 30–39.
- [126] X Rong Li and V P Jilkov. “Survey of maneuvering target tracking. Part I. Dynamic models”. In: *Aerospace and Electronic Systems, IEEE Transactions on* 39.4 (2003), pp. 1333–1364.
- [127] Yoshiaki Kuwata et al. “Safe Maritime Autonomous Navigation With COLREGS, Using Velocity Obstacles”. In: *IEEE Journal of Oceanic Engineering* 39.1 (2014), pp. 110–119.
- [128] D. Fathi. *ShipX Vessel Responses (VERES)*. 2004.
- [129] K. D. Do, Z. P. Jiang, and J. Pan. “Underactuated ship global tracking under relaxed conditions”. In: *IEEE Transactions on Automatic Control* 47.9 (2002), pp. 1529–1536.
- [130] Y.-K. Choi et al. “Continuous Collision Detection for Two Moving Elliptic Disks”. In: *IEEE Transactions on Robotics* 22.2 (2006), pp. 213–224.
- [131] S Axler, F W Gehring, and K A Ribet. *Integers, Polynomials, and Rings*. Ed. by S. Axler, F.W. Gehring, and K.A. Ribet. 1st ed. Springer, 2004.



# Declaration of Authorship

I, Mohamed Elsayed Hasan Abdelaal, born on 01.01.1988 in Cairo, hereby declare that I have written the present work about "Nonlinear Model Predictive Control for Trajectory Tracking and Collision Avoidance of Surface Vessels" independently and have not used any sources other than those specified, and that I have followed the general principles of scientific work and publications, as defined in the guidelines of good academic practice of the Carl von Ossietzky University of Oldenburg.

Oldenburg, 20 October 2018

\_\_\_\_\_  
Signature